# Test applications of advanced seismic assessment guidelines

**13 October 2004**

***Prepared for:*** The Pacific Earthquake Engineering Center
Task 508 Project

***By:*** RUTHERFORD & CHEKENE
Consulting Engineers
427 Thirteenth Street
Oakland, California 94618

Joe Maffei – Principal Investigator
Yuki Nakayama – Structural Designer
Danya S. Mohr – Structural Designer
Wiliam T. Holmes – Project Principal

## Executive Summary

For many utility and transportation networks, buildings are key components. Predicting the post-earthquake functionality of utility buildings is a crucial step in evaluating the likelihood that a distribution network will be able to provide electricity, gas, water, or communications services to the residents of an earthquake-affected area.

Advanced Seismic Assessment Guidelines, applicable to Utility buildings, were developed by Stanford University [Bazzurro et al 2004] as part of the PEER Lifelines Program, Building Vulnerability Studies (Project Task Number 507). The subject project, Task 508, applies these state-of-the-art Guidelines in a detailed fashion to two example buildings, each with differing features and functions within the electric and gas utility network.

The objectives of the test applications are to:

- Identify potential difficulties that Structural Engineers would encounter in using the procedures described in the Advanced Seismic Assessment Guidelines.
- Recommend possible revisions to the procedure to address any identified difficulties.
- Identify and make recommendations on other issues related to assessing the seismic reliability of utility structures and systems

The first building to be studied is a 3-story steel moment-frame building. The second building is a typical type of utility structure of composite concrete and steel (mill building) construction.

The findings of the project include the following:

- The Advanced Seismic Assessment Guidelines are a logical and rational method that appears to be technically sound.
- The Guidelines can be implemented using a variety of structural analysis approaches, ranging from hand-calculated building response to fully computerized analysis of intact and damaged structures.
- The results of the procedure depend on the technical definition of what collapse potential should correspond to a red-tag, yellow-tag, or green-tag occupancy. This report investigate several options for tagging criteria and generally recommends what is defined as Tagging Criteria D, with correlation to engineering judgment.
- The results of the procedure depend on key assumptions and practices related to evaluating the intact and damaged structure. These practices include:
  - Whether the analysis truly identifies and incorporates the structural behavior modes that will govern the seismic response. (This is a key aspect of any seismic evaluation procedure).
  - How degraded components are assumed to respond, which must be based on available research results and technical approaches.

  - Estimating the residual drift in a structure, and the effect of that residual drift on displacement demand. This report gives recommendations based on a structure's peak plastic drift, hysteresis loop shape, and strength degradation characteristics.

- For the most effective application of the Guidelines, research is needed on the structural response of degraded components, specifically in the following areas:

  - For steel moment frame structures, tests of beam-column connections are needed, where the tests are taken to displacements beyond flange fracture. (While there have been many tests of such connections, very few have continued testing beyond flange fracture.)

  - For concrete wall structures, a review and assessment of past laboratory testing would be useful, considering behavior modes including flexure, shear, and foundation rocking. There are a reasonable number of tests available, but appropriate recommendations for seismic evaluation assumptions have not been developed or verified.

- Advanced computer models of structural elements – in particular, multi-layer nonlinear finite element models of concrete walls, and nonlinear fiber models of fracturing steel beam connections – should be calibrated to experimental testing.

The conclusions of this report also summarize specific recommendations for engineers applying the Advanced Seismic Assessment Guidelines

# Table of Contents

## List of Figures

## List of Tables

# Notation

| | |
|---|---|
| $DS_i$ | $i^{th}$ structural damage state. |
| $Fs(S_a)$ | Fragility curve, cumulative probability distribution function of a S-state “capacity” measured in ground motion intensity terms. |
| $I$ | Moment of inertia of steel member. |
| $K_i$ | Global effective initial (elastic) stiffness for the $i^{th}$ damage state. |
| $K_{hi}$ | Global hardening stiffness for the $i^{th}$ damage state. |
| $K_{si}$ | Global softening stiffness for the $i^{th}$ damage state. |
| $k_i$ | Component effective initial (elastic) stiffness for the $i^{th}$ damage state. |
| $k_{hi}$ | Component hardening stiffness for the $i^{th}$ damage state. |
| $k_{si}$ | Component softening stiffness for the $i^{th}$ damage state. |
| $P$ | Mean annual frequency of exceeding the *Sa(Ti)* associated with collapse of the damaged structure. |
| $P_o$ | Mean annual frequency of exceeding the *Sa(Ti)* associated with collapse of the intact structure. |
| $MAF$ | Mean Annual Frequency = $1/RP$ |
| $N_c$ | Total number of beam connections. |
| $N_f$ | Number of fractured beam connections. |
| $R_i$ | Normalized base shear, = $V_i/V_{yi}$ |
| $RP$ | Return period. |
| $S_a$ | Spectral acceleration, or spectral acceleration to achieve a damage state. |
| $S_{a\ 10/50}$ | Spectral acceleration with a 10% probability of exceedance in 50 years. |
| $S_{a\ 5/50}$ | Spectral acceleration with a 5% probability of exceedance in 50 years. |
| $S_{a\ 2/50}$ | Spectral acceleration with a 2% probability of exceedance in 50 years. |
| $S_{a(cap)i}$ | Spectral acceleration to cause collapse of the damaged structure. |
| $S_{a(cap-\phi)i}$ | Spectral acceleration at the period of the intact structure that corresponds to $S_{a(cap)i}$ taken at the period of the damaged structure. |
| $S_d$ | Spectral displacement. |
| $T_1$ | Fundamental period of intact structure. |
| $T_i$ | Fundamental period of structure in the $i^{th}$ damage state. |
| $V$ | Base shear. |
| $V_y$ | Yield base shear. |
| $\alpha$ | Modal participation factor, assumed to be 0.9 |
| $\beta_U$ | Dispersion measurement representing epistemic uncertainty. |
| $\beta_R$ | Dispersion measurement representing aleatory variability. |
| $\beta$ | Dispersion measurement representing uncertainty and variability; equal to the square root sum of the square of $\beta_U$ and $\beta_R$. |
| $\Delta$ | Global displacement, typically taken at the roof level. |
| $\Delta_{rs}$ | Expected absolute value of the global residual displacement based on a static, monotonic pushover analysis. |
| $\Delta_{rd}$ | Expected absolute value of the global residual displacement based on a dynamic nonlinear analysis. |
| $\Delta_{re}$ | Effective reduction in global displacement capacity caused by residual displacement. |
| $\Delta_{yi}$ | Yield displacement. |

$\mu_i$ Global ductility ratio, $\Delta_i/\Delta_{yi}$

## Abbreviations

IDA Incremental Dynamic Analysis.
NSP Nonlinear Static Procedure of Analysis.
SPO Static Push-Over Curve of force versus displacement results from the NSP.

# 1. Introduction

### *Background*

One aspect of reducing the potentially costly and destructive impacts of earthquakes to society is to improve the earthquake resistance of utility and transportation networks, or "lifelines". Protecting these infrastructure networks requires understanding the seismic vulnerability of each of the components of the networks, understanding the most effective ways to reduce their seismic vulnerability, and understanding the inter-related importance of the components.

For many utility and transportation networks, buildings are key components. Predicting the post-earthquake functionality of utility buildings is a crucial step in evaluating the likelihood that a distribution network will be able to provide electricity, gas, water, or communications services to the residents of an earthquake-affected area.

A rational and practical approach to evaluating or reducing the seismic vulnerability of an infrastructure network starts with developing fragility curves for all components of the network. Recent research has led to improved methods of establishing fragility curves for utility buildings.

Advanced seismic assessment guidelines were developed by Stanford University (C. Allin Cornell, Paolo Bazzurro, Charles Menun, Maziar Motahari) as part of the PEER Lifelines Program, Building Vulnerability Studies (Project Task Number 507). The final product of the guidelines is a set of fragility curves for structural limit states directly related to post-earthquake building occupancy status, namely green, yellow, or red tagging.

The subject project, Task 508, applies these guidelines in a detailed fashion to two example buildings. Two utility buildings, with differing properties, are chosen for the test applications.

### *Objectives*

The objectives of the test applications are to:

- Identify potential difficulties that Structural Engineers would encounter in using the procedures described in the Advanced Seismic Assessment Guidelines.
- Recommend possible revisions to the procedure to address any identified difficulties.
- Identify and make recommendations on other issues related to assessing the seismic reliability of utility structures and systems

### *Scope*

The scope of the project includes a test application, to two real buildings, of the advanced seismic assessment guidelines. The first building to be studied is a 3-story steel moment-frame building. The second building is a typical type of utility structure of composite concrete and steel (mill building) construction. The scope includes developing specific performance predictions for the two structures, and identifying and commenting on, from the practicing engineer's perspective, issues related to the seismic assessment guidelines and the broader objectives of assessing the reliability of lifeline systems affected by building seismic vulnerability.

For each test building the scope includes the following topics:

- NSP analysis of undamaged building
- NSP analyses of damaged building
- NSP to ida conversion
- Occupancy status of damaged building
- Ground motion associated with limit state
- Computation of fragility curves

The detailed evaluations using the Guidelines have also led to study of integral technical issues including:

- Computer modeling issues for steel moment frame and concrete wall structures
- The spectrum analysis approaches ranging from "hand" adjustments on elastic models to fully computerized modeling of damaged structures.
- Estimating residual drift and its effect.
- Including the effect of building period shift
- Post-earthquake occupancy (tagging) criteria
- Post-earthquake inspection

Throughout the project, Rutherford and Chekene worked closely with the Project 507 researchers to ensure that our interpretations and use of the guidelines were correct, and to ensure that our recommendations complemented the intentions of the Guidelines.

# 2. Test Application 1: steel moment frame building

## *2.1. Description of the Structure*

The first example application is a service center and operations building, three stories, with a steel moment-resisting frame as the seismic-force-resisting system. (See Figure 2-1.) The building was designed in 1988. The rectangular plan measures 98 feet by 217 feet and the total floor area is 62,600 sq ft. Figure 2-2 shows a plan of typical floor framing for the building.

The floors and roof of the structure consist of lightweight concrete fill over metal deck. The floors and roof are supported by composite steel beams and girders, which spanning to steel columns. The columns bear on a foundation consisting of precast concrete piles and reinforced concrete pile caps, which are interconnected by concrete grade beams. Table 2-1 shows the building dead loads, floor masses, and story heights.

As shown in Figure 2-1, the steel moment frames are located around the building perimeter, with an additional two transverse frames bordering a two-story atrium near the building center. Figure 2-3 shows elevations of the moment frames analyzed, including member sizes. Grade 36 steel was used for the beams of the moment frames, while A572 Grade 50 steel was used for the columns. Table 2-1 shows the expected yield strengths for each material, taken from FEMA 356.

The building has a regular configuration, with no soft or weak stories, or other code-identified irregularities.

The building houses a communications facility that is used during storms and other emergencies. This call center was intended to be operational after an earthquake, so the building was designed as an essential facility using an importance factor of 1.5. This means that the structural frame is 50 percent stiffer (and stronger) than one would expect from a non-essential steel moment frame from the same era.

The steel moment frames are designed and specified to “pre-Northridge” standards, meaning that the connections can be susceptible to fracture near the welds of the beam to the column.

The building is located at a site of high seismicity. The short period design spectral acceleration, for a ground motion with a 5% probability of exceedence in 50 years, is 1.69g, as shown in Table 2-1. The building is on a Type D soil profile. The spectral acceleration at the building period of 0.78 seconds is governed by the short period plateau acceleration of the design spectra.

**Table 2-1: Building Loads and Properties**

| **Building Dead Load** | |
|---|---|
| Ceiling & Mech. | 6 psf |
| Partitions | 10 psf |
| 4 ½” LWC over 3” Metal Deck | 44 psf |
| Beams | 8 psf |
| Columns | 3 psf |
| Total | 71 psf |
| | |
| Exterior Walls ($2^{nd}$ & $3^{rd}$ stories) | 15 psf |

| **Floor** | **Story Ht. (ft)** | **Area ($ft^2$)** | **Floor DL (K)** | **Floor Mass ($k\text{-}s^2/ft$)** | **Floor LL (K)** |
|---|---|---|---|---|---|
| Roof | 14’ | 21266 | 1638 | 50.9 | 851 |
| $3^{rd}$ | 14’ | 21266 | 1638 | 50.9 | 2127 |
| $2^{nd}$ | 15.5’ | 20146 | 1431 | 44.4 | 2015 |
| | | Totals | 4707 | 146.2 | 4993 |

| **Estimated Material Properties** | | |
|---|---|---|
| Columns | A572 Grade Sc | Fy=55ksi |
| Beams | A36 | Fy=51ksi |

| **Site Seismicity Data** | From USGS National Seismic Hazard Maps | | | |
|---|---|---|---|---|
| | PGA | $S_s$ (g) | $S_1$ (g) | $S_a$ (g) * |
| 10% / 50 yr. | 0.61 | 1.28 | 0.67 | 1.28 |
| 5% / 50 yr. | 0.75 | 1.69 | 0.92 | 1.69 |
| 2% / 50 yr. | 0.96 | 2.04 | 1.25 | 2.04 |
| MCE | | | | 1.50 |
| DBE | | | | 1.00 |

*At building period = 0.78s
Soil Type D

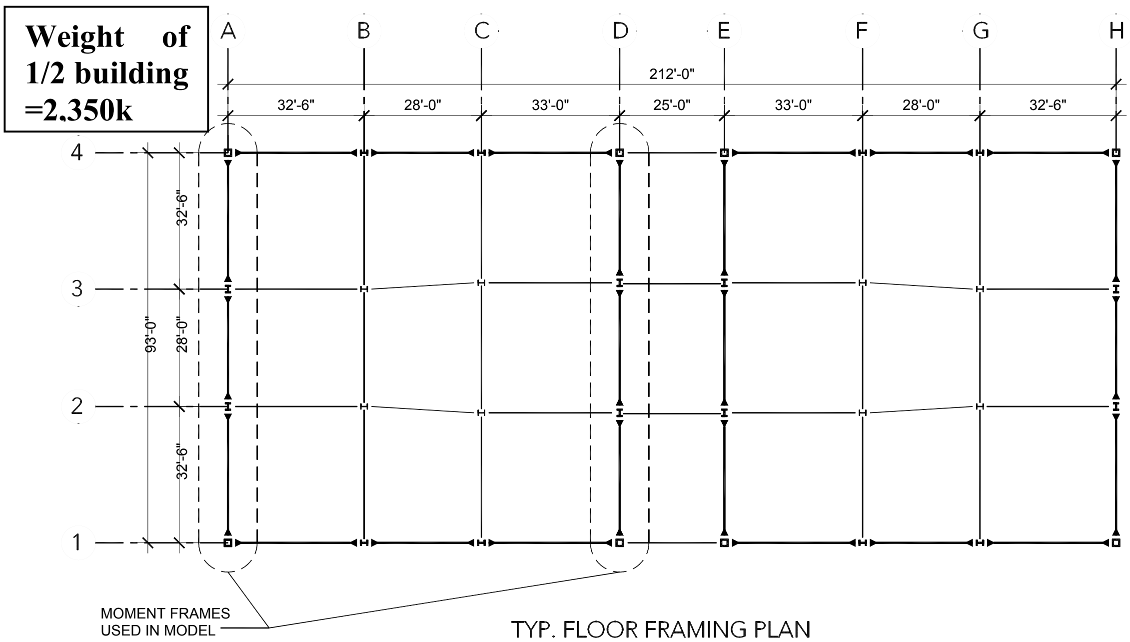


**Figure 2-1:** **Typical floor framing showing moment frames included in model**

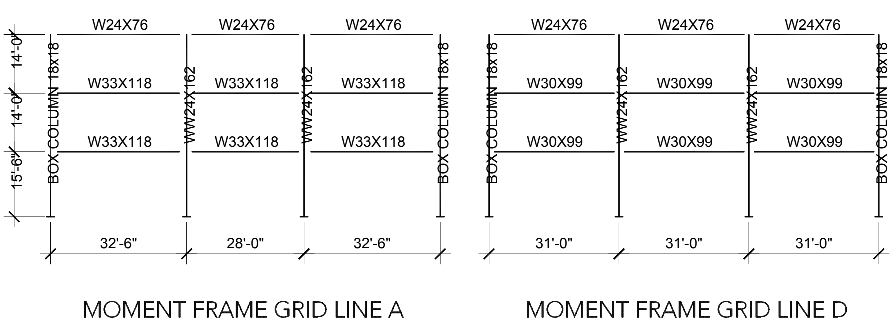


**Figure 2-2:** **Elevation of moment frames included in model**

**Figure 2-3:** **Photo of the building exterior**

## 2.2. *Seismic evaluation of the intact structure*

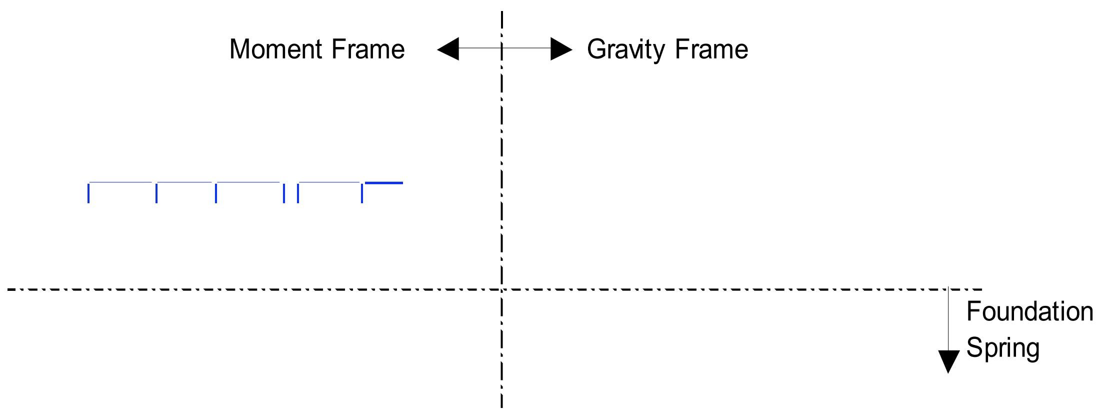


**Table 2-2:** **Beam Hinge Properties, determined using FEMA 356 Table 5-6.**

| Size | $L_b$ (ft) | a | b | c | $Q_C/Q_B$ | $\theta_C/\theta_B$ | $\theta_E/\theta_B$ |
|---|---|---|---|---|---|---|---|
| W33x118 | 30.71 | 0.008 | 0.023 | 0.2 | 1.036 | 2.20 | 4.39 |
| W33x118 | 25.92 | 0.008 | 0.023 | 0.2 | 1.043 | 2.42 | 5.02 |
| W30x90 | 29.21 | 0.013 | 0.025 | 0.2 | 1.052 | 2.74 | 4.48 |
| W30x90 | 28.92 | 0.013 | 0.025 | 0.2 | 1.053 | 2.76 | 4.52 |
| W24x76 | 30.71 | 0.020 | 0.029 | 0.2 | 1.064 | 3.15 | 4.09 |
| W24x76 | 29.21 | 0.020 | 0.029 | 0.2 | 1.068 | 3.26 | 4.25 |
| W24x76 | 28.92 | 0.020 | 0.029 | 0.2 | 1.068 | 3.28 | 4.28 |
| W24x76 | 25.92 | 0.020 | 0.029 | 0.2 | 1.076 | 3.54 | 4.66 |

**Figure 2-4:** **Analysis model including gravity frames**

## 2.3. *Seismic evaluation of the damaged structure*

**Table 2-3:** **Ground acceleration for damage states**

| $DS_i$ | Period(sec) | $S_{a\ 10/50}$ | $S_{a\ 5/50}$ | $S_{a\ 2/50}$ |
|---|---|---|---|---|
| Intact | 0.81 | 1.25 | 1.69 | 2.04 |
| $DS_2$ | 0.88 | 1.15 | 1.58 | 2.04 |
| $DS_3$ | 0.99 | 1.02 | 1.40 | 1.90 |
| $DS_4$ | 1.03 | 0.98 | 1.35 | 1.82 |

**Table 2-4:** **Tagging Criteria**

| $DS_i$ | Roof Drift % | $S_a$ to get to $DS_i$ | $S_{a(cap)}$ | $S_{a(cap-\phi)}$ | $S_{a(cap-\phi)}/S_{ai}$ | Tagging State |
|---|---|---|---|---|---|---|
| $DS_2$ | 1.74 | 1.11 | 2.55 | 2.55 | 2.30 | *Green* |
| $DS_3$ | 3.25 | 1.76 | 2.30 | 2.47 | 1.40 | *Green* |
| $DS_4$ | 4.04 | 1.87 | 2.03 | 2.28 | 1.22 | *Green* |

**Table 2-5: Median roof drifts and median $S_a$ corresponding to structural limit states.**

| Structural Limit State: | Onset of Damage | Onset of Yellow | Onset of Red | Collapse |
|---|---|---|---|---|
| Median Roof Drift: | 1.38% | 5.50% | 8.00% | 7.70% |
| Median $S_a$: | 0.86g | 2.05g | 2.50g | 2.50g |

**Table 2-6: Uncertainty Values**

| Structural Limit State | Onset of Damage | Onset of Yellow | Onset of Red | Collapse |
|---|---|---|---|---|
| $\beta_u$ | 0.30 | 0.60 | 0.60 | 0.50 |
| $\beta_r$ | 0.00 | 0.26 | 0.33 | 0.33 |
| $\beta$ | 0.25 | 0.65 | 0.68 | 0.60 |

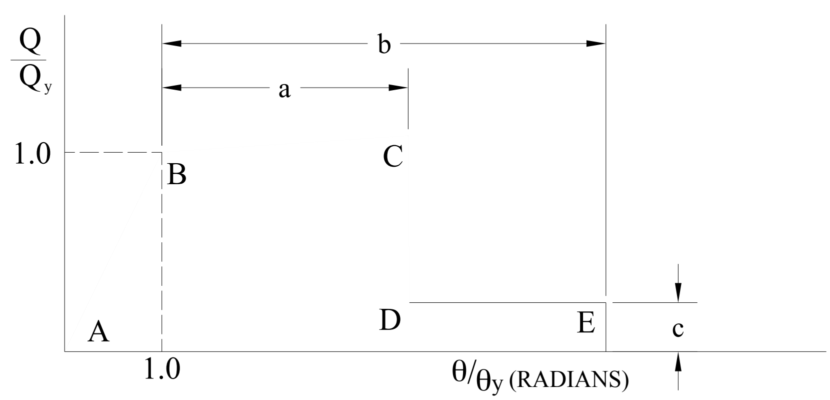


**Figure 2-5: Generalized Force-Deformation Relation for Steel Elements or Components**

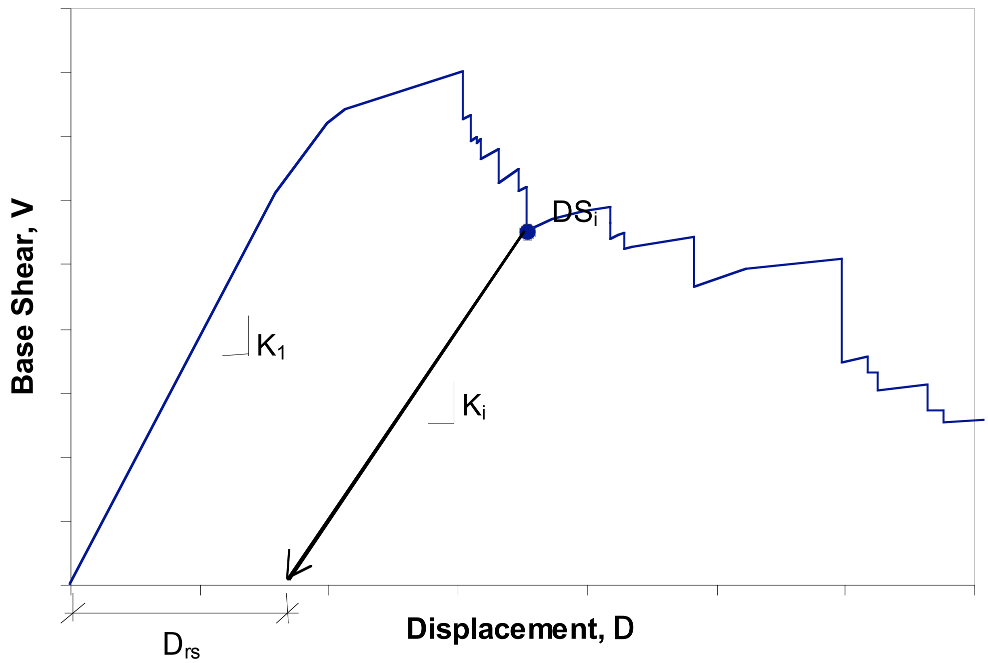


**Figure 2-6:** **Assumed global unloading stiffness from DSi**

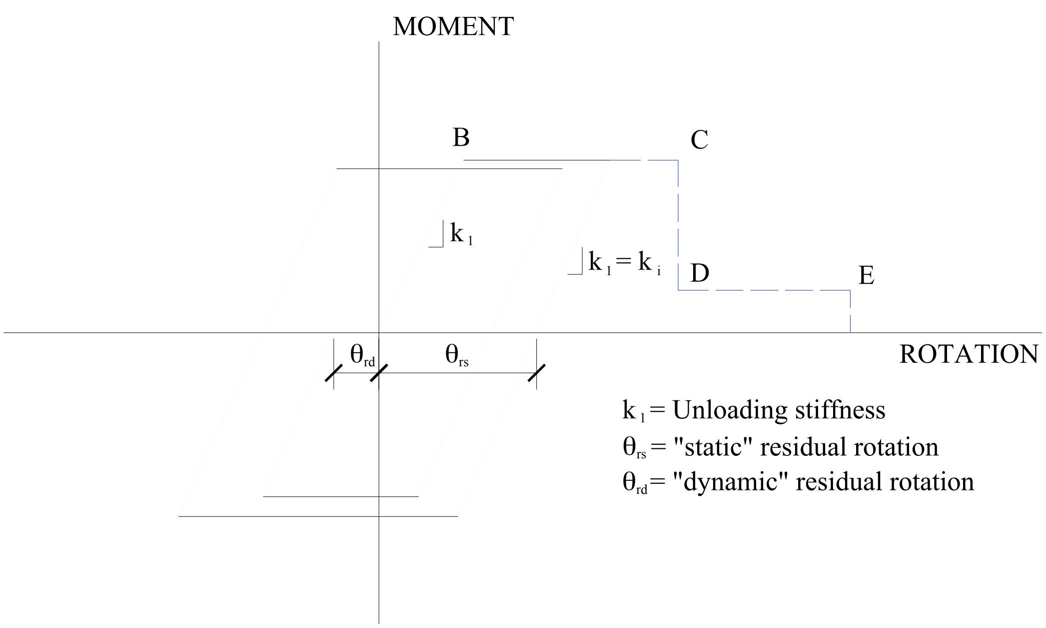


**Figure 2-7:** **Assumed unloading cyclic behavior for connections whose flanges have not fractured**

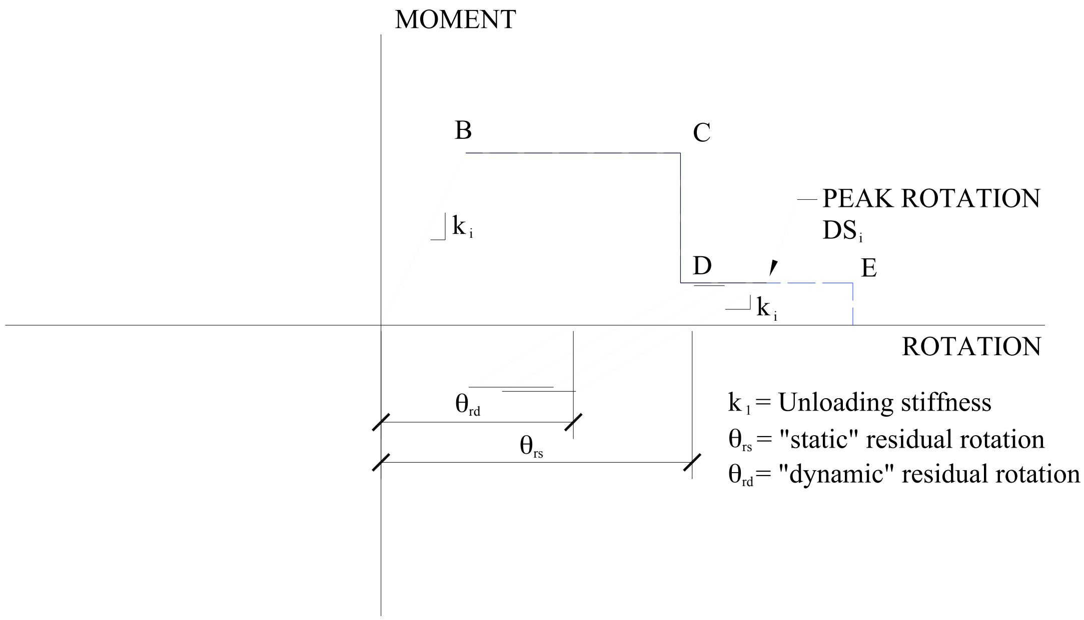


**Figure 2-8:** **Assumed unloading and cyclic behavior of connections whose flanges have fractured.**

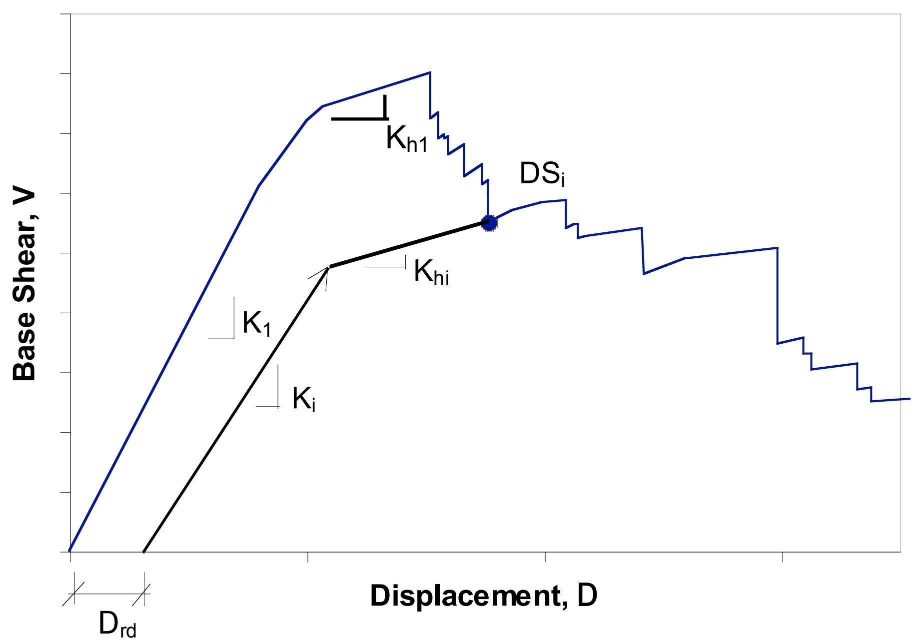


**Figure 2-9:** **Assumed global reloading of a structure that has been subjected to DSi**

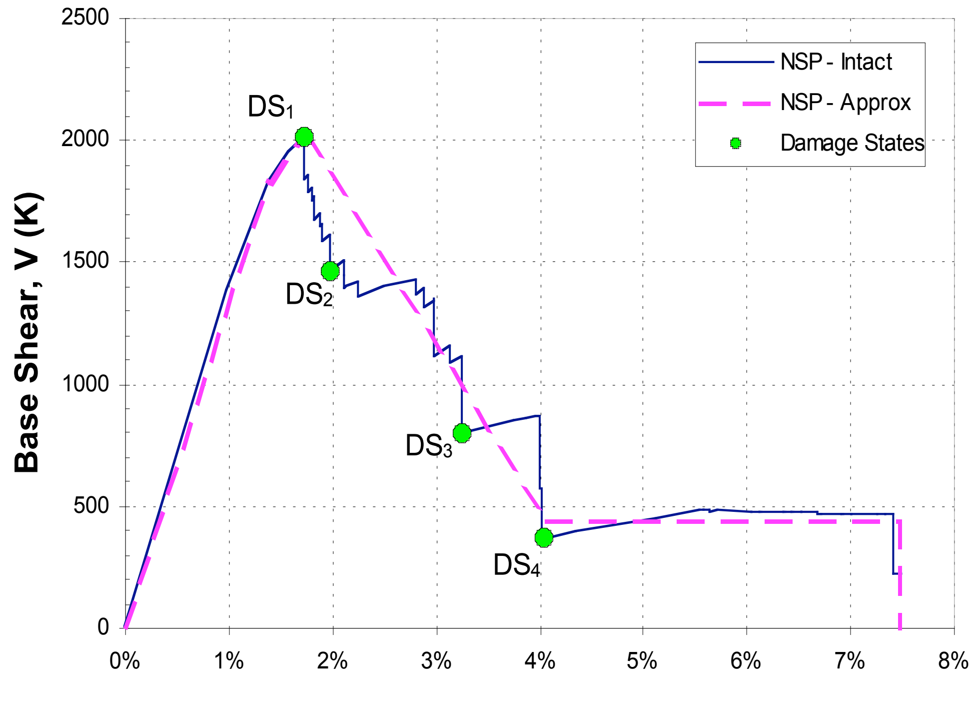


**Figure 2-10: Pushover curve for the Intact structure**

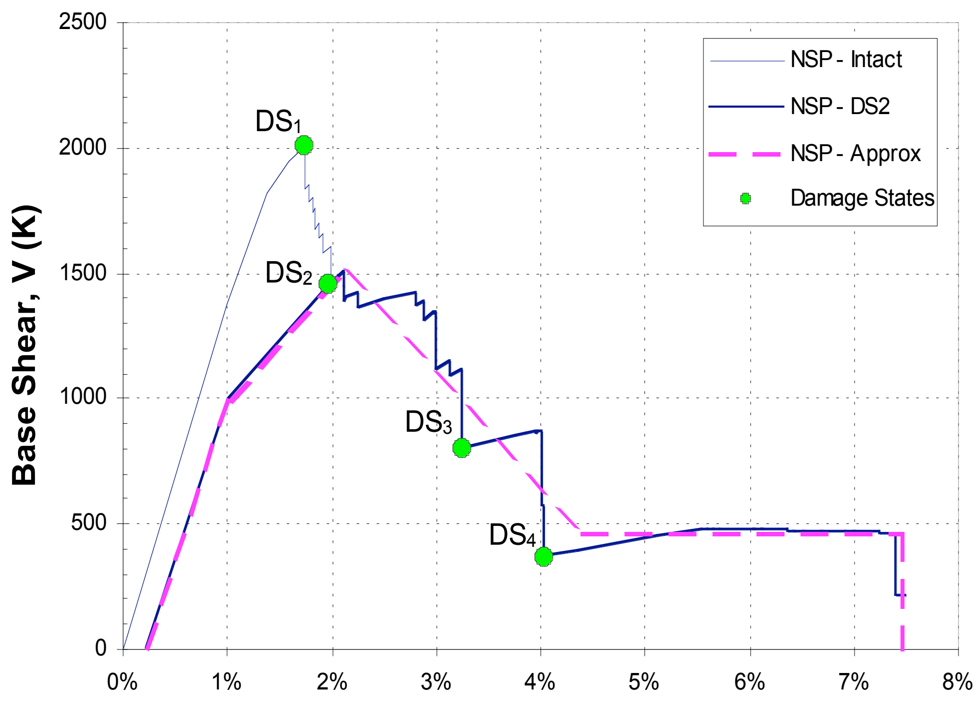


**Figure 2-11: Pushover curve for DS2**

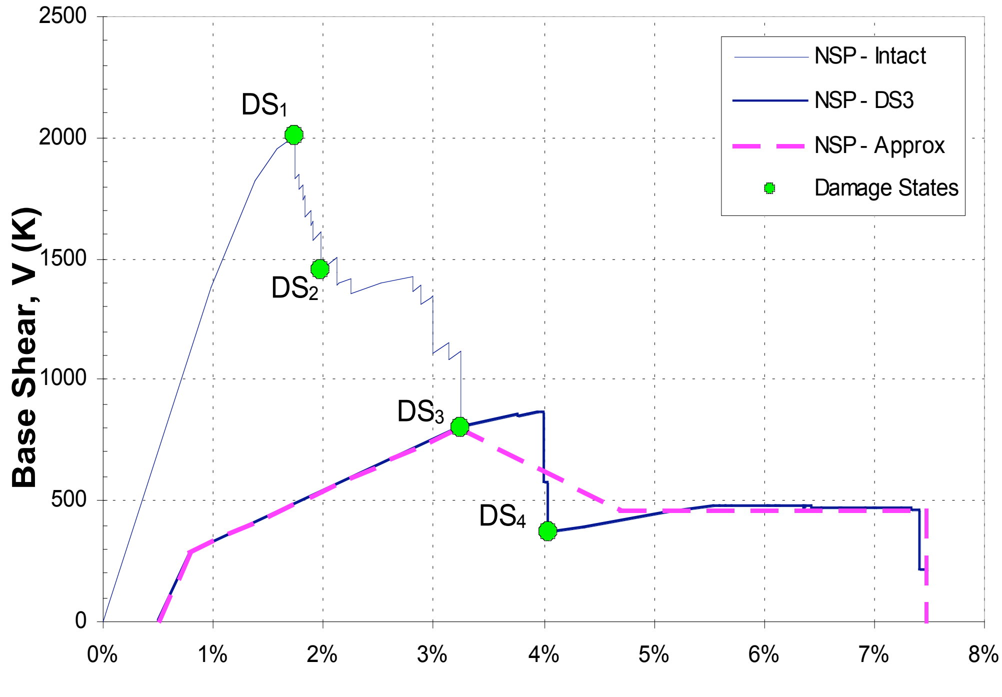


**Figure 2-12:** **Pushover curve for DS3**

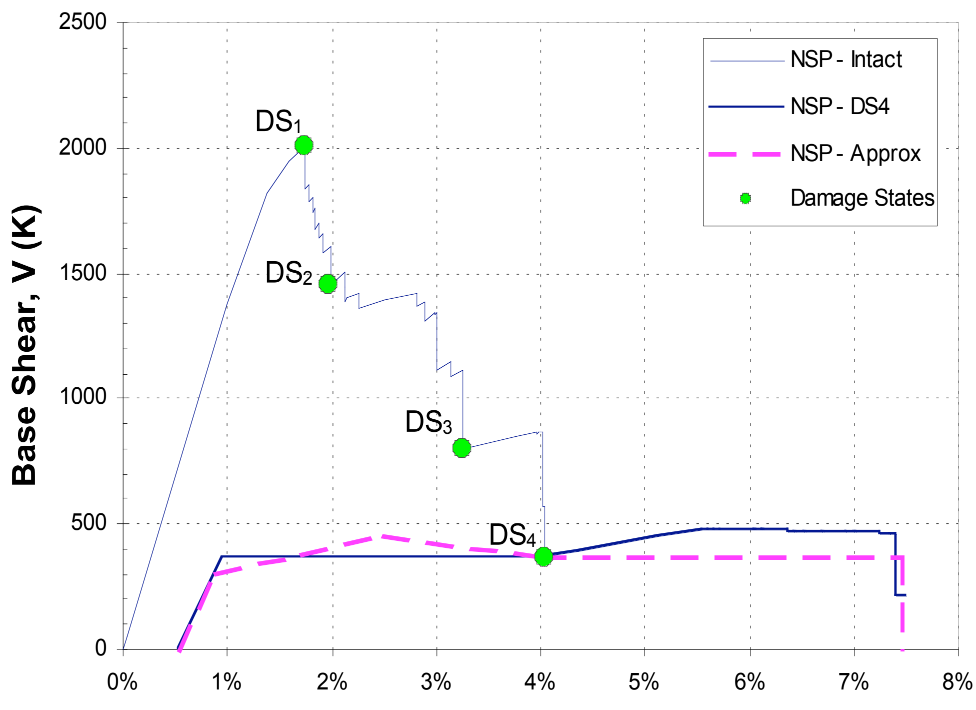


**Figure 2-13:** **Pushover curve for DS4**

## 2.4. Inferred dynamic behavior (SPO2IDA)

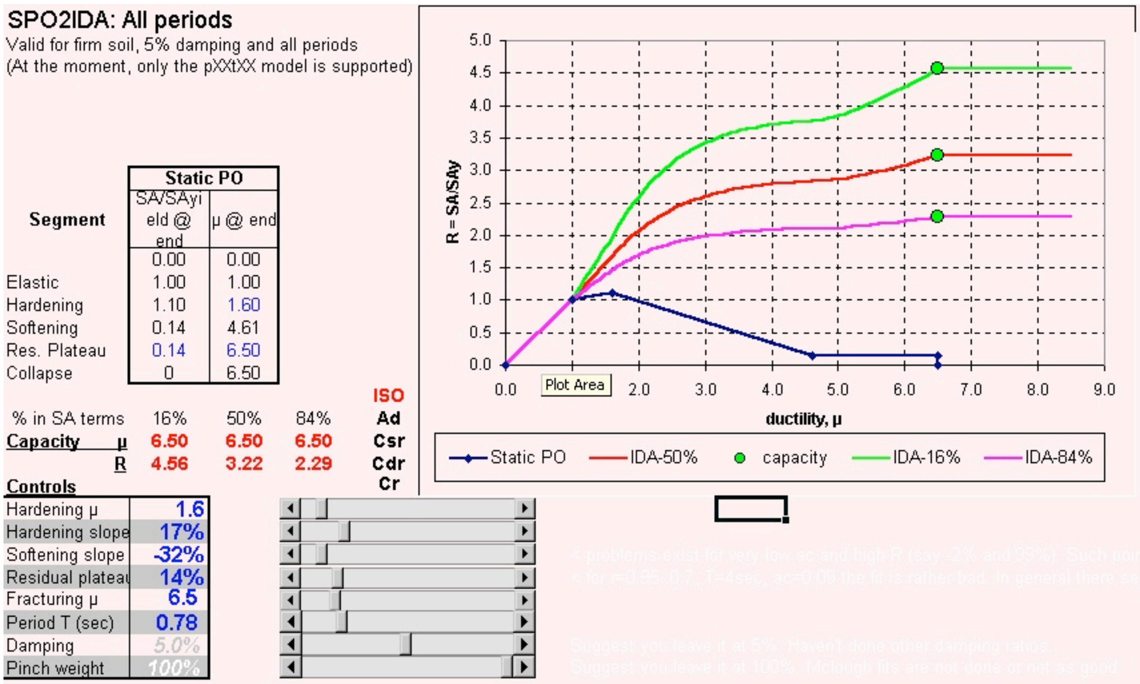


Figure 2-14: Example of SPO to IDA spreadsheet

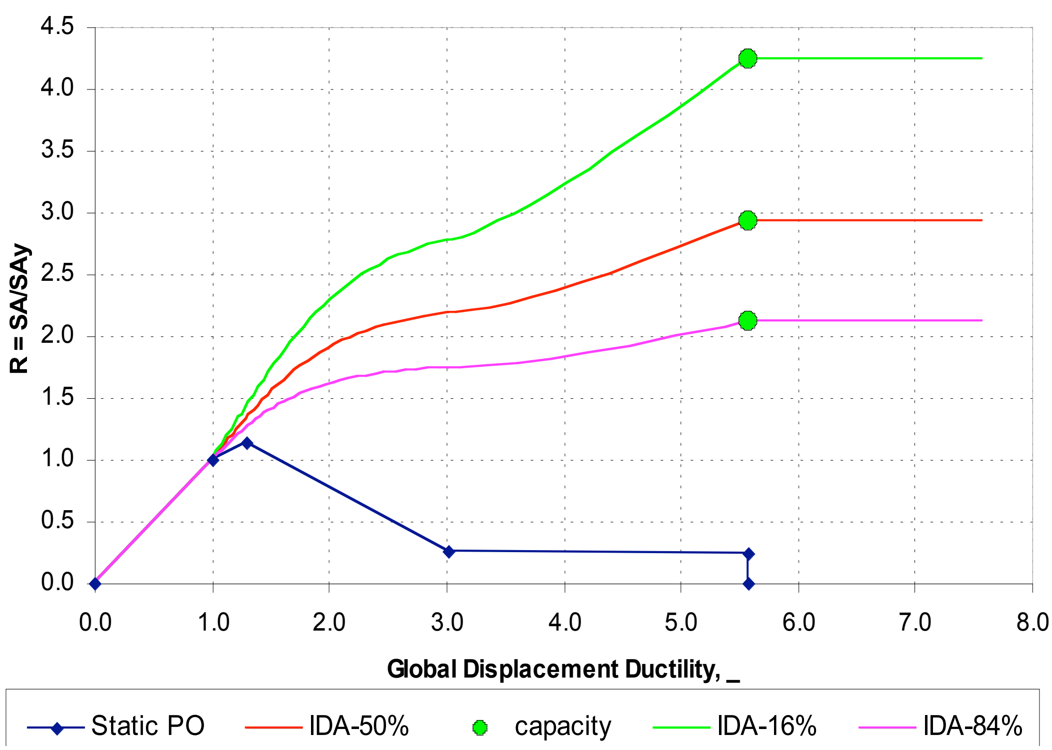


Figure 2-15: Normalized IDA for Intact structure

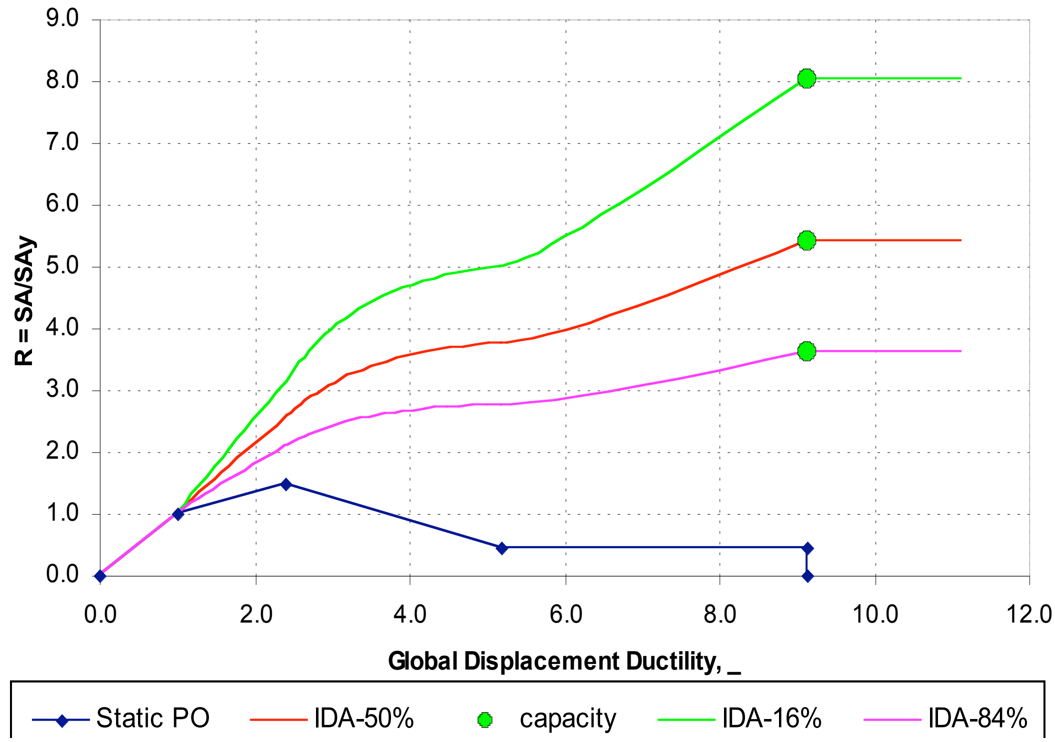


**Figure 2-16:** **Normalized IDA for DS2**

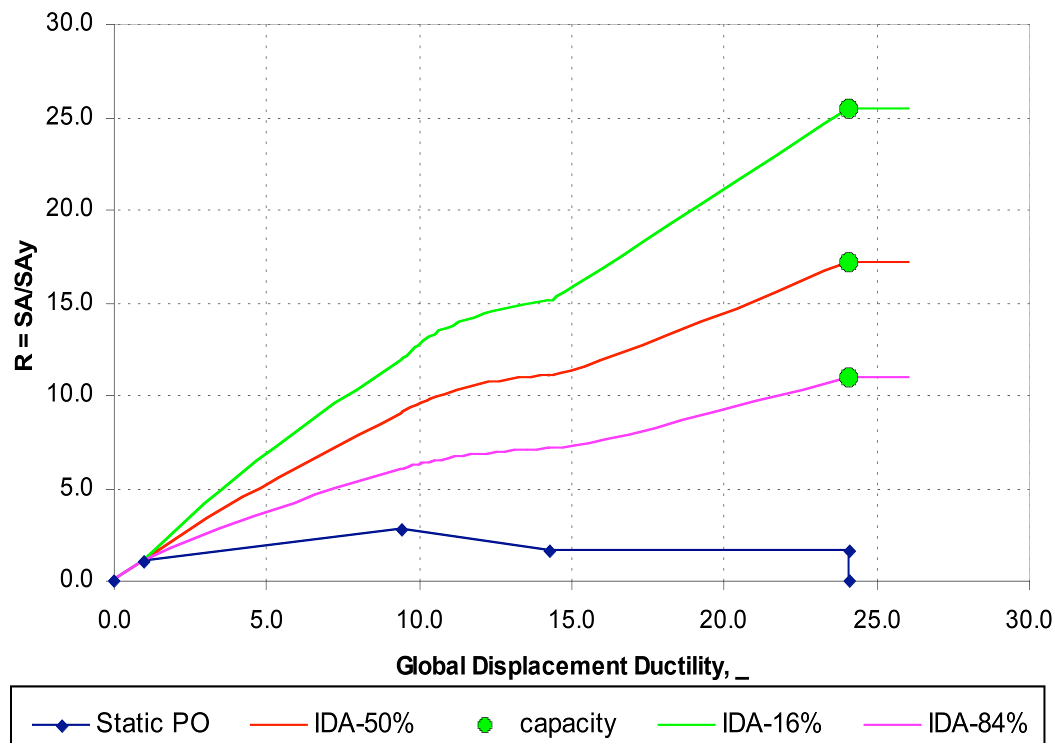


**Figure 2-17:** **Normalized IDA for DS3**

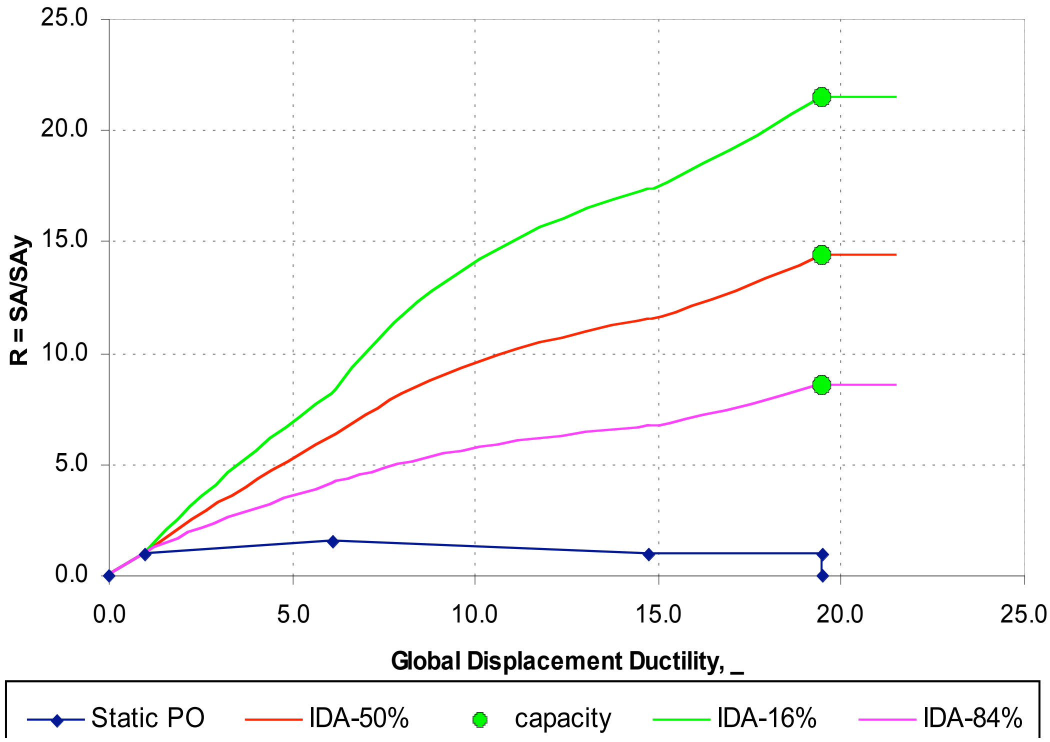


**Figure 2-18: Normalized IDA for DS4**

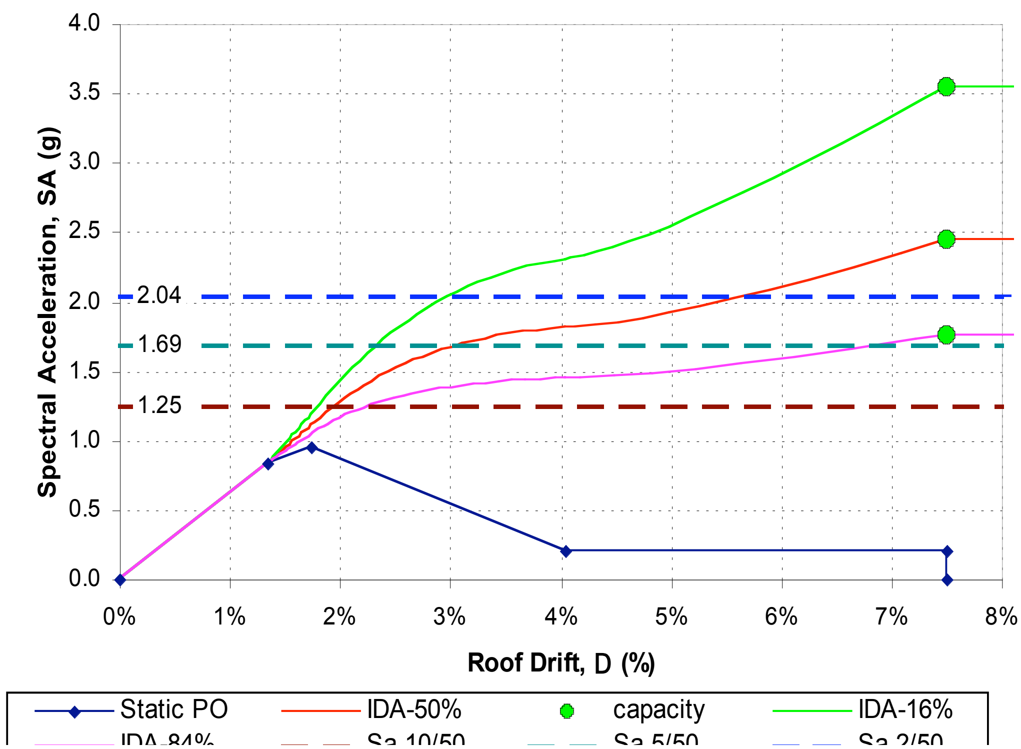


**Figure 2-19: Intact IDA**

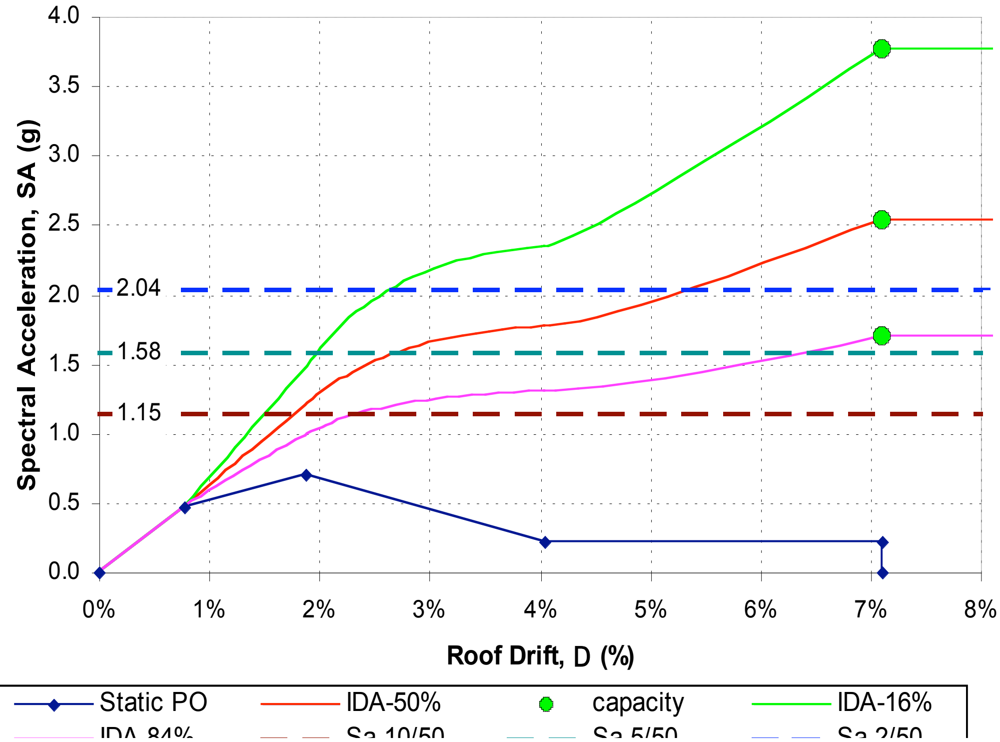


**Figure 2-20: DS2 IDA**

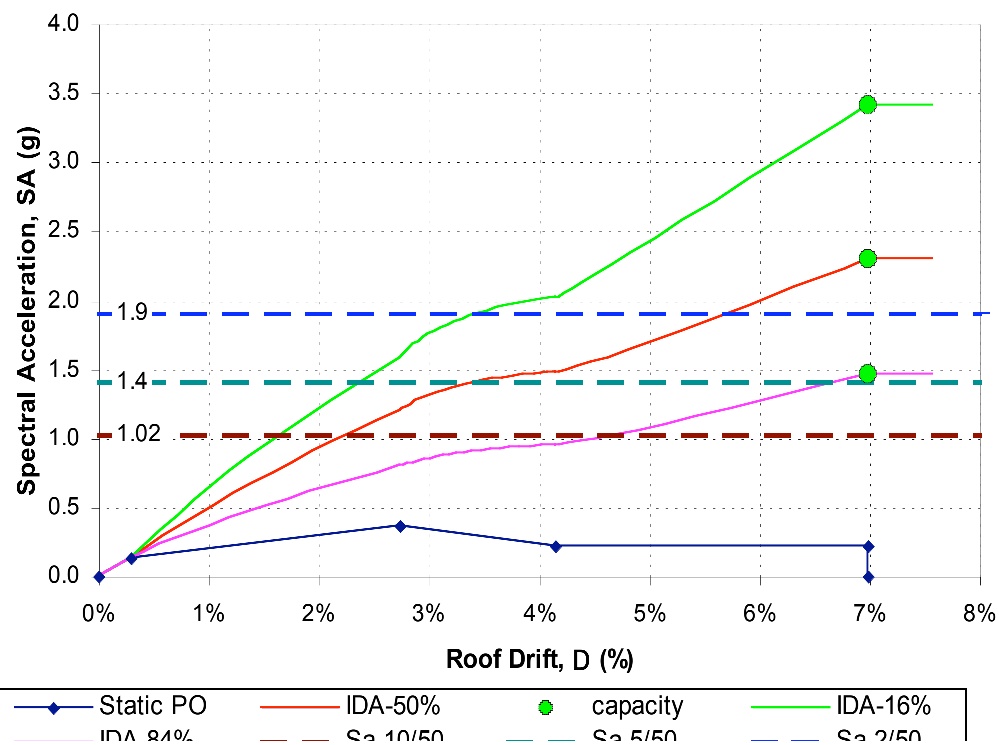


**Figure 2-21: DS3 IDA**

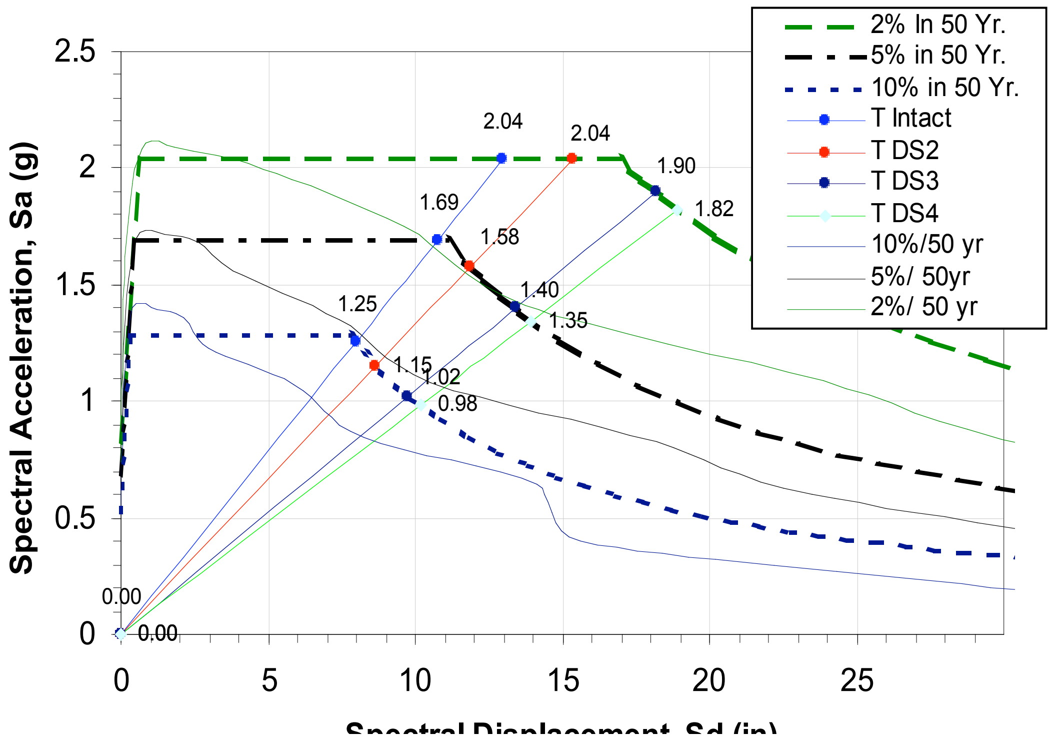


Figure 2-22: Response spectrum of intact and damage states

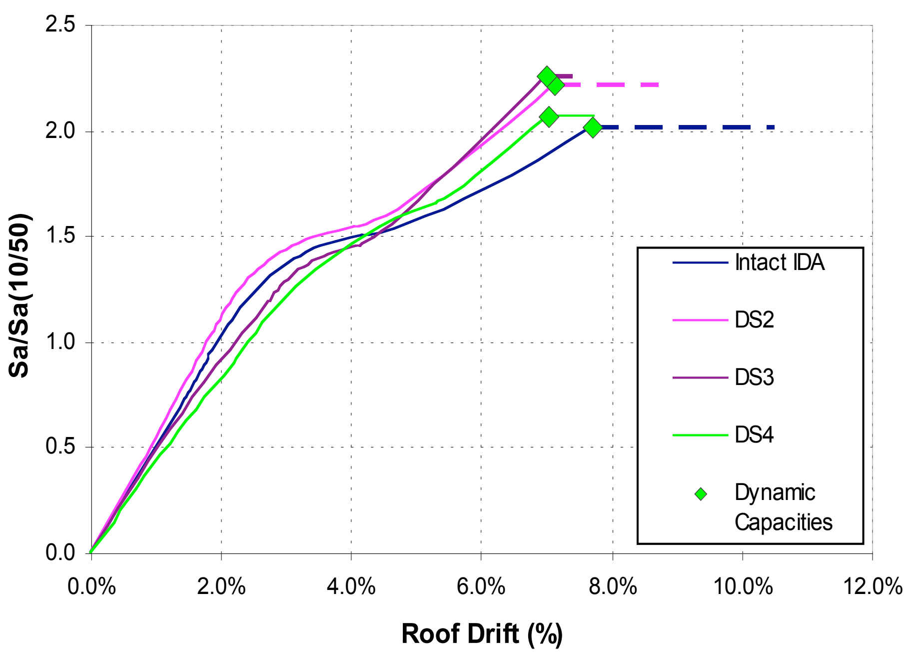


Figure 2-23: IDA, Roof Drift vs. Sa/Sa(10/50) for intact and damage states

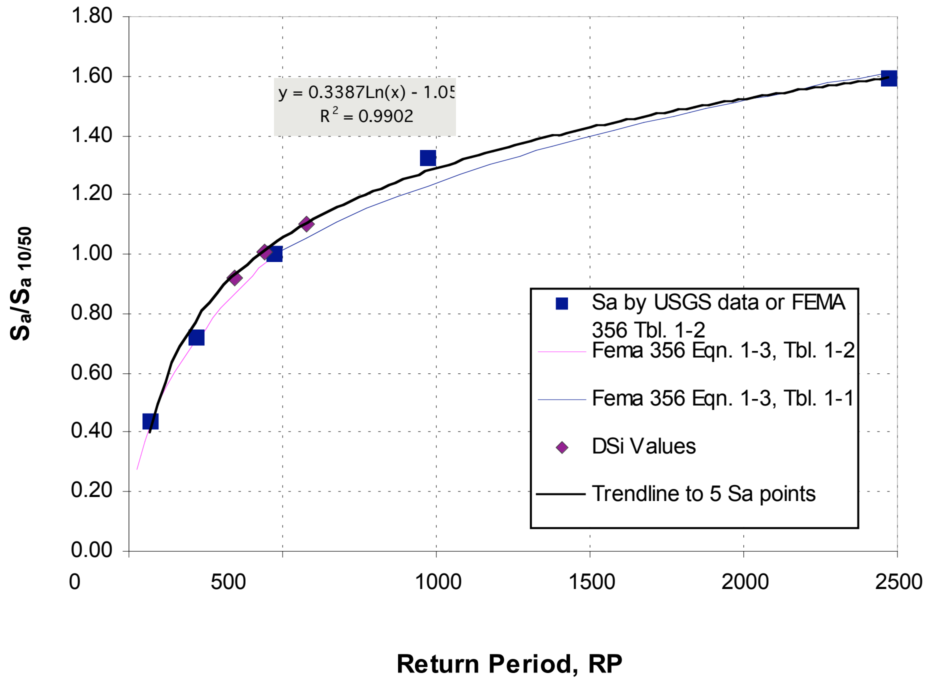


**Figure 2-24: Relationship between Sa and return period, RP, for the building site**

## 2.5. *Post-earthquake tagging limit states*

## 2.6. *Fragility curves*

## 2.7. *Summary of steps*

This section summarizes the steps used in applying the Guidelines to the structure of Analysis Run 120.

***Step 1: Nonlinear Static Procedure of the Intact Building***

1.1 Model structure using SAP2000 Non-Linear.

1.2 Beam hinges are modeled according to FEMA 356 section 5.5.2.2.2, see Figure 2-5 and **Error! Reference source not found.** for beam hinge properties.

1.3 Obtain SPO for Intact structure.

1.4 The specific damage states are chosen based on points where a significant loss of lateral force capacity occurs.

***Step 2: SPO curves for the damaged building.***

2.1 The building is assumed to unload linearly, see (Figure 2-6). The unloading stiffness, $K_i$, is determined using a linear model of the structure in $DS_i$. This model is constructed by reducing the stiffness of damaged beams. For beams whose end connections remain within the elastic or hardening region of the moment-rotation curve (Figure 2-7), the beam stiffness remains unchanged. For beams whose end connections have "fractured" or gone past point D on the moment-rotation curve (Figure 2-8), the stiffness is reduced to approximate that for a beam with fractured flanges. For a beam that fails on one end, the moment of inertia is reduced to 2/3 *I*, for a beam that had fails on both ends it is reduced to 1/3 *I*.

2.2 The residual deformation resulting from this unloading is $\square_{rs}$ as shown Figure 2-6. The dynamic residual displacement, $\square_{rd}$, is estimated to be $0.3 * \square_{rs}$ for a steel moment frame building according to ($\gamma_1$=0.3).

$$\square_{rd} = \gamma_1 * \square_{rs}$$

2.3 Determine the effective loss of deformation capacity $\square_{re}$, which is a function of $\alpha_i$. See Table for the $\gamma_2$ values for the damage states.

$$\square_{re} = \gamma_2 * \square_{rd} = \gamma_1 \gamma_2 * \square_{rs}$$

2.4 The hardening stiffness, Khi, for the damaged structure is determined by the ratio of fractured connections to the total number of connections.

$$K_{hi} = (1 - N_f/N_c) * K_{h1}.$$

2.5 The SPO of the damaged structure meets the SPO of the intact structure at the defined $DS_i$ point and then follows the SPO of the intact structure. Given the two points, $DS_i$ and $\square_{re}$, and the two slopes $K_i$ and $K_{hi}$, the SPO curves for the damaged structure can be created, see (Figure 2-9).

***Step 3: Inferring dynamic response from static response, SPO to IDA.***

3.1 The SPO results from Step 2 are approximated into a quadralinear curve, see (Figure 2-10) - (Figure 2-13).

3.2 The quadralinear approximation for the damaged structure is shifted to account for the effect of residual deformation. $\square_{re}$ is subtracted from all deformation capacities on the SPO.

3.3 Normalize the SPO by $\square_y$ and $V_y$.

$$R = V/V_y \qquad \square = \square/\square_y$$

3.4 Input the SPO approximation into the SPO2IDA spreadsheet in terms of $R$ and $\square$; see (Figure 2-14) for an example of the SPO2IDA spreadsheet interface.

3.5 The IDA curve representing the median (50%) is used, see (Figure 2-15) - (Figure 2-18).

3.6 The IDA output is "de-normalized" to produce *Roof Drift* vs. $S_a$, see (Figure 2-19) - (Figure 2-21).

$$S_a = RV_y/W\alpha \qquad \textit{Roof Drift} = \square_y$$

3.7 To compare the IDA results for Intact structure and each of the damage states on the same graph, the ordinate ($S_a$) value is normalized by $S_{a(10/50)}$ , (Figure 2-23). The SPO for each damage state has a slightly different initial stiffness therefore it has a different $T$ and results in different $S_{a(10/50)}$ values.

3.8 The $S_{a(10/50)}$ values are determined for each damage state using the response spectrum for the site. Spectral values for 0.2s and 1.0s are taken from USGS National Seismic Hazard Mapping Project website (http://geohazards.cr.usgs.gov/eq/index.html). Soil profile type B is used.

3.9 $S_{a(cap)}/S_{a(10/50)}$ is taken as the point on the 50% IDA plot where the curve becomes horizontal.

#### *Step 4: Occupancy Status for Damaged Building (Tagging Criteria C).*

4.1 Using the SPO for the intact structure (Figure 2-10), determine the displacement at which each of the damage states occurs.

4.2 Using the Intact IDA curve (Figure 2-19) and the displacement values from step 4.1, determine the corresponding $S_a$ for each of the $DS_i$.

4.3 Determine the $S_{a(cap-\phi)i}$ for each damage state using their respective 50% IDA values.

4.4 The tagging states are determined based on the structure's ability to sustain an aftershock proportional to the main shock.

- *Green*, if $S_{a(cap-\phi)}/ S_{ai} > 1.0$
- *Yellow*, if $0.75 < S_{a(cap-\phi)}/ S_{ai} < 1.0$
- *Red*, if $S_{a(cap-\phi)}/ S_{ai} < 0.75$

4.5 Create a plot of Roof Drift vs. $S_{a(cap-\phi)}/S_a$, with the tagging limit states included, see **Error! Reference source not found.**.

#### *Step 5: Ground motion level associated with a structural limit state.*

5.1 Onset of damage is taken as the first significant point of yielding.

5.2 Determine the roof drift levels associated with each structural limit state using the tagging criteria and **Error! Reference source not found.**.

5.3 The resulting main shock ground motion values causing the structure to reach the incipient limit states are obtained using **Error! Reference source not found.**, these values are shown in **Error! Reference source not found.**.

5.4 The aleatory variability values, $\beta_r$, are taken from the SPO2IDA spreadsheet for the global ductility ratios corresponding to the specific limit states. The epistemic uncertainty values, $\beta_u$, are taken from Table 2e of the PG&E Advanced Seismic Assessment Guidelines. The term $\beta$ is calculated as the square root sum of the squares of $\beta_u$ and $\beta_r$ for each tagging state, (**Error! Reference source not found.**).

***Step 6: Computation of Fragility Curves***

6.1 The fragility curves are created using the ground motion intensities and the dispersion values obtained in Step 5; the fragility curves are plotted using the relationship described in the guidelines. The curves are plotted for the probabilities $p = \{0.05, 0.25, 0.5, 0.75, 0.95\}$ versus the corresponding Sa:

$$S_a = S^s_{cap} e^{x\beta}$$

for the values of x equal to {-1.65, -0.67, 0.0, 0.67, 1.65}, see (**Error! Reference source not found.**).

# 3. Study of analysis assumptions for Test Application 1

## *3.1. Variation in assumptions for the intact structure*

**Table 3-1: Assumptions used in the nonlinear static procedure**

| **Run number** | **101** | **102** | **103** |
|---|---|---|---|
| Foundation model (fixed/modeled) | Fix | | |
| Panel zone modeled (no/linear/nonlinear) | No | | |
| Vertical distribution of forces (ubc/uniform) | Ubc | | |
| Beam component curve used | 1 | | |
| Gravity framing included (yes/no) | No | | |
| Direction of analysis (transverse/longitudinal) | Tr | | |
| Software used (SAP/Perform) | SAP | | |
| Variability of steel connections (y/n) | No | | |
| Local collapse criterion | None | | |

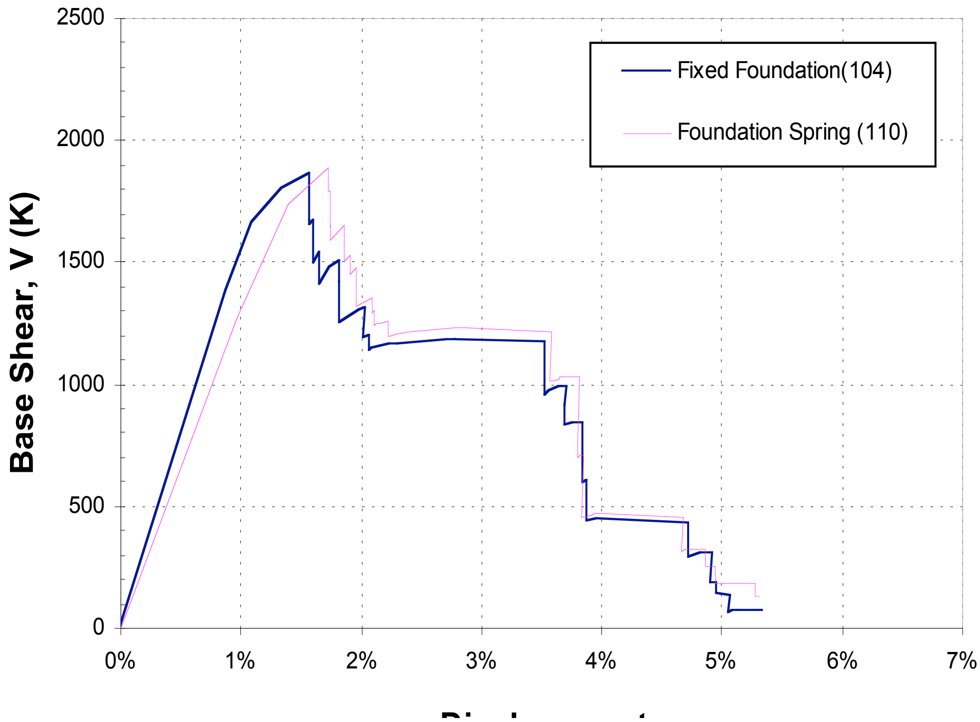


**Figure 3-1: Comparison of intact pushover curves showing the effect of foundation flexibility**

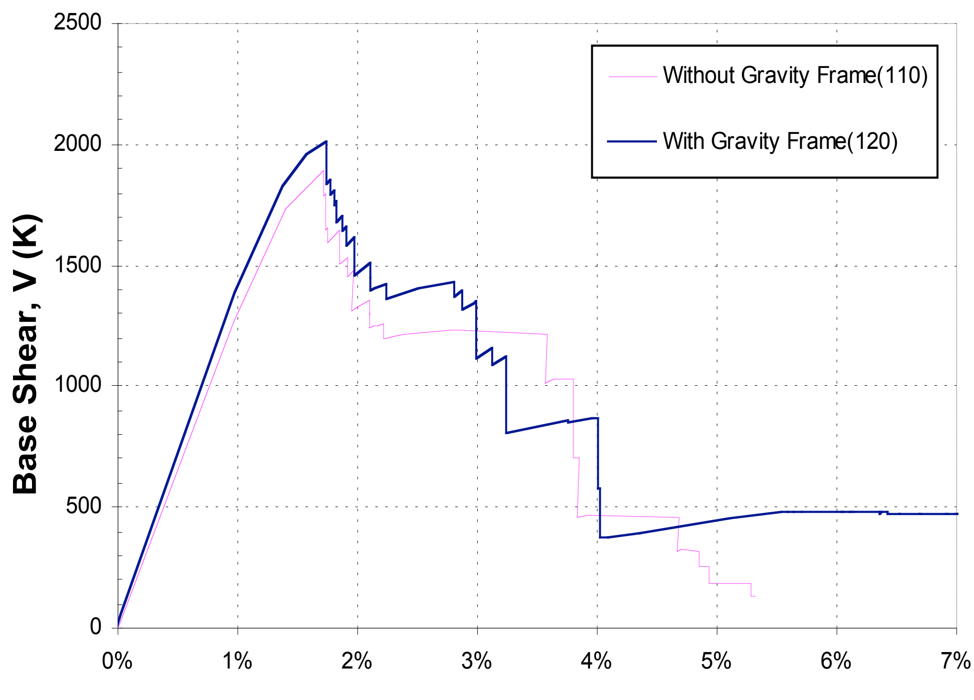


**Figure 3-2: Comparison of intact pushover curves showing the effect of gravity frame**

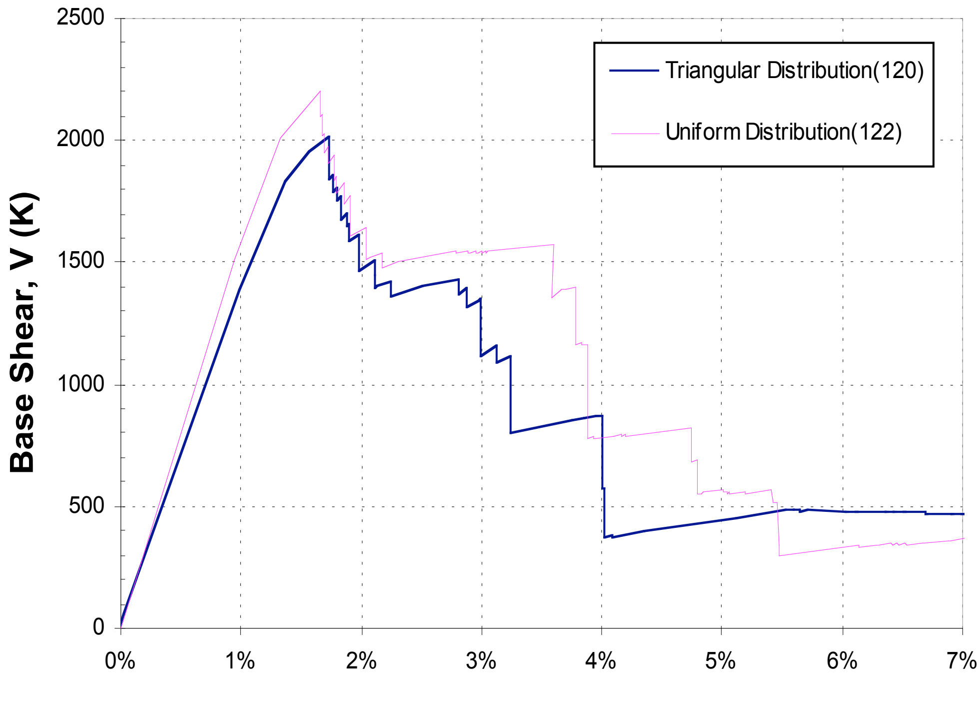


**Figure 3-3: Comparison of intact pushover curves showing the effect of vertical distribution of lateral load**

### *3.2. Study of assumptions for the damaged structure*

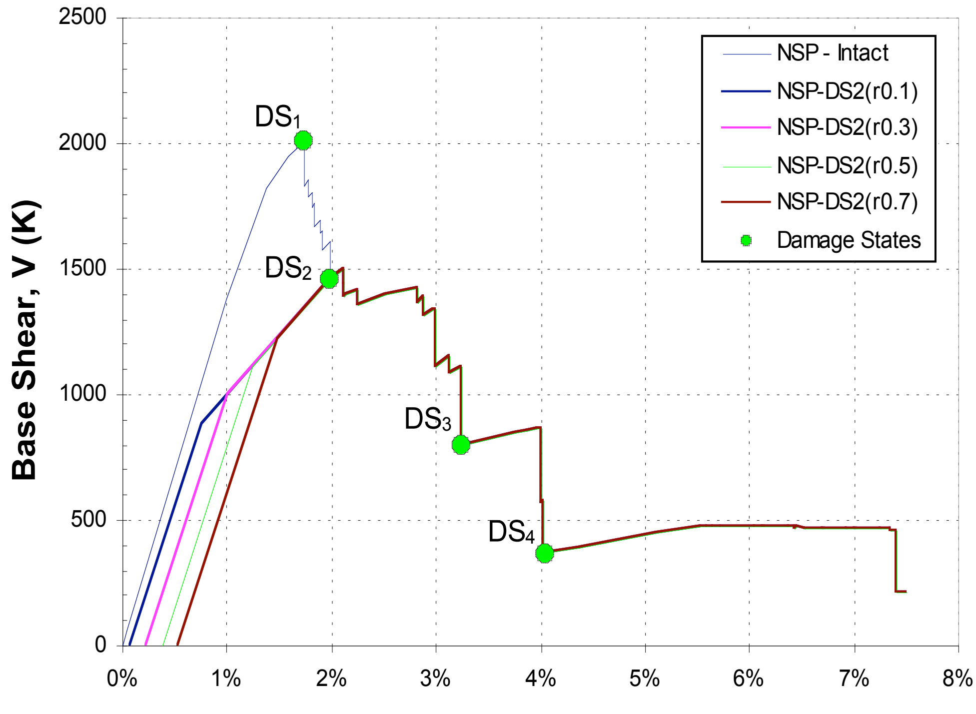


**Figure 3-4: Pushover curves for damage state2, with different estimates of effective residual drift, $\Box_{\gamma e}$**

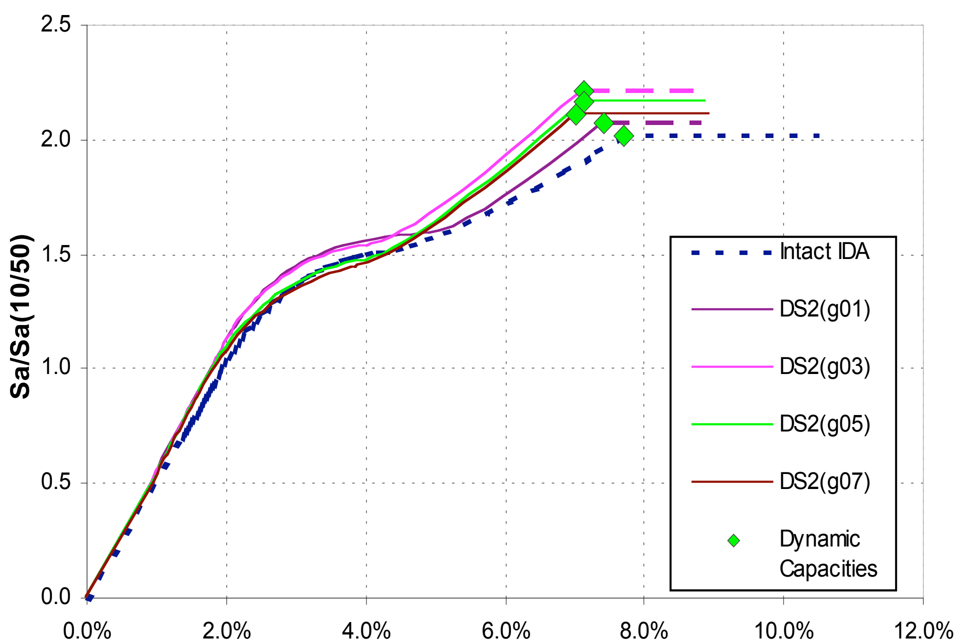


**Figure 3-5: Incremental dynamic analysis(IDA) resluts as influenced by effective residual drift, $\Box_{\gamma e}$**

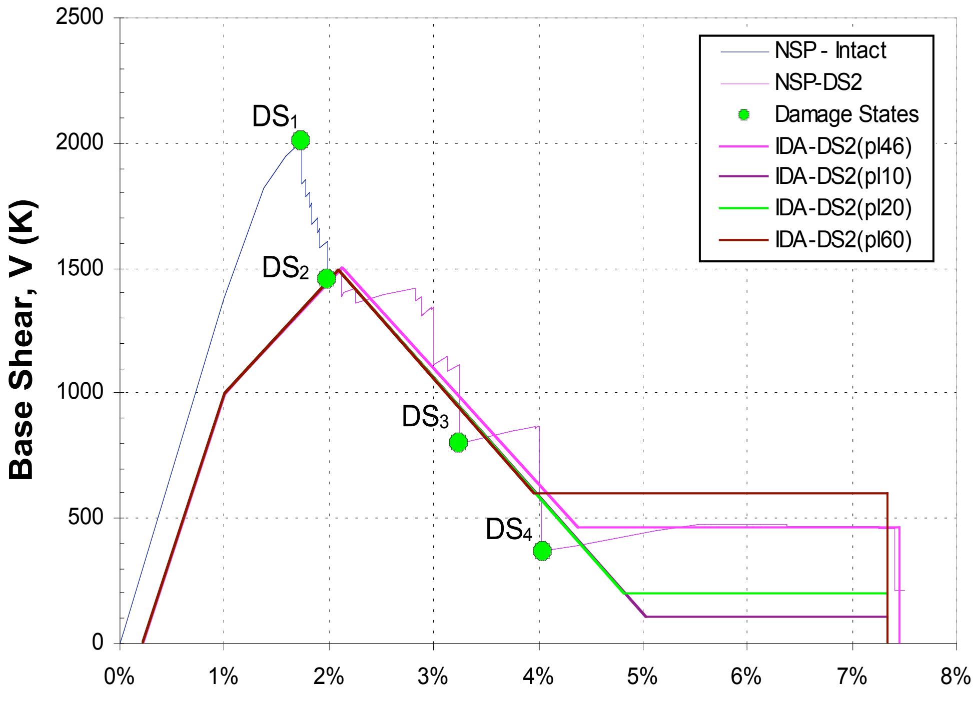


**Figure 3-6:** **Pushover curves for damage state2, with different estimates of post-fracture plateau strength**

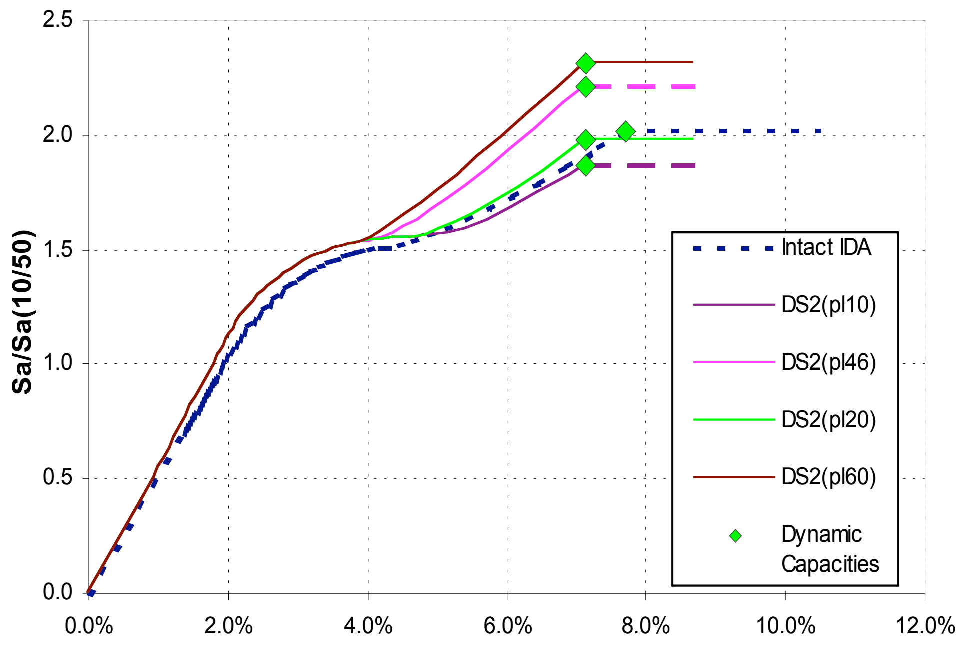


**Figure 3-7:** **Incremental dynamic analysis(IDA) results as influenced by post-fracture plateau strength**

# 4. Test Application 2: Mill Building

## 4.1. Description of the Structure

The second example is a substation building designed in 1921, of a type referred to as a mill building. The building has an open interior framed with exposed steel columns and trusses, which provide gravity support. The exterior walls of the building are cast-in-place concrete and provide the building's resistance to seismic forces.

The drawings that describe the original building, provided by PG&E, are listed in Table 4-xx. The building has a regular configuration with a rectangular plan measuring 94 feet by 42 feet, as shown in Figure 4-1. The building was designed so that a 37-foot-long addition could be constructed at each end, which would have increased the building size to 168 feet by 42 feet. The additions were never built. (New equipment at the substation has generally been added outdoors, so new building space was not needed.) Figure 4-2 shows the exterior and part of the interior of the building.

**Table 2 Construction drawings for example building 2.**

| Topic | Drawing Numbers | Date |
|---|---|---|
| Structural steel framing plans and details | 34768, 34769 | 8 October 1920 |
| Foundation plan | 34697 | 23 August 1921 |
| Plans, elevations, sections, and details | 34746–34754 | 17 September 1921 |
| Reinforcement plan for walls | 41179 | 24 September 1921 |

***Steel framing***

The left half of Figure 4-1 shown the steel framing that forms a hip roof. Roof trusses span across the short direction of the building and support hip trusses and 8-inch I-beam purlins. The truss members are typically double angles connected with gusset plates, stitch plates, and rivets. The rivets are ¾-inch diameter installed in 13/16" diameter holes. Most of the rivets are shop installed, which the drawings indicate with open circles. At the field splices of the steel assemblies, the drawings show filled circles to indicate field rivets.

The roof framing allows an open interior, with columns are on the building perimeter. Twelve main columns support the roof trusses. The columns are built-up sections approximately 10 inches square, consisting of a 10" x 5/16" web plate riveted to four 5" x 3½" x 5/16" angles. See Figure 4-2(c). Each column is has four anchor bolts at the base, 1" diameter by 2'-6" long. Three additional columns -- 8" wide-flange sections -- support the 15" deep I-beams at the north and south eaves of the building. Two columns are at the south end and one column is at the north end. These columns each have two anchor bolts.

At the east and west eaves, in the building longitudinal direction, trusses connect between the columns forming "sway frames". The end bays in the longitudinal direction also have angle bracing in a chevron configuration, with 2½" x 2" x ¼" single angles, as shown in Figure 4-

3. Along the ridge of the building, a "ridge sway frame" is created with trusses connecting between the building transverse trusses.

### *Foundation*

The building foundation consists of spread footings under each column, connected by a continuous 12" x 18"grade beam around the building perimeter.. The grade beam has longitudinal reinforcement consisting of four 7/8" square bars. The footings have tapered sides so that they form a truncated pyramid shape. No reinforcement is shown for the footings. There is a 4" slab on grade, presumably unreinforced and not connected to the foundation.

### *Roof*

The steel roof purlins support a 5" thick concrete roof slab reinforced with 4" x 16" #6/10 "Clinton Fabric" (i.e., welded wire reinforcement.) For gravity loads, the roof slab spans one way between purlins, apparently with 6-gage wires (area 0.029 in$^2$) at a 4-inch spacing parallel to the span, and 10 gage wires (area 0.014 in$^2$) at a 16-inch spacing perpendicular to the span. The roof is topped with clay tile, and two skylights in the western slope of the roof penetrate the 5" slab.

### *Walls*

The building's exterior walls are built of 6-inch-thick reinforced concrete. The reinforcement is specified as square "corrugated bars". The walls are typically reinforced with a single curtain of 3/8" square bars at a spacing of 12 inches in each direction. The walls connect to the perimeter grade beam with ½" x 3'-0" dowels at a 2'-0" spacing.

The concrete mix is specified as "1-2-4" apparently specifying the relative amounts of cement to sand to gravel. This indicates that cement represents 1/7, or 14%, of the total volume of dry ingredients. For comparison, in current construction a typical 5-sack mix with a design strength of 3000 psi contains cementitious material (cement plus flyash) that represents 9% of the total dry volume.

### *Connections between concrete and steel elements*

The apparent construction sequence of the structure was that the foundation was built, then the complete steel framing, then the concrete walls and roof. Portions of the steel framing, including the outer column flanges are embedded in the concrete walls. The inside face of the concrete wall is approximately flush with the inside of the outer column flange. The longitudinal trusses connect to each column at this outer flange, and thus one angle of each double-angle member is embedded in the concrete wall. The single-angle chevron braces are also embedded in the concrete wall. Because of the embedded steel members, we expect that there will be full composite action between the steel framing and the concrete walls, meaning that the steel members can be assumed to act like reinforcement in the walls.

### *1996 seismic retrofit*

The concrete mix is specified as "1-2-4" apparently indicating the ratio of cement to sand to gravel. This indicates that cement represents 1/7, or 14%, of the total volume of dry ingredients. For comparison, in current construction a typical 5-sack mix with a design strength of 3000 psi contains cementitious material (cement plus flyash) that represents 9% of the total dry volume.

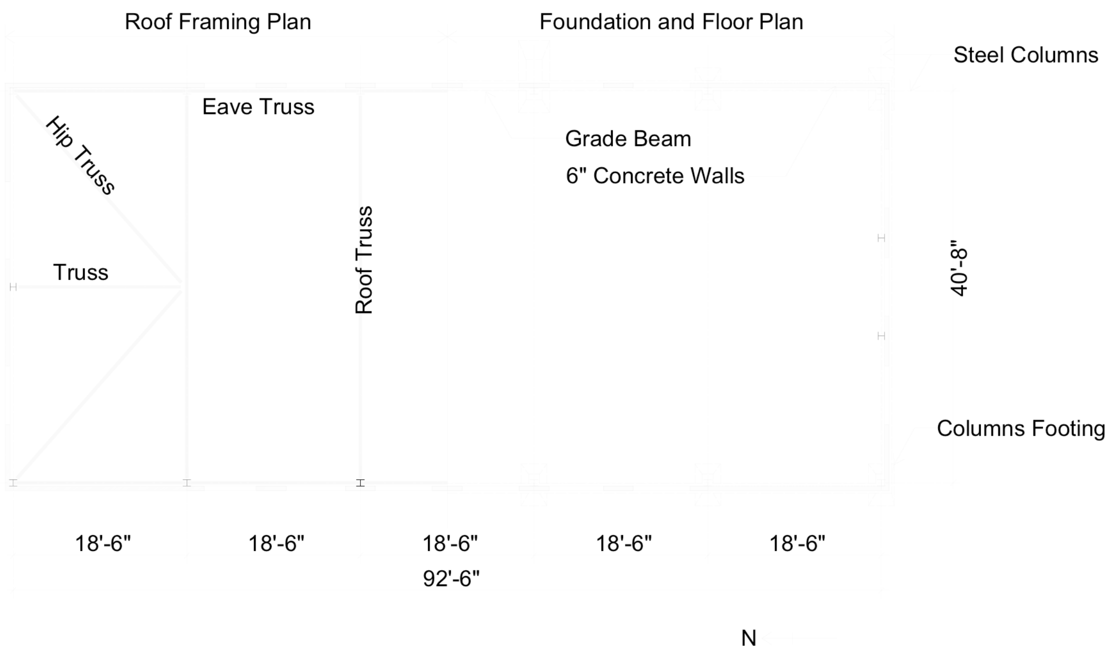


**Figure 4-1: Roof Framing, Foundation and Floor Plan of the building**


**Figure 4-2:** **Photos of the building: (a) Exterior. (b) Interior showing existing steel framing, added horizontal steel beam for wall out-or-plane support, and added steel members for roof diaphragm bracing. (c) Close up of existing steel column made up of four angles riveted to a web plate**

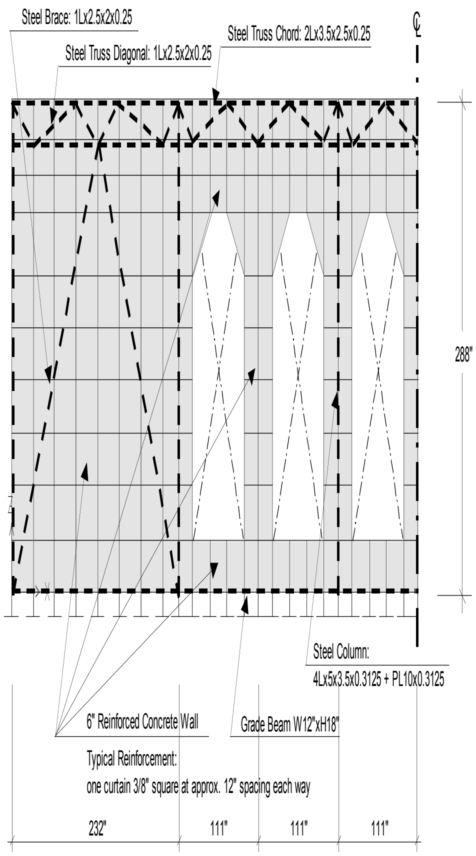


**Figure 4-3: Summary of structural design and dimensions (*RAM Perform* model)**

**Table 4-3: Assumed expected material strength properties (Year of construction =1921)**

| Material | Expected Strength | Basis |
|---|---|---|
| Structural Steel | $f_y$ = 30.8 ksi | From FEMA 356 tables 5-2 and 5-3: 28ksi*1.1 |
| Concrete | $f'_c$ = 3750 psi | From FEMA 356 tables 6-3 and 6-4: 2500psi*1.5 |
| Reinforcing Steel | $f_y$ = 41.3 ksi | From FEMA 356 tables 6-1 and 6-4: 33ksi*1.25 |

## 4.2. Seismic evaluation of the intact structure

**PG&E project: Pushover Analysis of Mill building**

**- Progress & Results-**

-Elastic model-

Model: SAP Planar shell element model on non-tension foundation
Weight (1/2 of bldg): 360(k)
Roof displacement(1g): 0.054(in)
Stiffness: 6679(k/in)
Period: 0.074(sec)
f'c: 3750(psi)
fy: 30.8(ksi)

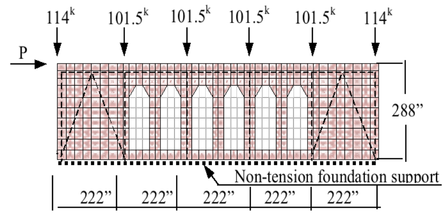


-Hand Calculations for strength-

A) Concrete wall pier without steel column (3 total):
- DL assuming concrete wall pier taken roof load = 23.0(k)
- $M_{CR}$(cracking strength) = 715(k-in)
- Mn(flexural strength at DL=23.0k) = 59(k-ft)= 710(k-in)
- V*(shear corresponding to Mn) = 28.1(k)
- Shear strength in diagonal tension (DL=33.8k):
  - Low ductility = 38.0(k)
  - High ductility = 20.4(k)
- Sliding shear strength = 23.4(k)
- $(Ec)_{eff} = (EI)_{eff} / I_{gross}$ = 589(ksi)→0.3EcIg

B) Concrete wall pier with steel column (2 total):
- DL assuming concrete wall pier taken roof load = 50.0(k)
- Mn(flexural strength at DL=50.0k) = 307(k-ft)= 3680(k-in)
- V*(shear corresponding to Mn) = 45.5(k)
- Shear strength in diagonal tension (DL=33.8k):
  - Low ductility = 82.0(k)
  - High ductility = 25.8(k)
- Sliding shear strength = 152(k) (limit 650psi)
- $(Ec)_{eff} = (EI)_{eff} / I_{gross}$ = 1880(ksi)→0.6EcIg

C) Concrete wall segment 20'-long with steel column and brace:
- DL assuming concrete wall pier taken roof load = 81.4(k)
- Mn(flexural strength at DL=81.4k) = 9320(k-ft)= 112000(k-in)
- V*(shear corresponding to Mn) = 1380(k)
- Shear strength in diagonal tension (DL=81.4k):
  - Low ductility = 535(k)
  - High ductility = 248(k)
- Shear strength in diagonal tension (Ne=146k ):
  - Low ductility = 650(k)
  - High ductility = 364(k)
- Shear strength in diagonal tension (Ne=-117k ):
  - Low ductility = 443(k)
  - High ductility = 156(k)
- Sliding shear strength = 936(k) (limit 650psi)
- $(Ec)_{eff} = (EI)_{eff} / I_{gross}$ = 0.6EcIg
- First foundation uplift = 48.6(k)
- Uplift of entire end wall = 113, 369(k)

D) Concrete roof diaphragm (5"):
At a section through skylights
- Shear strength in diagonal tension:
  - Low ductility = 580(k)
  - High ductility = 177(k)
- Sliding shear strength = 679(k)
- Diaphragm shear demand at 1g lateral force = 116(k)

At Wall
- Shear strength in diagonal tension:
  - Low ductility = 1090(k)
  - High ductility = 331(k)
- Sliding shear strength = 1272(k)
- Diaphragm shear demand at 1g lateral force = 296(k)

E) Concrete spandrel (6"):
- Shear strength in diagonal tension:
  - Low ductility = 130(k)
  - High ductility = 55.5(k)
- Sliding shear strength = 257(k) (limit 650psi)
- Flexural strength(Mu) = 14840, 5770(k-in)
- $V_{Mu}$ = 286(k)

**Figure 4-4: Summary of dead load and strength calculation for the mill-building example**

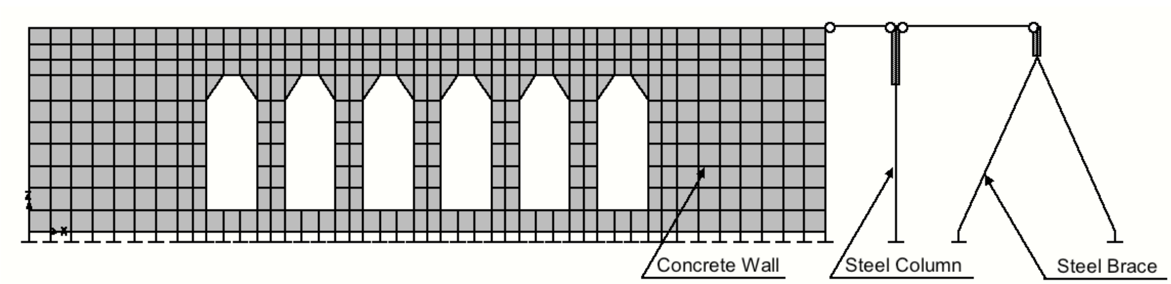


**Figure 4-5:** ***SAP*** **pushover model**

**Force Distribution on Non-tension foundations**

| | Case | Lateral load at zero uplift | Δ(in) Kn(k/in) | Force distribution(kip) EW1 | EW2 | WP1 | WP2 | WP3 | WP4 | WP5 | Shear force(kip) SP1 | SP2 | SP3 | SP4 | SP5 |
|---|---|---|---|---|---|---|---|---|---|---|---|---|---|---|---|
| A | Fixed Foundation | 360k(1.0g) (100%) | 0.054 (6679) | 169 (47%) | 169 (47%) | 3.4 (0.9%) | 6.1 (1.7%) | 3.4 (0.9%) | 6.1 (1.7%) | 3.4 (0.9%) | 34.8 | 9.7 | 8.0 | 8.0 | 9.7 |
| B | Non-tension 1st Fndn uplift @EW1 | 376k (100%) | 0.063 (5997) | 168 (44%) | 183 (47%) | 4.0 (1.8%) | 6.3 (1.7%) | 3.9 (1.7%) | 6.5 (1.7%) | 4.0 (1.8%) | 37.1 | 9.7 | 9.5 | 8.4 | 11.4 |
| C | Non-tension Fndn uplift @EW1 & 1st uplift @EW2 | 587k (100%) | 0.111 (4340) | 233 (40%) | 311 (53%) | 7.1 (1.2%) | 10.9 (1.9%) | 6.7 (1.1%) | 10.9 (1.9%) | 7.1 (1.2%) | 57.1 | 15.0 | 17.7 | 13.4 | 20.5 |
| D | 1st Flexural hinge @WP1,3,5 | 700k (100%) | 0.139 (4026) | 271 (39%) | 375 (54%) | 8.9 (1.3%) | 13.6 (1.9%) | 8.3 (1.2%) | 13.6 (1.9%) | 9.1 (1.3%) | 68.7 | 17.9 | 22.6 | 16.2 | 26.4 |
| E | 1st Shear failure @EW2 | 1146k (100%) | 0.256 (3835) | 416 (36%) | 632 (55%) | 17.0 (1.5%) | 24.6 (2.2%) | 14.1 (1.2%) | 24.4 (2.1%) | 17.6 (1.5%) | 116.7 | 34.5 | 38.4 | 25.5 | 51.1 |
| F | Max load assuming no element yielding | 1174k (100%) | 0.372 (242) | 421 (36%) | 653 (56%) | 17.6 (1.5%) | 24.9 (2.1%) | 14.2 (1.2%) | 24.7 (2.1%) | 18.2 (1.5%) | 151.3 | 20.3 | 38.2 | 5.1 | 21.5 |

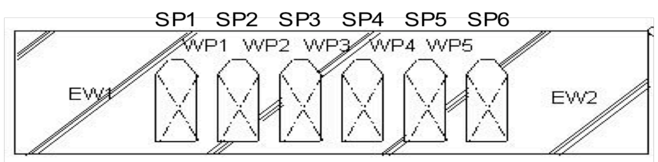


**Fig. Analysis model**

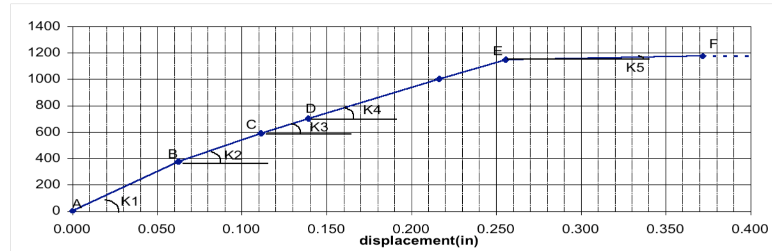


**Fig. P - Δ relationship**

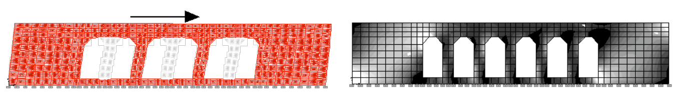

**A. Fixed Foundation**

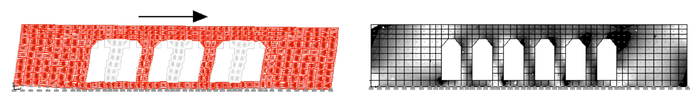

**D. 1st Flexural hinge @WP1,3,5**

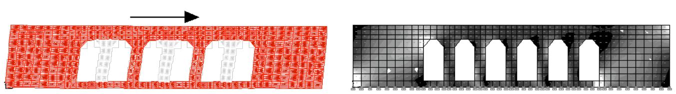

**B. Non-tension 1st Fndn uplift @EW1**

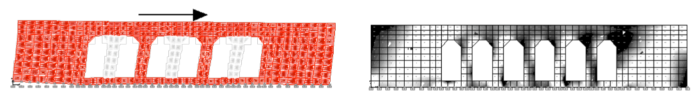

**E. 1st Shear failure @EW2**

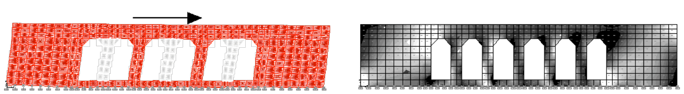

**C. Non-tension Fndn uplift @EW1 & 1st uplift @EW2**

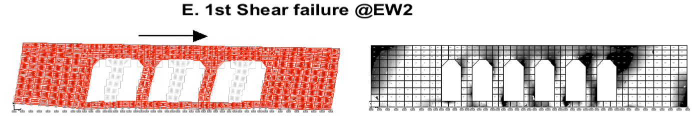

**F. Max load assuming no element yielding**

**Fig. Deformation and stress**

**Figure 4-6: Pushover curve developed from linear *SAP* model, neglects spandrel degradation**

**Reaction force of Non-tension foundations**

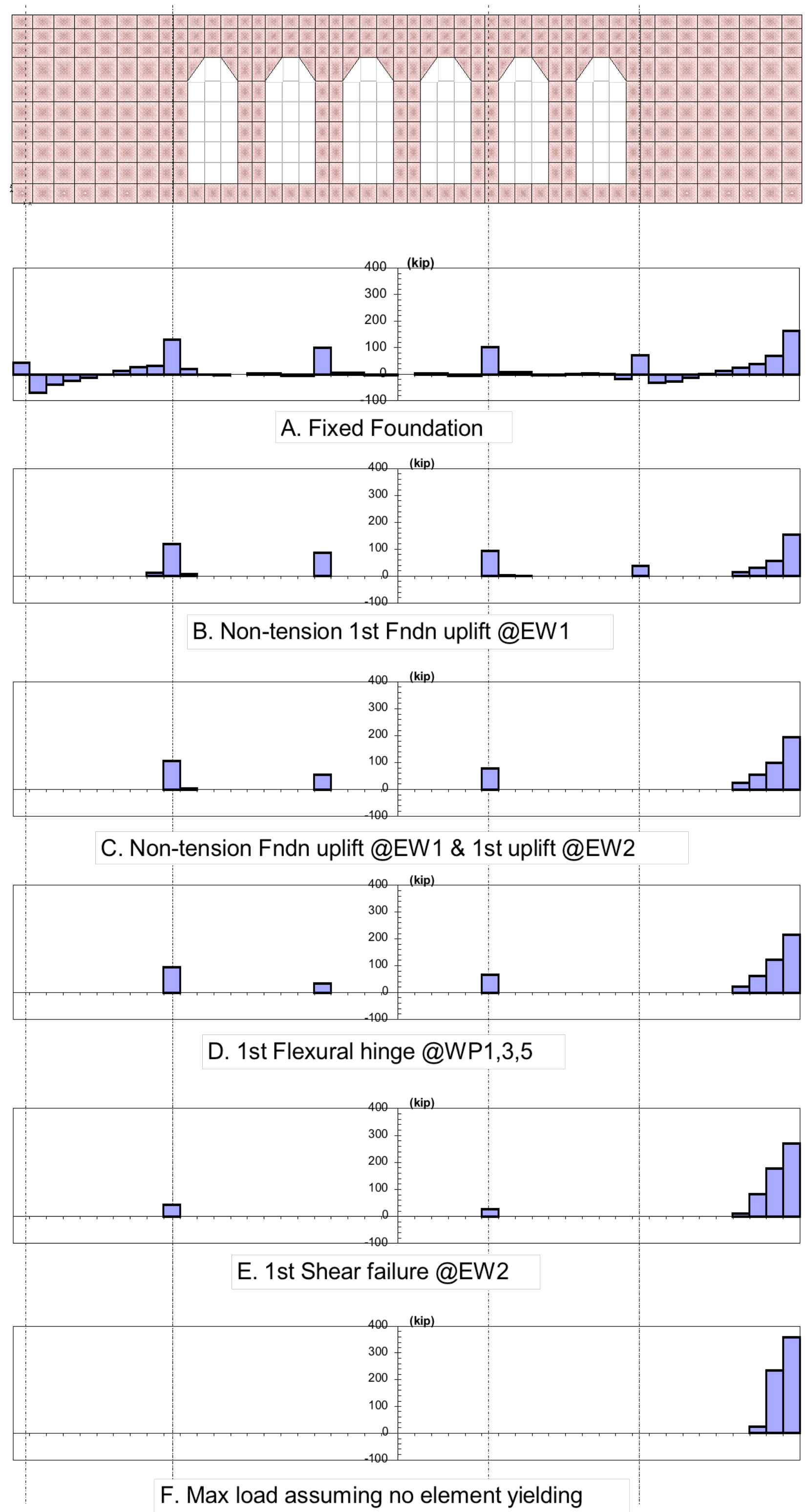


**Figure 4-7: Foundation reaction forces from *SAP* model**

**Table 4-4: Concrete wall *RAM Perform* [2004] input properties**

| | |
|---|---|
| Reinforcing Steel | $K_0$ = 29,000 ksi (= $E_s$)<br>$F_U$ = 41.3 ksi (= $f_y$) |
| Inelastic Concrete Material | $K_0$ = 3,491 ksi (= $E_c$)<br>$F_U$ = 3.75 ksi (= $f'_c$)<br>$D_L$ = 0.003<br>$D_R$ = 0.006<br>$F_R/F_U$ = 0.2 |
| Inelastic Shear Material | $K_0$ = 580 ksi(= $G_{eff} = 0.17E_c = 10\rho E_s$)<br>$F_U$ = 0.75 ksi (= $12.2\sqrt{f'_c}$)<br>$D_L$ = 0.0075 (□ = 5.8)<br>$D_R$ = 0.0085 (□ = 6.6)<br>$F_R/F_U$ = 0.4 |
| Diagonal Compression Material | Same as inelastic concrete material |

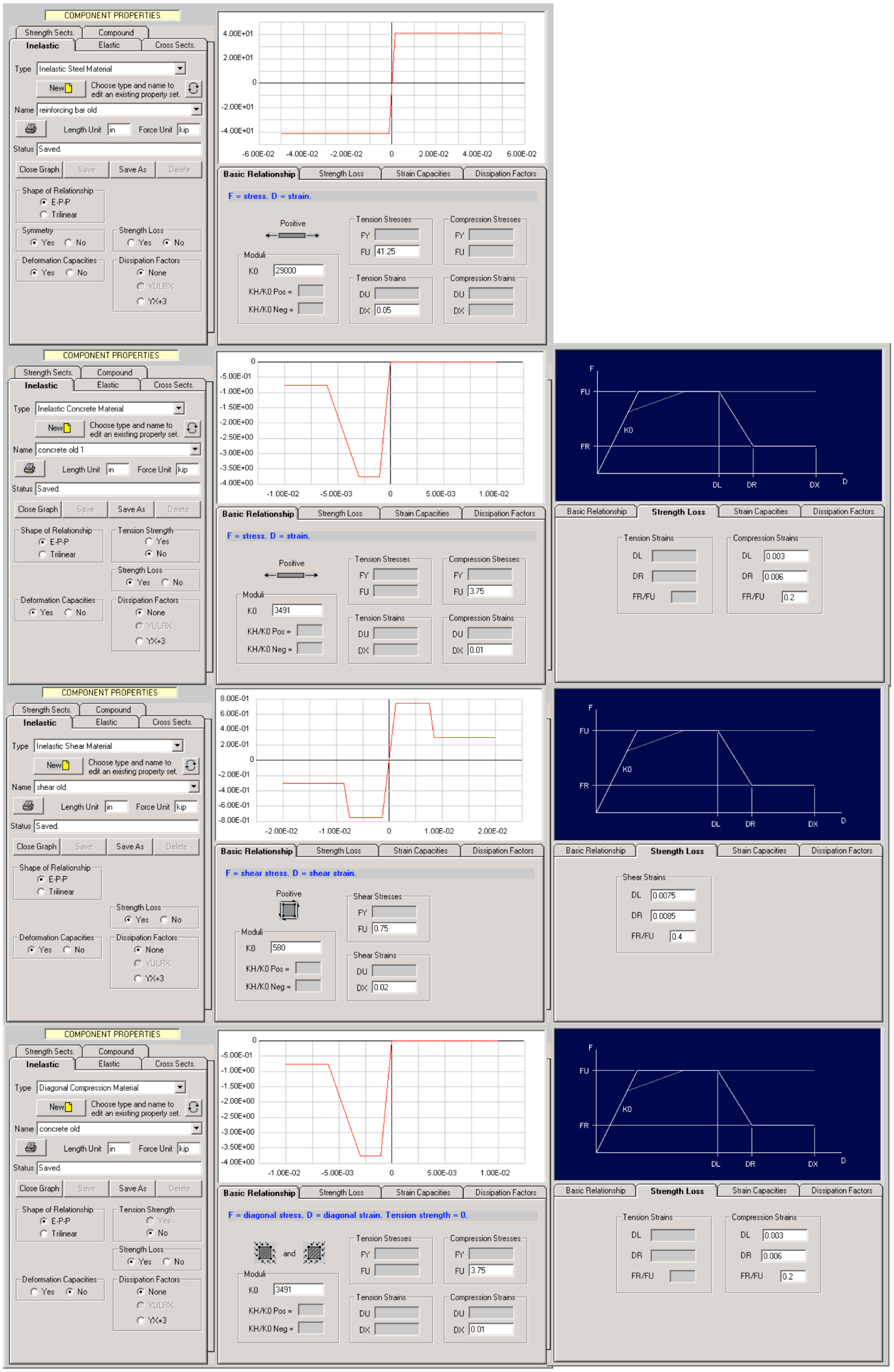
COMPONENT PROPERTIES
Strength Sects.
Compound
Inelastic
Elastic
Cross Sects.
Type Inelastic Steel Material
New
Choose type and name to edit an existing property set.
Name reinforcing bar old
Length Unit in
Force Unit kip
Status Saved
Close Graph
Save
Save As
Delete
Shape of Relationship
E-P-P
Trilinear
Symmetry
Yes
No
Strength Loss
Deformation Capacities
Dissipation Factors
None
YULRX
YX+3
Basic Relationship
Strength Loss
Strain Capacities
Dissipation Factors
F = stress, D = strain.
Positive
Moduli
K0 29000
KH/K0 Pos =
KH/K0 Neg =
Tension Stresses
FY
FU 41.25
Compression Stresses
Tension Strains
DU
DX 0.05
Compression Strains
Type Inelastic Concrete Material
Name concrete old 1
Tension Strength
K0 3491
FU 3.75
DX 0.01
Tension Strains
DL
DR
FR/FU
Compression Strains
DL 0.003
DR 0.006
FR/FU 0.2
F
FU
FR
K0
D
Type Inelastic Shear Material
Name shear old
F = shear stress, D = shear strain.
K0 580
Shear Stresses
FU 0.75
Shear Strains
DX 0.02
DL 0.0075
DR 0.0085
FR/FU 0.4
Type Diagonal Compression Material
Name concrete old
F = diagonal stress, D = diagonal strain. Tension strength = 0.
and
K0 3491
FU 3.75
DX 0.01
DL 0.003
DR 0.006
FR/FU 0.2

**Figure 4-8: *Ram Perform* Input Properties for the Intact Structure**

(a)

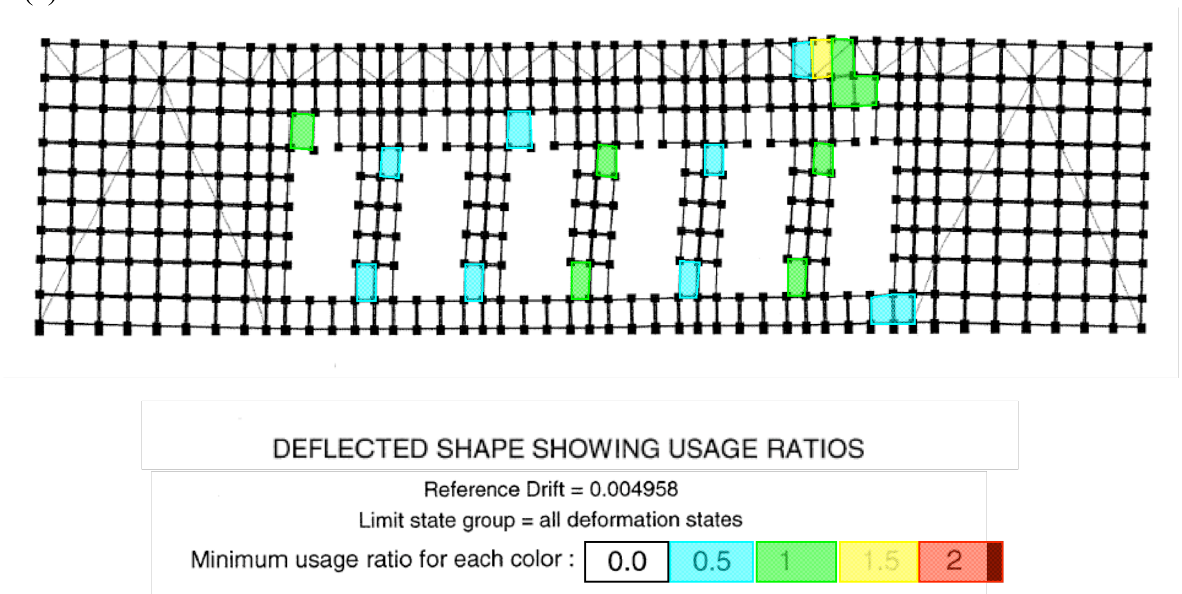


(b)

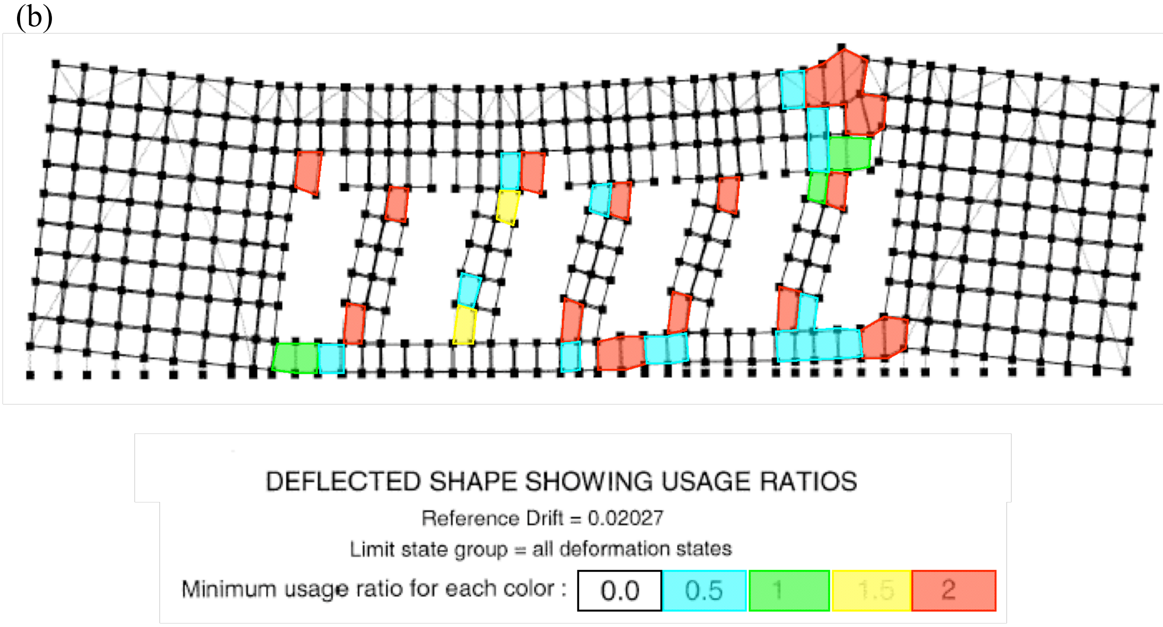


**Figure 4-9:** **Non linear finite element model using *RAM Perform* at (a) 0.5% Roof Drift and (b) 2.0% Roof Drift**

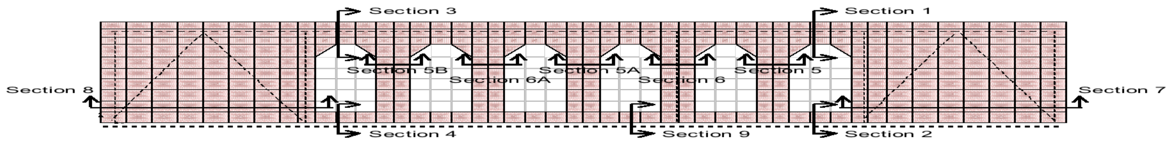


| Stractural Member | Structure Section | Governed by | Hand Calc | Peak Value from Ram Perform | | | | Roof Drift when Peak Occurs |
|---|---|---|---|---|---|---|---|---|
| Peak Vertical Capacity of Roof Spandrel | Section 1 | Shear Strength in Diagonal Tension | 130 k | 210 k | | | | 0.30% |
| Peak Vertical Capacity of Floor Spandrel | Section 2 | - | - | 149 k | | | | 0.90% |
| Peak Vertical Capacity of Roof Spandrel | Section 3 | Shear Strength in Diagonal Tension | 130 k | 176 k | | | | 0.80% |
| Peak Vertical Capacity of Floor Spandrel | Section 4 | - | - | 78 k | | | | 0.37% |
| Peak Lateral Capcity of Wall Pier without Steel Column | Section 5 | Flexure (Mn) at top and bottom | 28 k | Horiz ontal | 41 k | Vertic al | 158 k | 0.83% |
| | Section 5A | | | | 40 k | | 145 k | 0.73% |
| | Section 5B | | | | 50 k | | 196 k | 0.80% |
| Peak Lateral Capcity of Wall Pier with Steel Column | Section 6 | Flexure (Mn) at top and bottom | 45 k | 61 k | | | | 0.45% |
| | Section 6A | | | 65 k | | | | 0.63% |
| Peak Lateral Capcity of End Wall | Section 7 | Foundation Uplift | 369 k | 571 k | | | | 0.31% |
| Peak Lateral Capcity of End Wall | Section 8 | Foundation Uplift | 113 k | 192 k | | | | 0.32% |

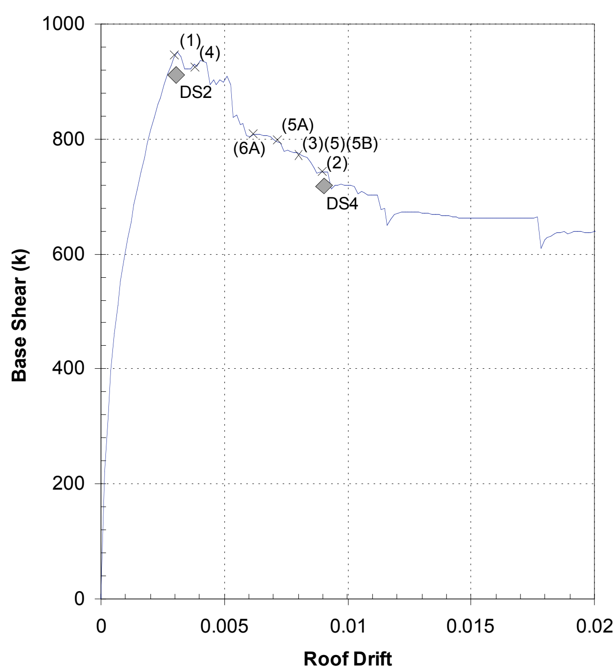

**Figure 4-10: Forces at key structure section cuts, by computer analysis and hand calculation, and points on the pushover curve when peak strength of each section is reached**

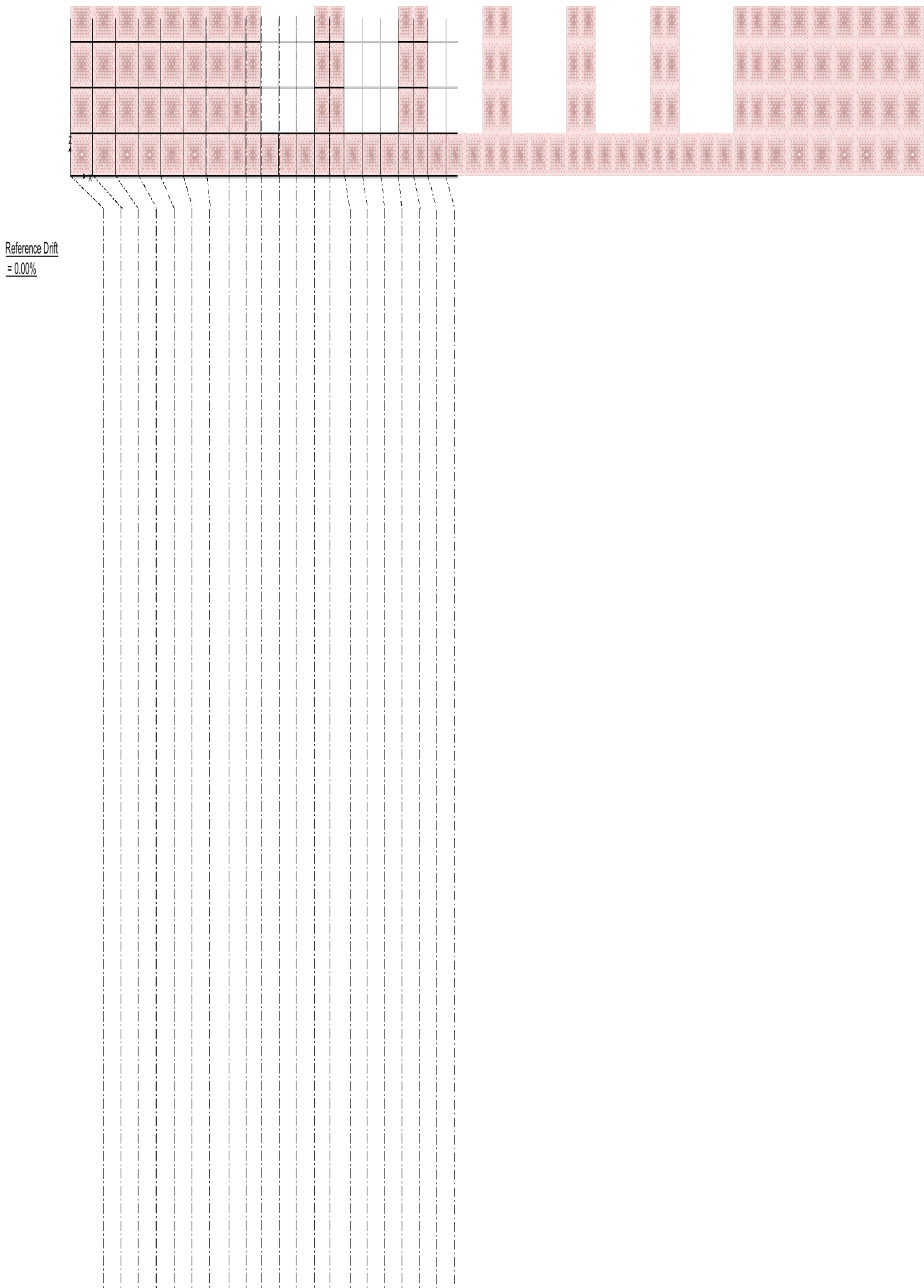

**Figure 4-11: Foundation reaction forces from RAM Perform pushover model**

## 4.3. Seismic evaluation of the damaged structure

**Table 4-5: Modeling of each damage state in *RAM Perform***

| Damage State | Roof Drift | Components modeled with damaged properties |
|---|---|---|
| Intact | 0 | None |
| DS2 | 0.3 % | Section 1: Spandrel |
| DS4 | 0.9 % | Section 1: Spandrel<br>Section 2: Grade Beam<br>Section 3: Spandrel<br>Section 4: Grade Beam<br>Section 5, 5A, 5B: Wall Pier without Steel Column<br>Section 6, 6A: Wall Pier with Steel Column<br>Section 9: Grade Beam |

**Table 4-6: Assumed fundamental period of vibration**

| Damage State | Roof Drift at 400kips Lateral Load | Stiffness/Intact | T (sec) |
|---|---|---|---|
| Intact | 0.040% | 1.00 | 0.20 |
| DS2 | 0.054% | 0.74 | 0.23 |
| DS4 | 0.069% | 0.58 | 0.26 |

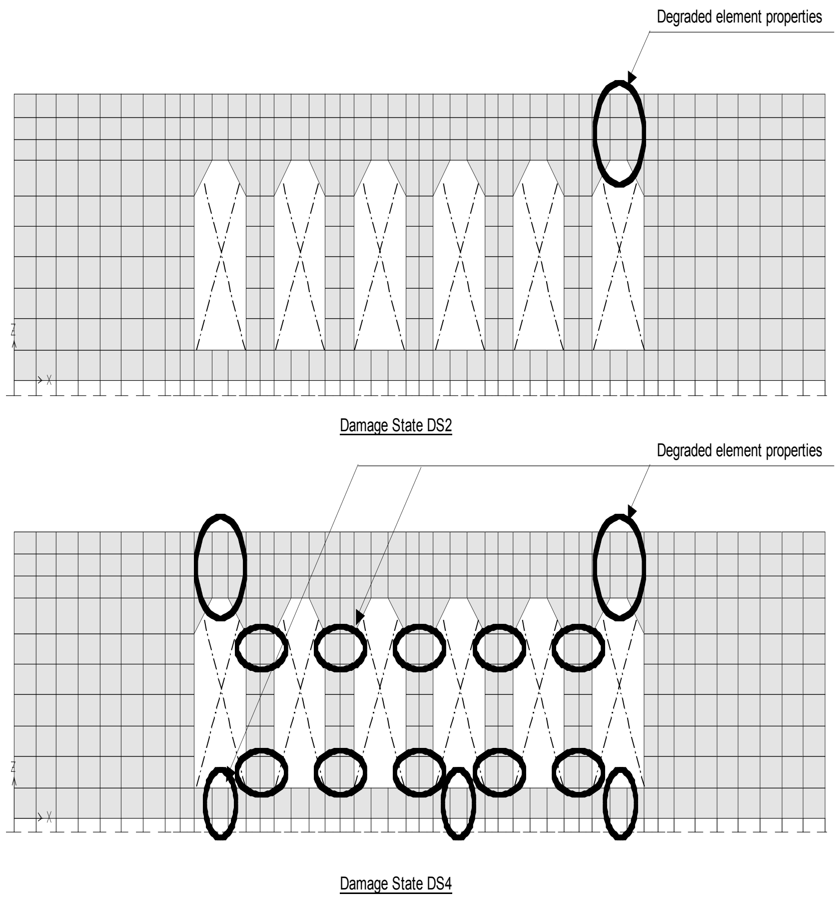


**Figure 4-12: Modeling of each damage state**

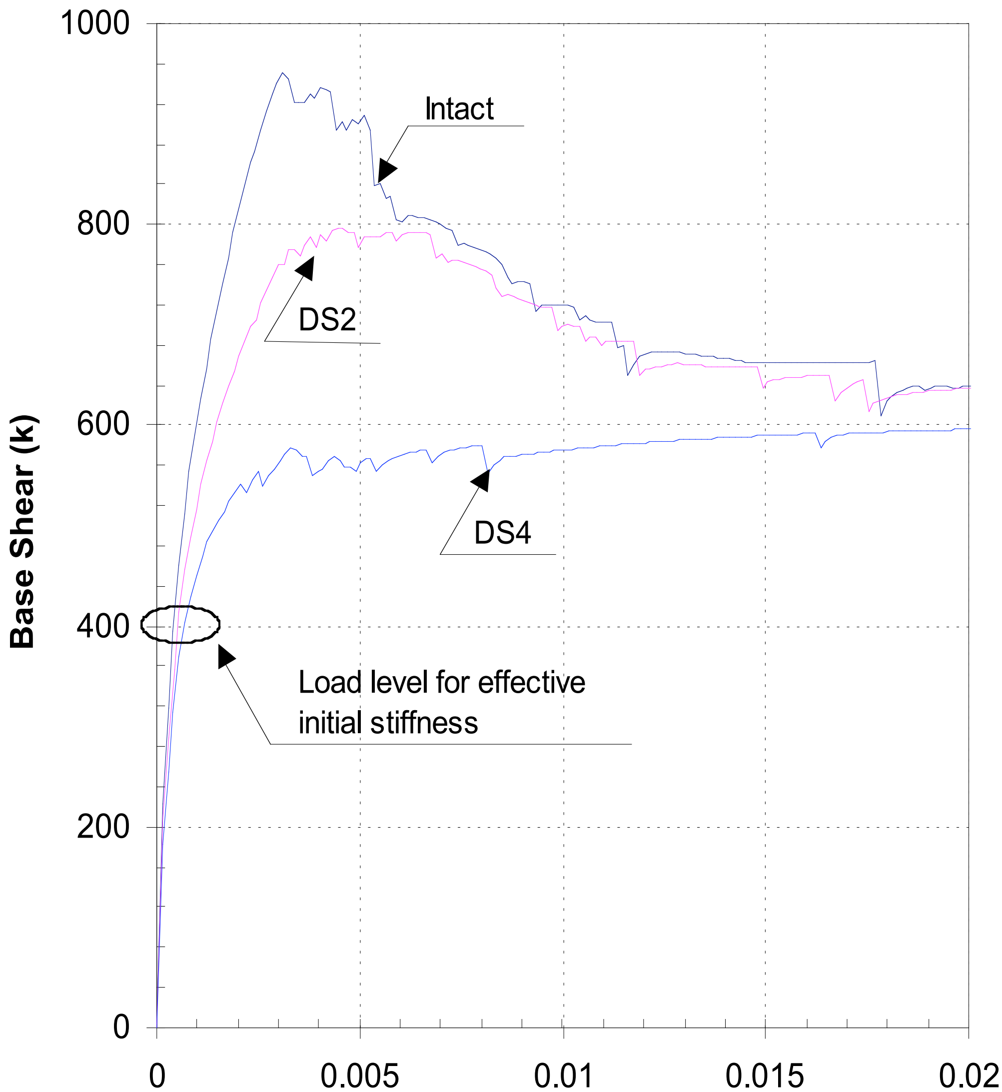


**Figure 4-13: Pushover curves for Intact structure and structure previously damaged to damage state DS2 and DS4**

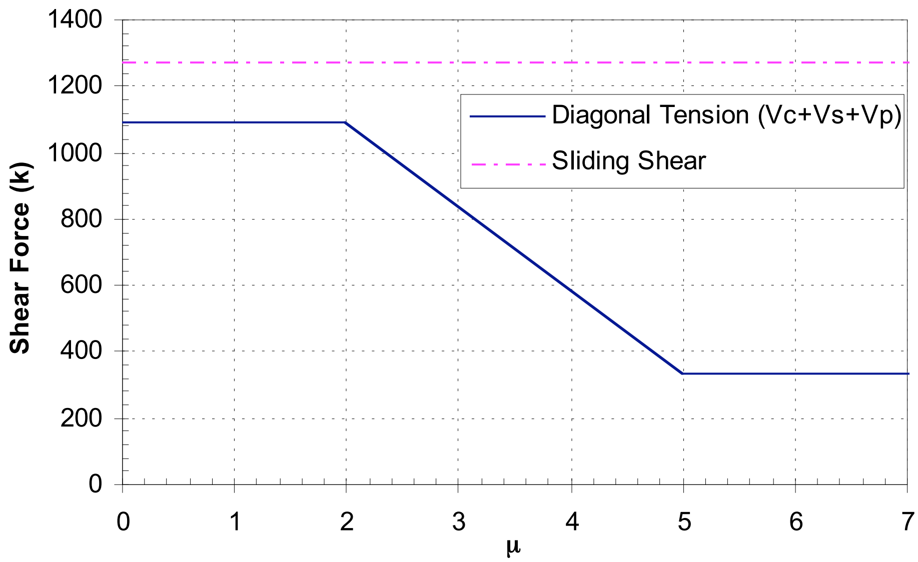


**Figure 4-14: Concrete shear strength behavior by FEMA 306**

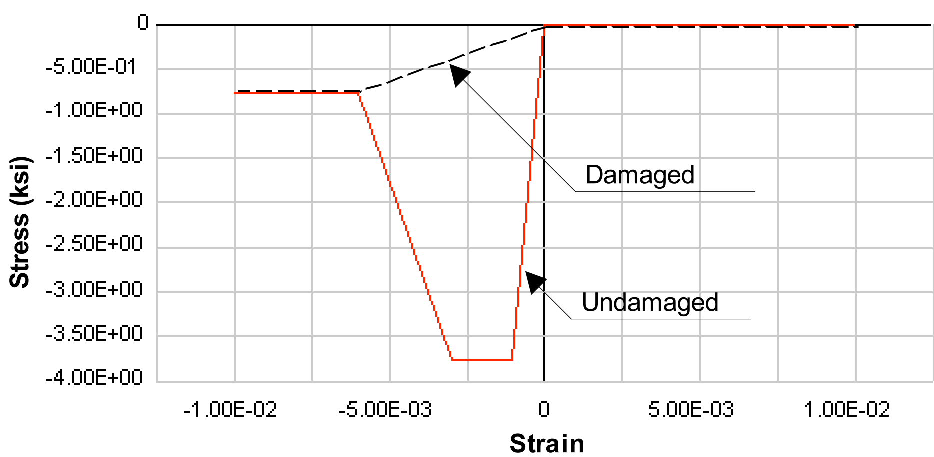


**Figure 4-15: Component material properties in *RAM Perform* for undamaged and damaged concrete**

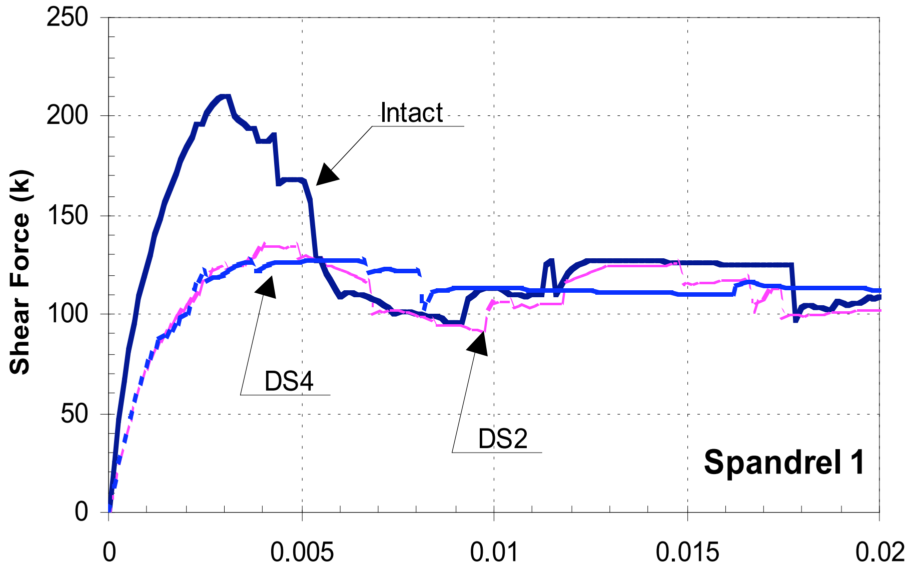


**Figure 4-16: Spandrel 1 section strength for Intact structure and damaged structures DS2 and DS4**

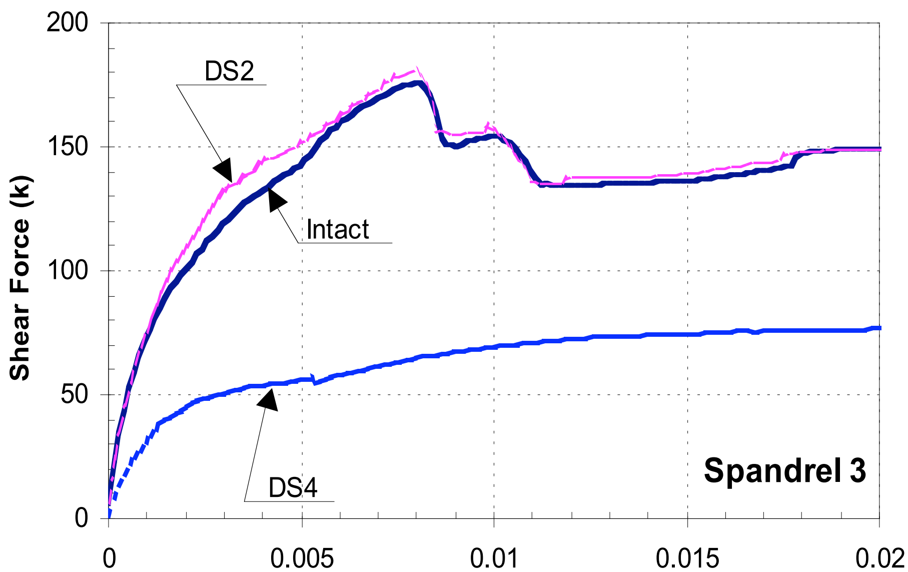


**Figure 4-17: Spandrel 3 section strength for Intact structure and damaged structures DS2 and DS4**

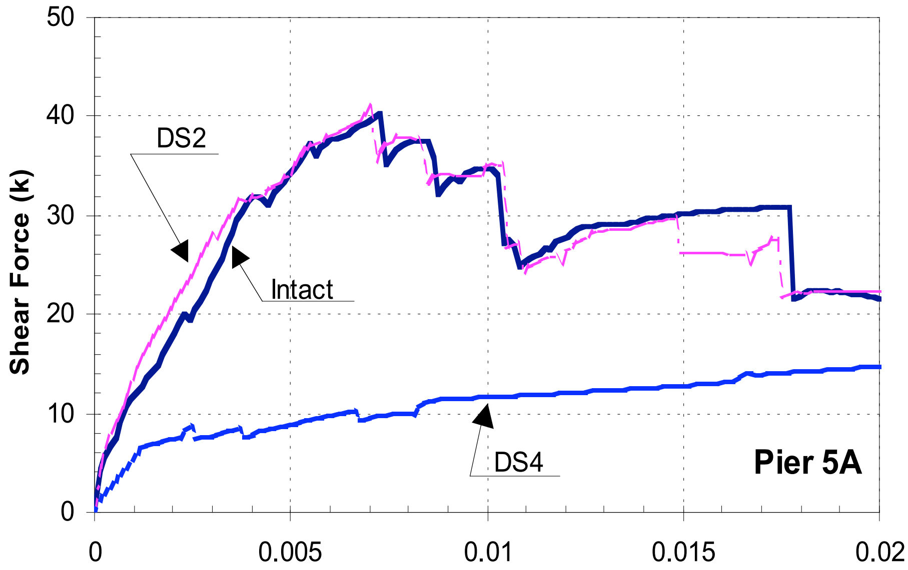


**Figure 4-18:** **Pier 5A section strength for Intact structure and damaged structures DS2 and DS4**

## *4.4. Inferred dynamic behavior (SPO2IDA)*

**Table 4-7:** **SPO2IDA Input**

| Damage State | Yield Point | | Peak Strength | | Beginning of Plateau | | SPO2IDA Input | | | | | Period T |
|---|---|---|---|---|---|---|---|---|---|---|---|---|
| | Roof Drift | V/W | Roof Drift | V/W | Roof Drift | V/W | Hardening □ | Hardening Slope | Softening Slope | Residual Plateau | Fracturing □ | |
| Intact | 0.0013 | 1.97 | 0.0035 | 2.62 | 0.0116 | 1.83 | 2.7 | 19.5% | -6.4% | 0.93 | 23.1 | 0.2 |
| DS2 | 0.0015 | 1.88 | 0.0054 | 2.24 | 0.0120 | 1.78 | 3.6 | 7.4% | -5.6% | 0.95 | 20.0 | 0.23 |
| DS4 | 0.0012 | 1.43 | 0.0100 | 1.63 | 0.0200 | 1.63 | 8.3 | 1.9% | 0.0% | 1.14 | 25.0 | 0.26 |

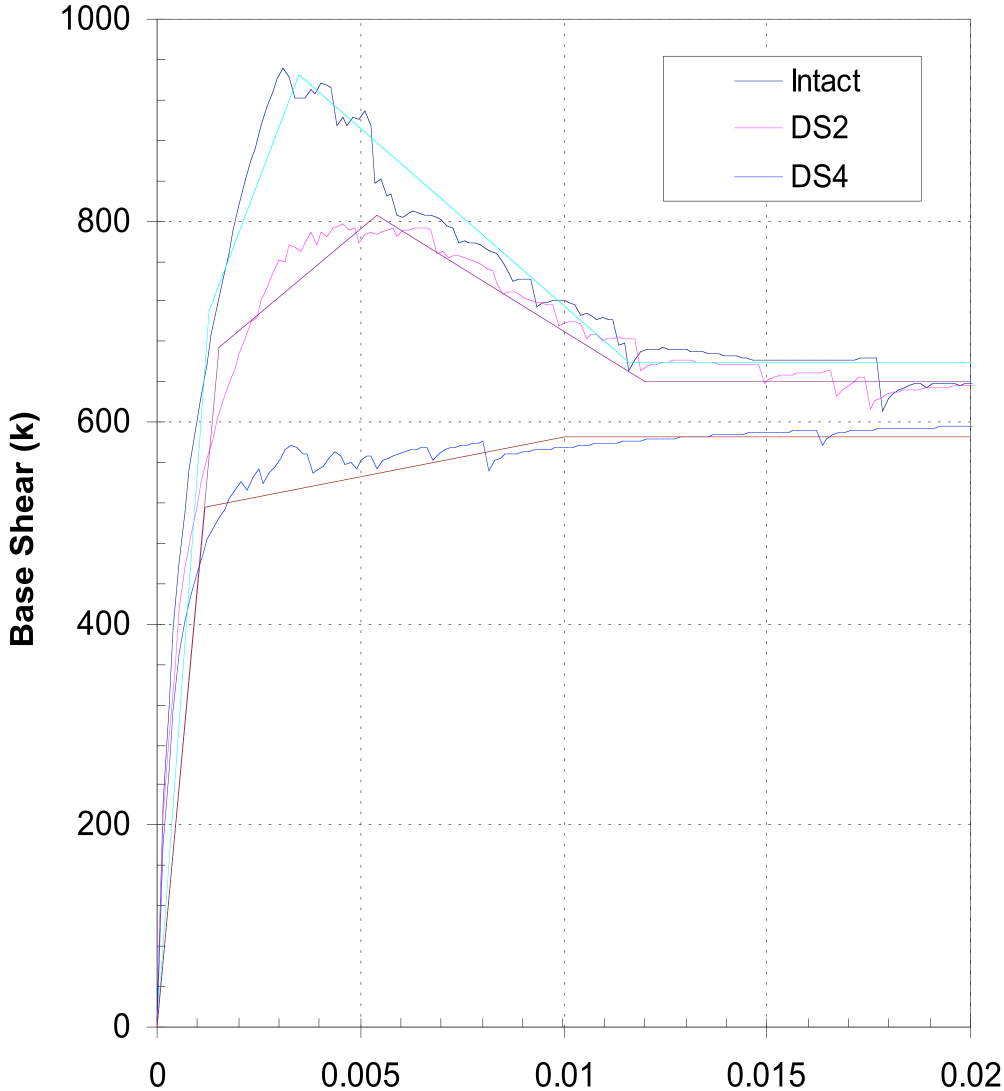


**Figure 4-19: Pushover curves and linear approximations**

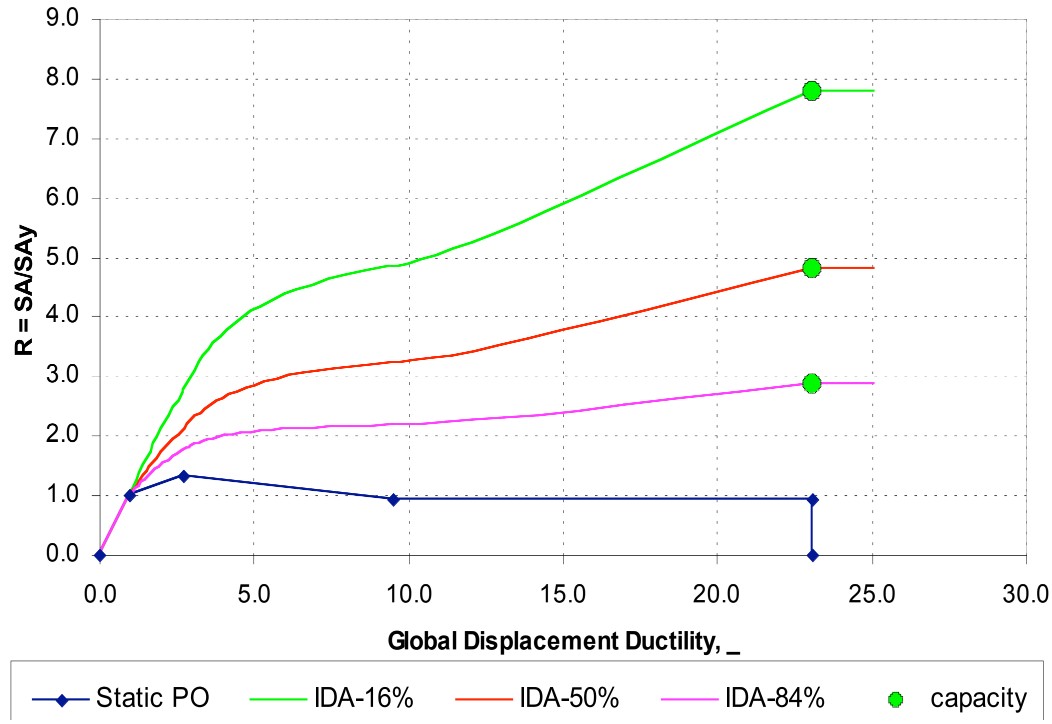


**Figure 4-20:** **SPO2IDA Intact (R vs. )**

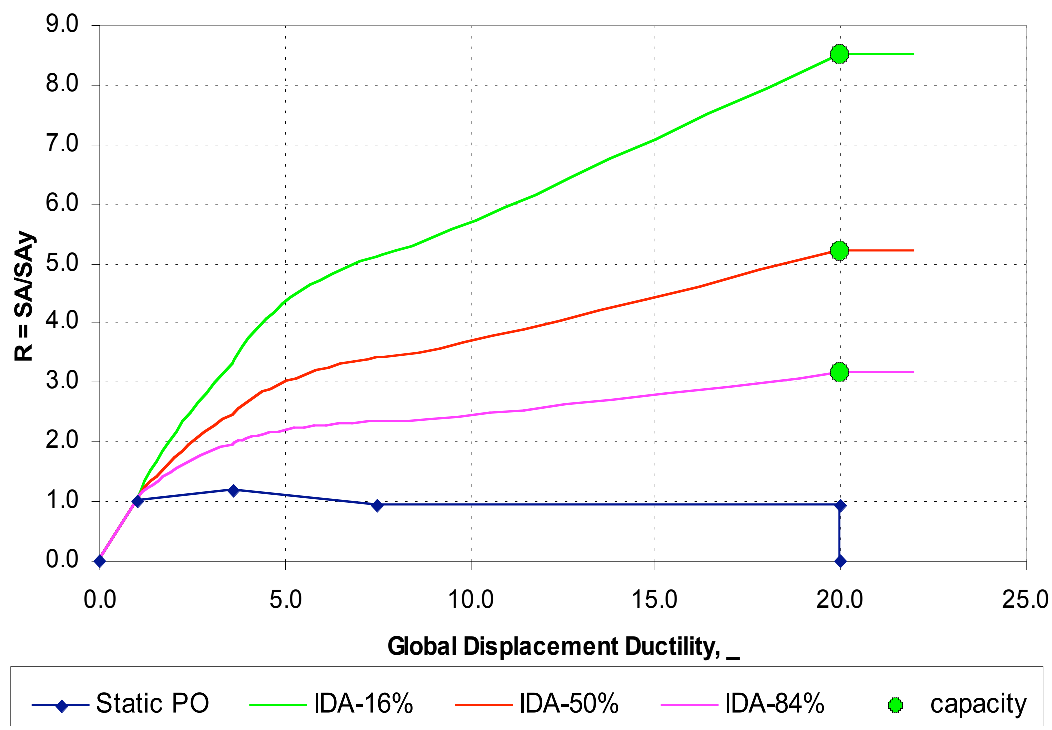


**Figure 4-21:** **SPO2IDA DS2 (R vs. )**

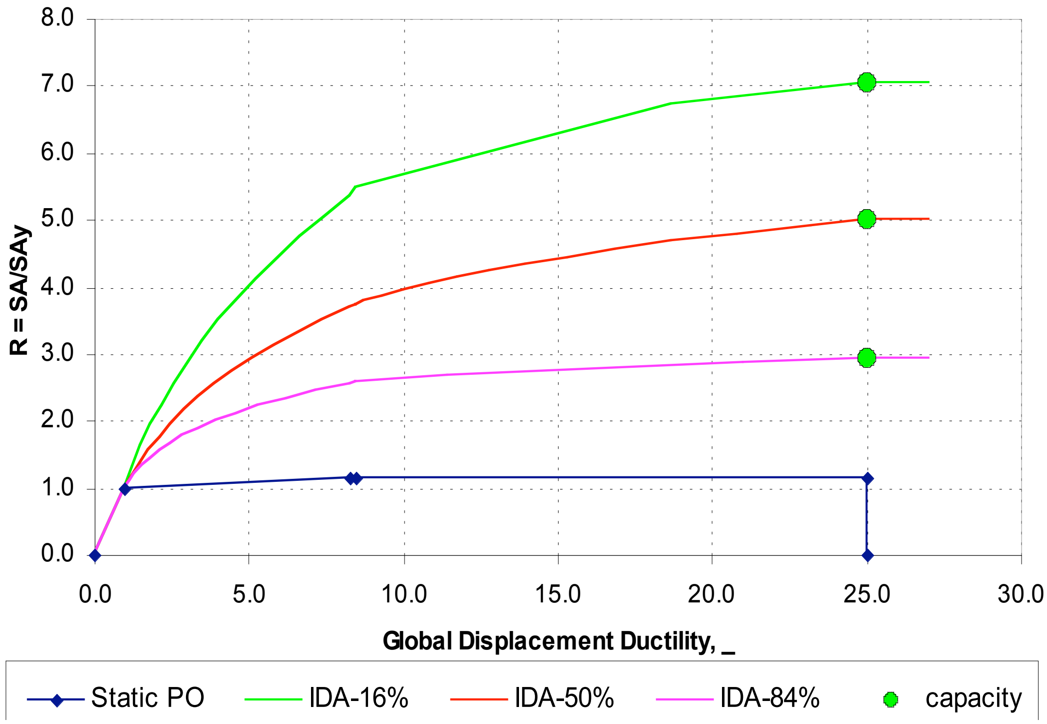


**Figure 4-22:** **SPO2IDA DS4 (R vs. )**

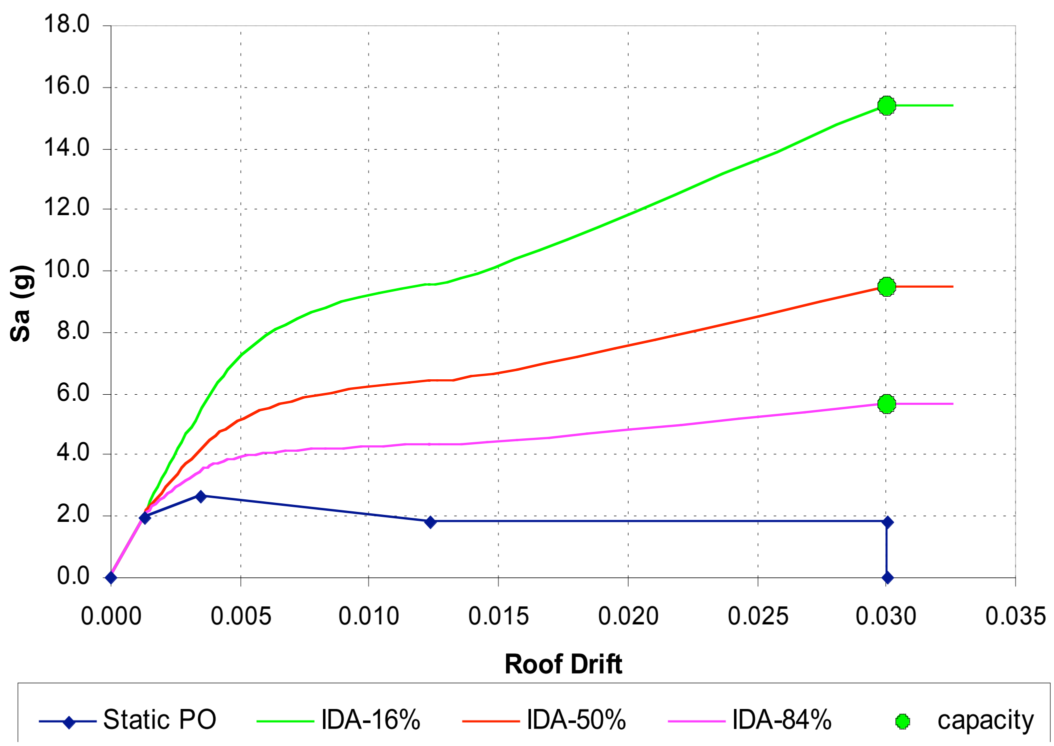


**Figure 4-23:** **SPO2IDA Intact (Sa vs. Roof drift)**

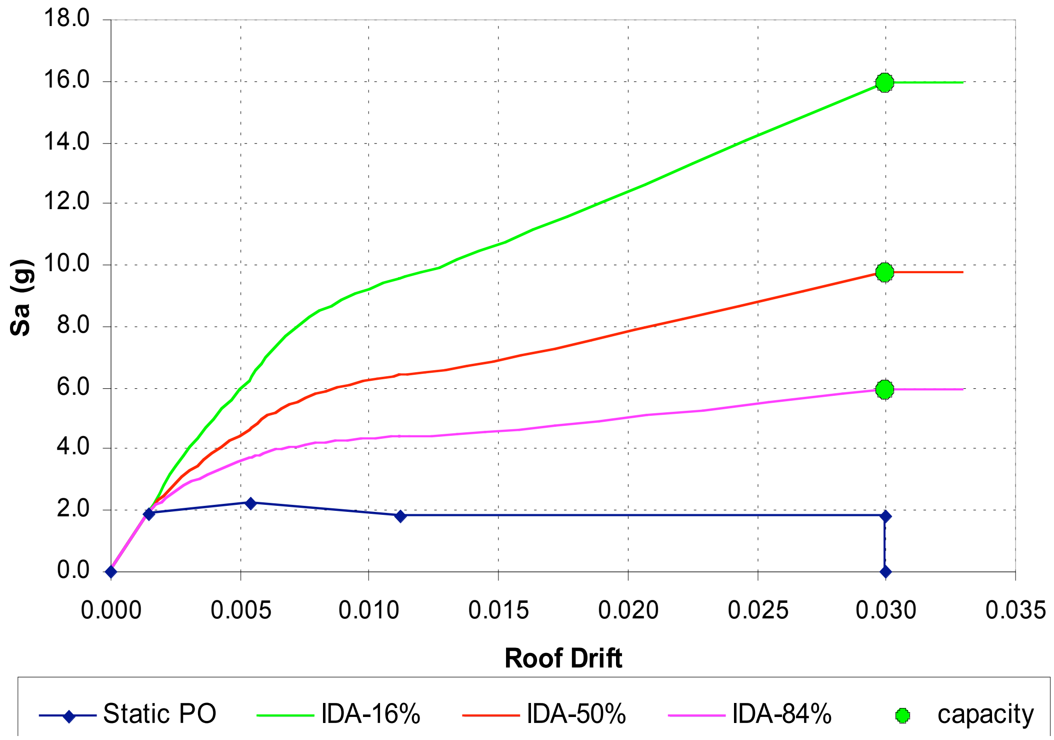


**Figure 4-24:** **SPO2IDA DS2 (Sa vs. Roof drift)**

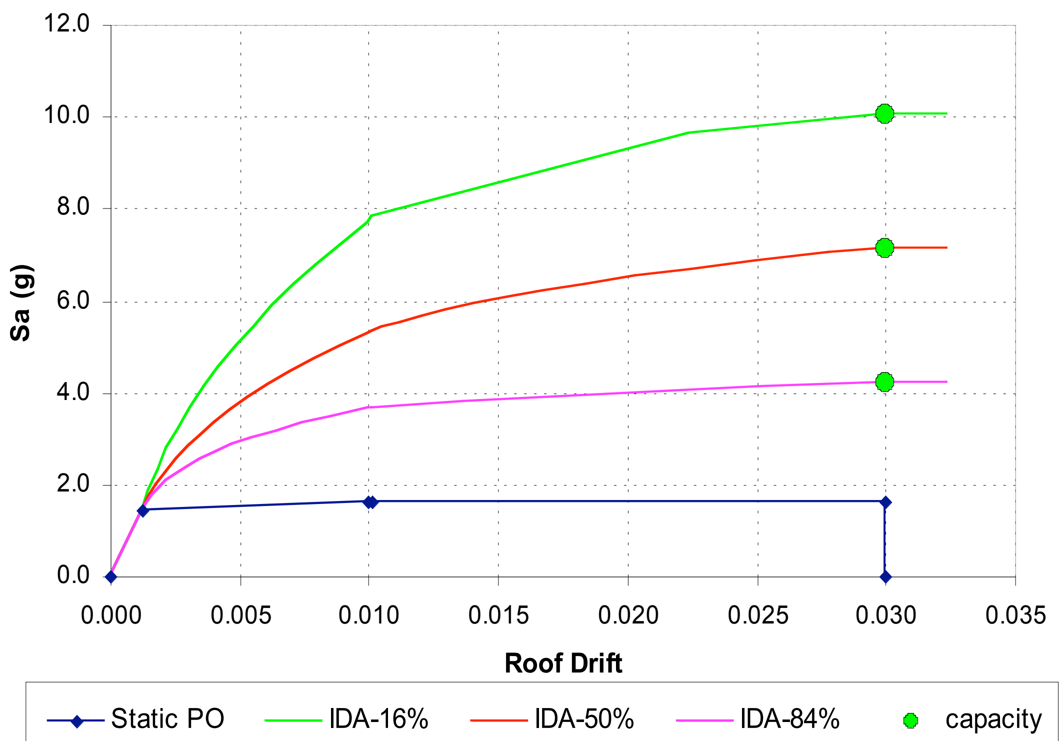


**Figure 4-25:** **SPO2IDA DS4 (Sa vs. Roof drift)**

**Table 4-8: Spectral Acceleration to Cause Each Damage State (From Figure 4-23)**

| Damage State | $S_A$ (g) |
|---|---|
| DS2 | 3.7 |
| DS4 | 6.1 |
| Collapse | 9.5 |

**Table 4-9: Spectral Acceleration to Collapse the structure in an aftershock**

| Damage State | IDA 50% $S_A$ (g) | IDA 84% $S_A$ (g) | Source |
|---|---|---|---|
| Intact | 9.5 | 5.6 | Figure 4-23 |
| DS2 | 9.8 | 5.9 | Figure 4-24 |
| DS4 | 7.2 | 4.2 | Figure 4-25 |

## 4.5. Post-earthquake tagging limit states

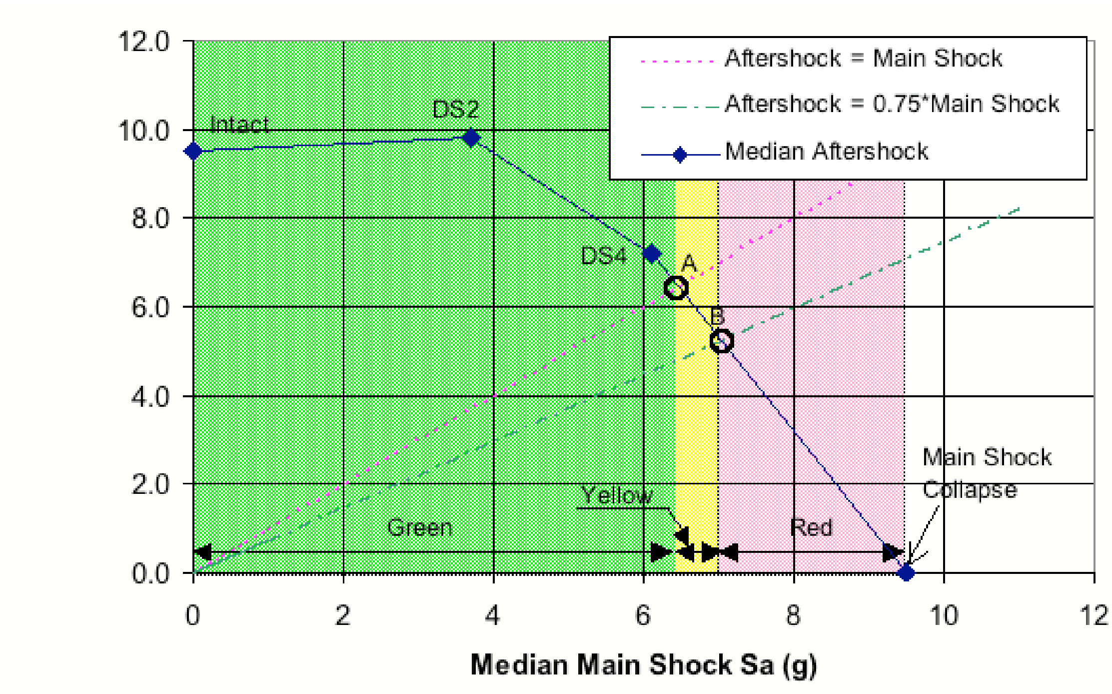


**Figure 4-26: Main Shock vs Aftershock to Cause Collapse Tagging Criteria C**

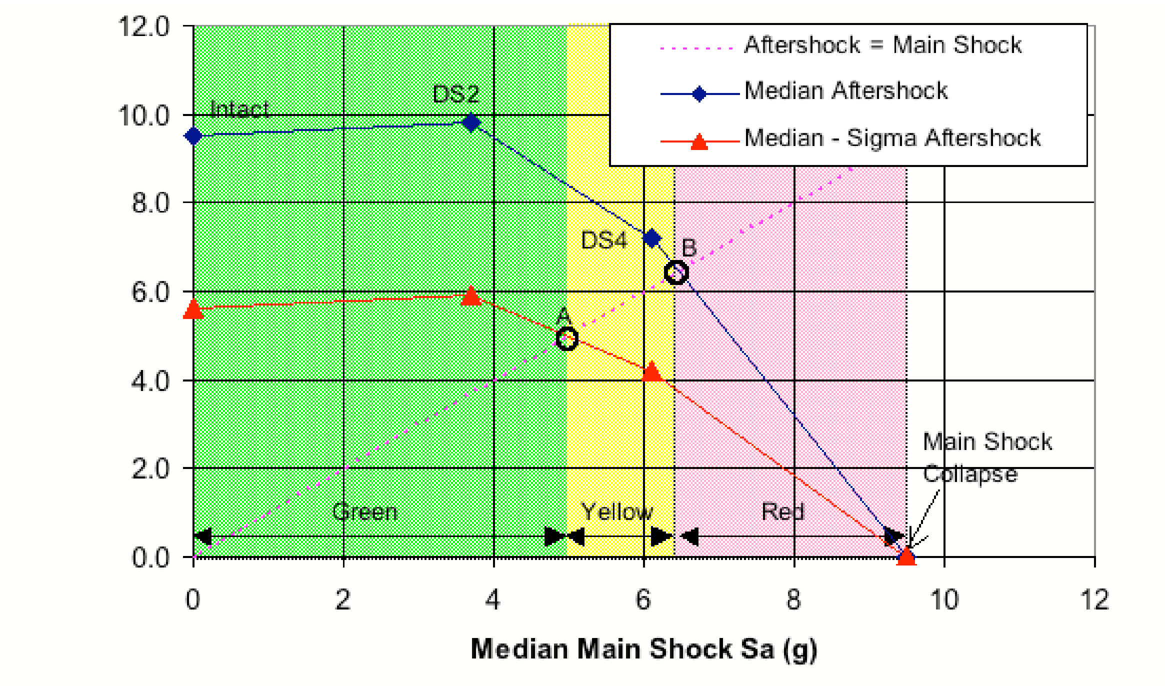


**Figure 4-27: Main Shock vs Aftershock to Cause Collapse Tagging Criteria D**

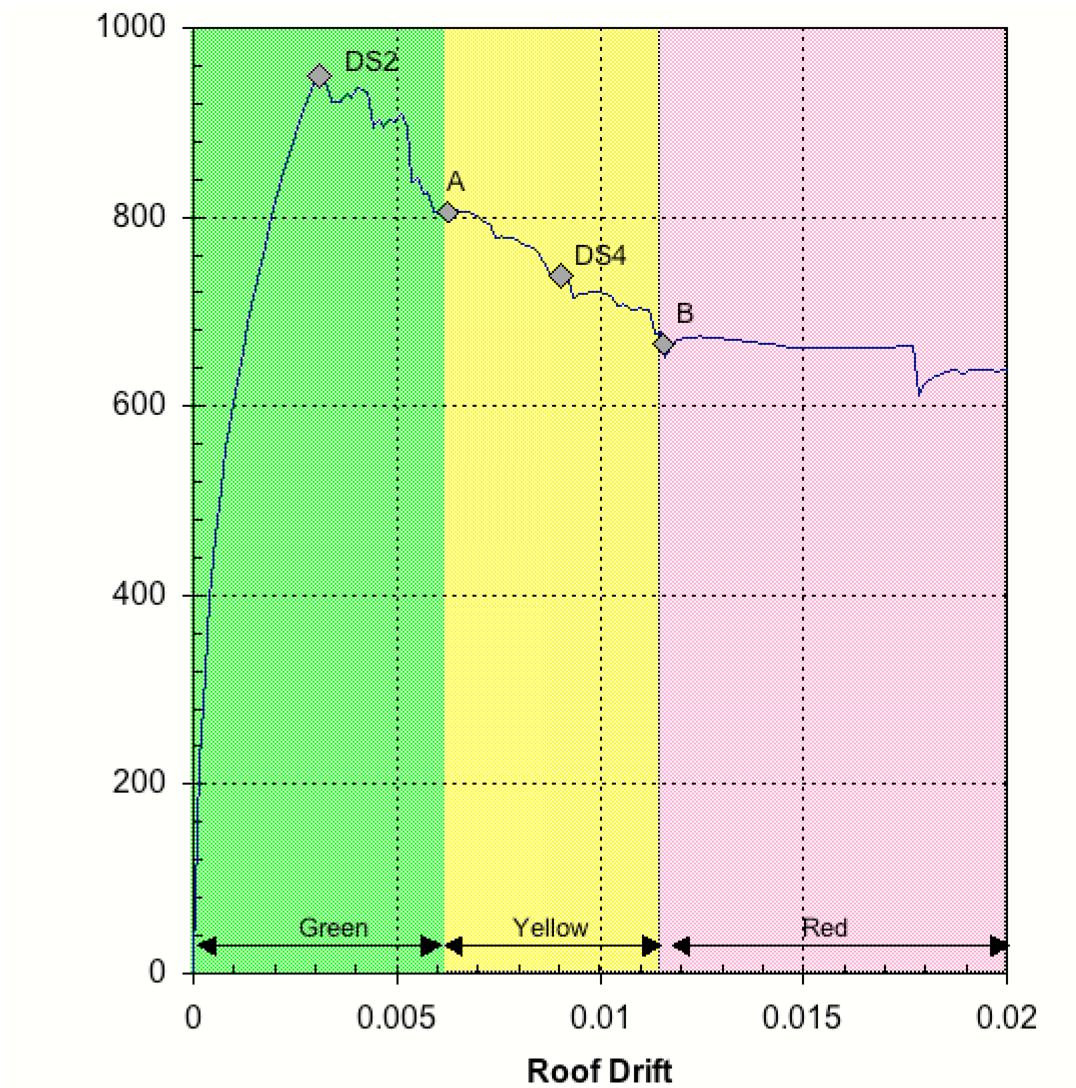


**Figure 4-28:** **Tagging limit states, per Criteria "D", on the Pushover Curve of the Intact Structure**

## *4.6. Fragility curves*

**Table 4-10:** **$\beta_R$ Values taken from the Intact Structure SPO2IDA Results, and $S_{a,\,cap}$ values**

| Damage State | Roof Drift | □ | $\beta_R$ | $S_{a,cap}$ (g) |
|---|---|---|---|---|
| Onset of Damage | 0.003 | 2.31 | 0.16 | 3.67 |
| Yellow | 0.006 | 4.81 | 0.32 | 5.51 |
| Red | 0.012 | 8.85 | 0.39 | 6.35 |
| Collapse | 0.030 | 23.1 | 0.52 | 9.45 |

**Table 4-11: Uncertainty Values for Fragility Curves**

| Uncertainty Value | Onset of Damage | Onset of Yellow | Onset of Red | Collapse | Basis |
|---|---|---|---|---|---|
| $\beta_U$ | 0.40 | 0.60 | 0.60 | 0.60 | Mill-type building, improved [Bazzuro 2002] |
| $\beta_R$ | 0.16 | 0.32 | 0.39 | 0.52 | From SPO2IDA |
| $\beta$ | 0.43 | 0.68 | 0.72 | 0.79 | SRSS of $\beta_U$ and $\beta_R$ |

**Table 4-12: Spectral Acceleration Values (in g) for Fragility Curves**

| $F_S(S_a)$ | $x$ | Onset of Damage | Onset of Yellow | Onset of Red | Collapse |
|---|---|---|---|---|---|
| 0.05 | -1.65 | 1.803 | 1.794 | 1.950 | 2.550 |
| 0.25 | -0.67 | 2.750 | 3.494 | 3.931 | 5.551 |
| 0.5 | 0 | 3.670 | 5.510 | 6.350 | 9.450 |
| 0.75 | 0.67 | 4.898 | 8.690 | 10.257 | 16.086 |
| 0.95 | 1.65 | 7.471 | 16.921 | 20.681 | 35.026 |

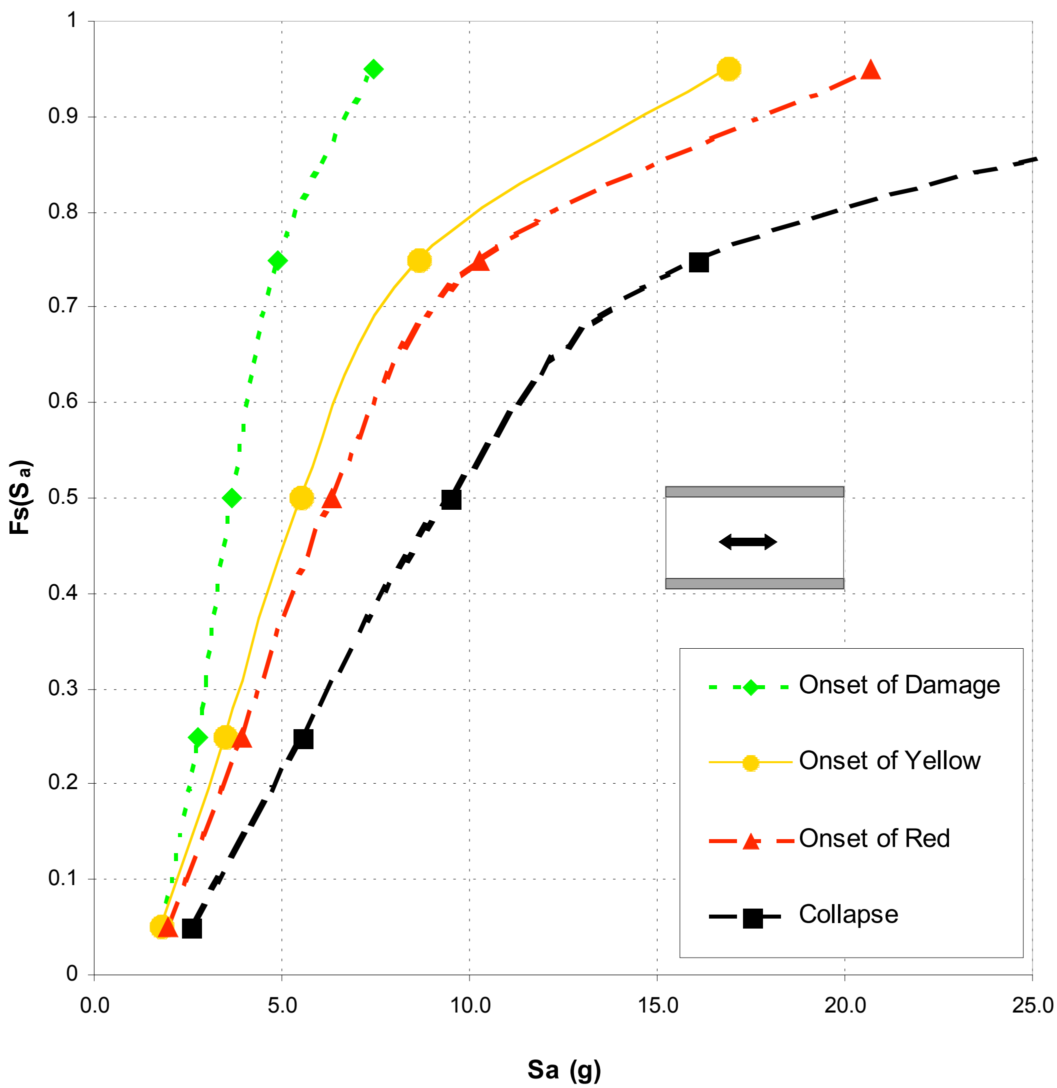


**Figure 4-29:** **Fragility Curves**

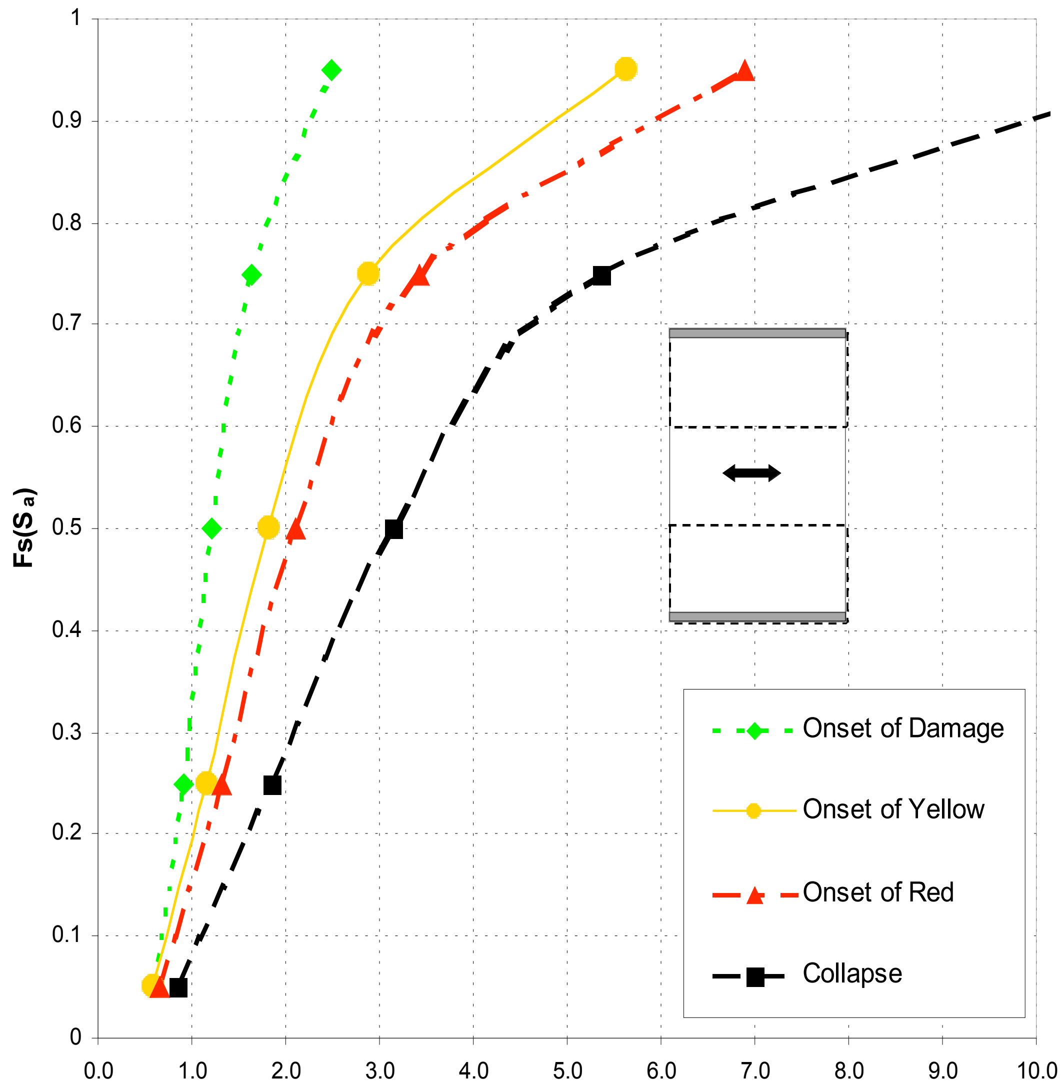


**Figure 4-30:** **Fragility Curves for a hypothetical building with 3 times the seismic weight per wall area**

# 5. Study of the finite element modeling assumptions for Test Application 2

### *5.1. Attempted Calibration of finite element model*

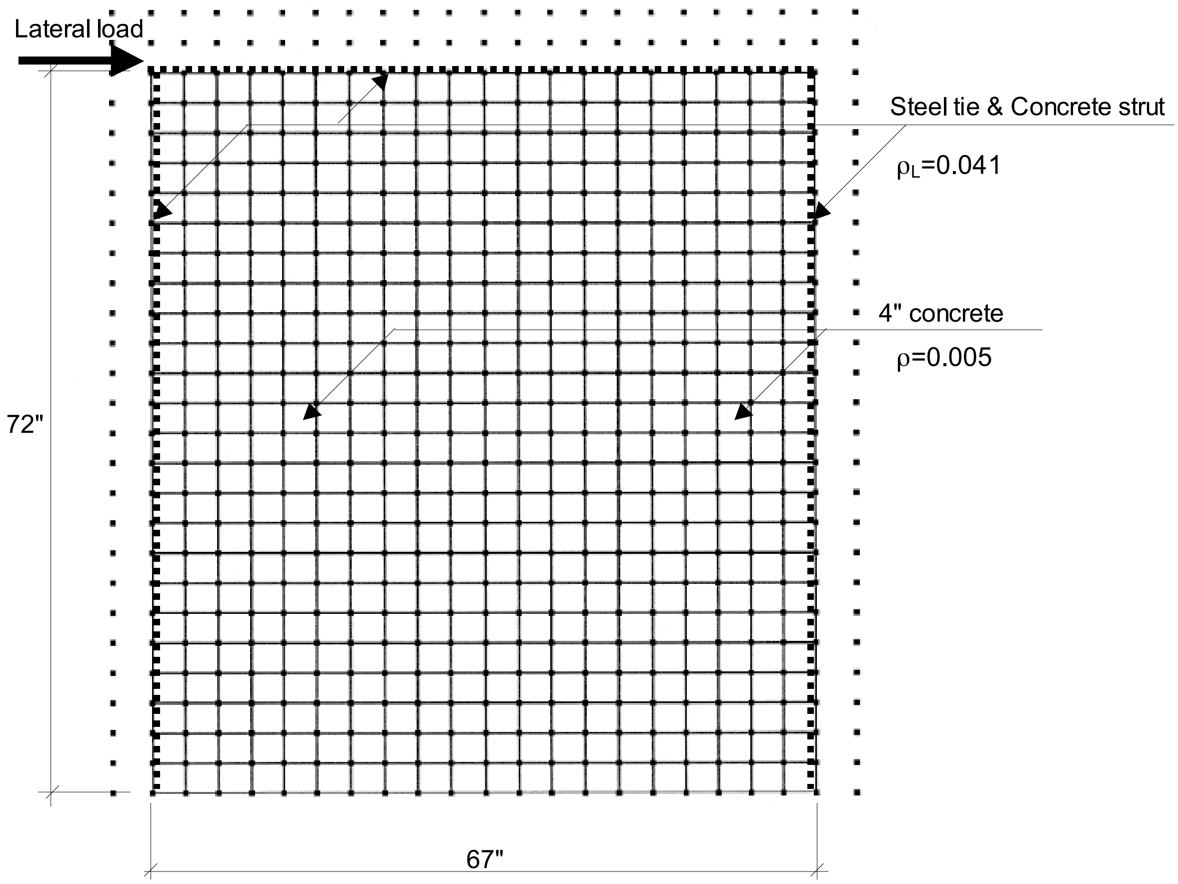


**Figure 5-1: Calibration to concrete wall test specimen, *RAM Perform* analysis model**

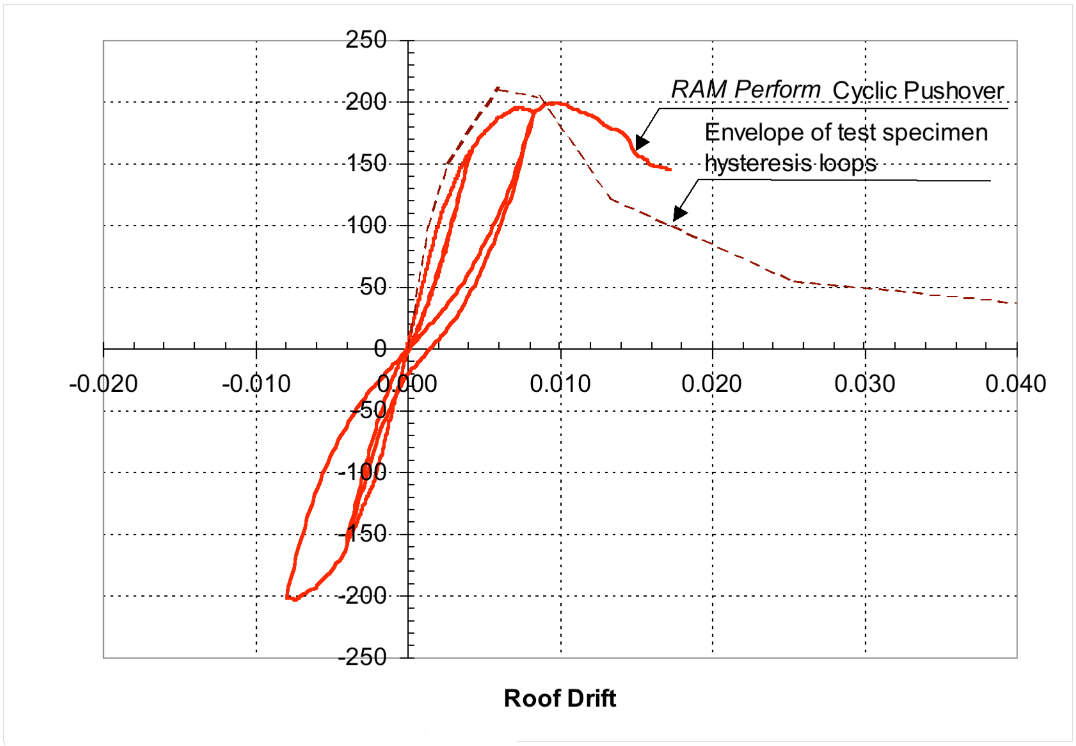


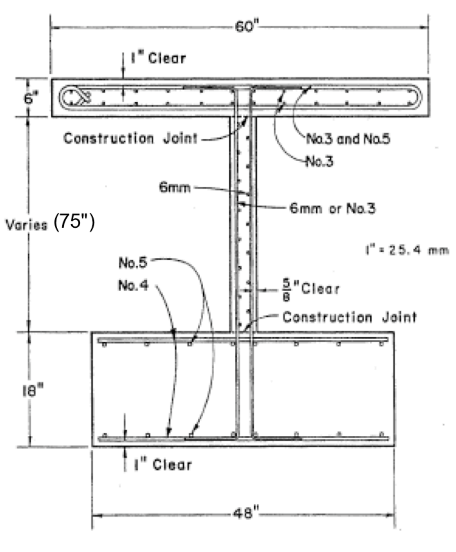


Fig. 3. Representative vertical section.

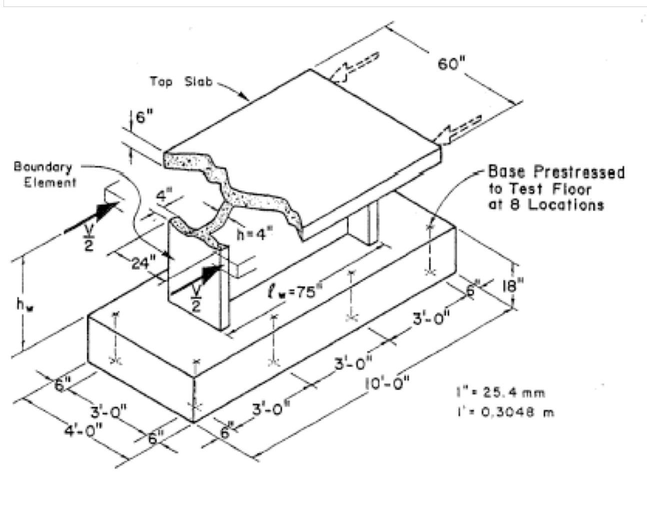


Fig. 1. Test specimen indicating application of load.

**Figure 5-2:** **Concrete wall test specimen (Barda 1974) and calibration of *RAM Perform* Cyclic Pushover (Run 4)**

(a)

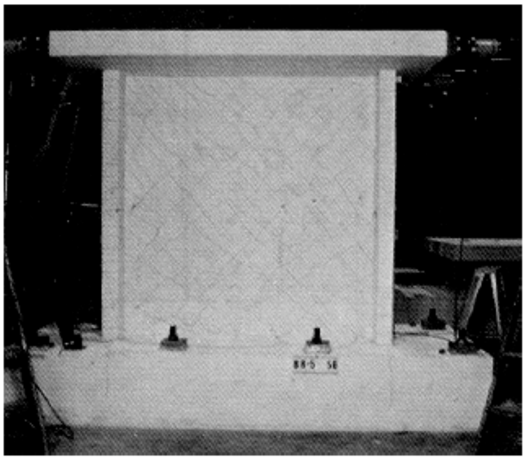

Test specimen at ultimate load
$\Delta = 0.2$ in $\Delta/h_w = 0.005$ $\lambda_Q = 1.0$

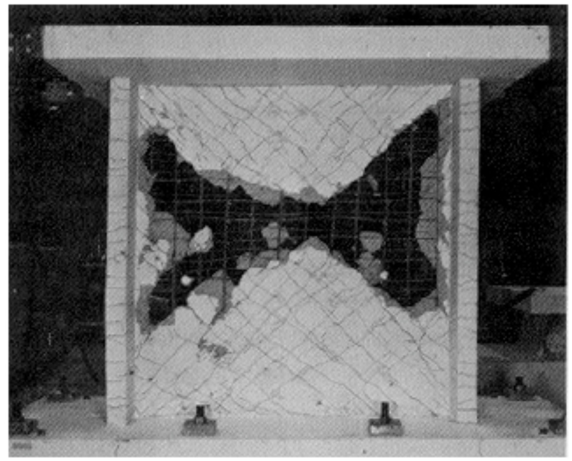

Test specimen at conclusion of loading
$\Delta = 3.0$ in $\Delta/h_w = 0.040$ $\lambda_Q = 0.2$

(b)

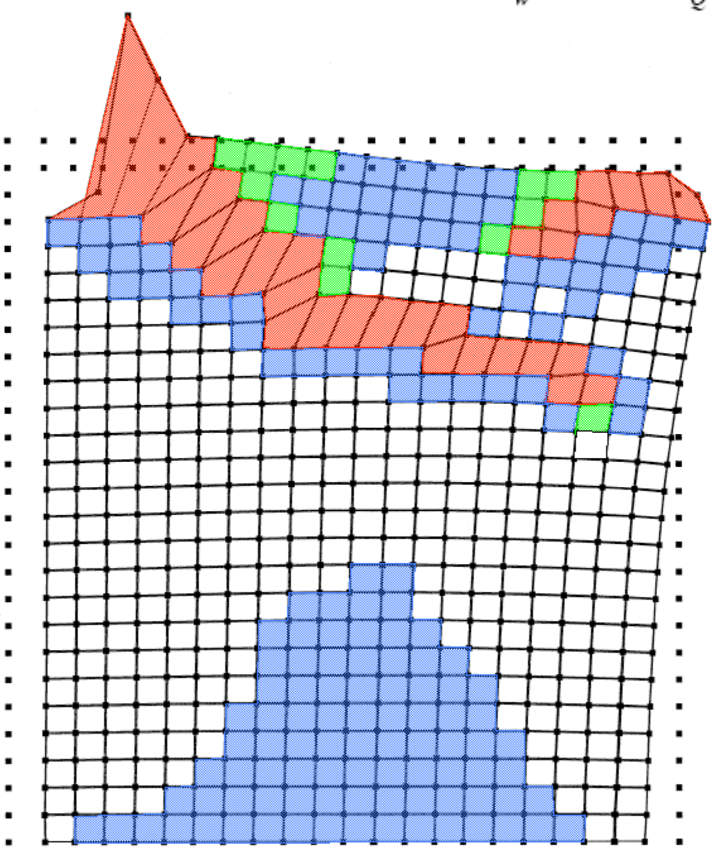

DEFLECTED SHAPE SHOWING USAGE RATIOS
Structure = exp-2 (yn)
Analysis Series = test-c (test-c)
Load Case = [6] = [5] + push3
Reference Drift = 0.01724
Limit state group = all deformation states
Minimum usage ratio for each color : 0.0 0.5 1 1.5 2

**Figure 5-3: (a) Photo of Damaged test specimen (Barda 1972) (b) Finite element model (Run 4)**

**Table 5-1: Concrete wall calibration to test specimen: *RAM Perform* [2004] input properties**

| | Run # | 0 | 1 | 2 | 3 | 4 | 5 | 6 | 7 | 8 | 9 | 10 | 11 | Note |
|---|---|---|---|---|---|---|---|---|---|---|---|---|---|---|
| Inelastic Steel Material | Shape | E-P-P | E-P-P | E-P-P | E-P-P | E-P-P | E-P-P | E-P-P | Trilinear | Trilinear | Trilinear | Trilinear | E-P-P | |
| | $K_0$ (ksi) | 29000 | 29000 | 29000 | 29000 | 29000 | 29000 | 29000 | 29000 | 29000 | 29000 | 29000 | 29000 | 29000 = $E_s$ |
| | $F_R$ (ksi) | 71 | 71 | 71 | 71 | 71 | 71 | 71 | 71 | 71 | 71 | 71 | 71 | 71 = $F_y$ |
| | $F_U$ (ksi) | - | - | - | - | - | - | - | 92.3 | 92.3 | 92.3 | 81.7 | - | 92.3 = 1.3 $F_y$, |
| | $D_U$ | - | - | - | - | - | - | - | 0.05 | 0.05 | 0.05 | 0.03 | - | 81.7 = 1.15$F_y$ |
| | $D_L$ | 0.1 | 0.1 | 0.1 | 0.1 | 0.1 | - | - | 0.033 | 0.033 | 0.033 | 0.033 | - | |
| | $D_R$ | 0.11 | 0.11 | 0.11 | 0.11 | 0.11 | - | - | 0.036 | 0.036 | 0.036 | 0.036 | - | |
| | $F_R/F_U$ | 0.05 | 0.05 | 0.05 | 0.05 | 0.05 | - | - | 0.05 | 0.05 | 0.05 | 0.05 | - | |
| Inelastic Concrete Material | $K_0$ (ksi) | 3300 | 3300 | 3300 | 3300 | 3300 | 3300 | 2310 | 2310 | 2310 | 2310 | 2310 | 3300 | 2310 = 2/3 $E_c$ |
| | $F_U$ (ksi) | 4.08 | 4.08 | 4.08 | 4.08 | 4.08 | 4.08 | 3.4 | 3.4 | 3.4 | 3.4 | 4.08 | 3.4 | 3.4 = $f'_c$,4.08 = |
| | $D_L$ | 0.003 | 0.003 | 0.003 | 0.003 | 0.003 | 0.003 | 0.002 | 0.002 | 0.002 | 0.002 | 0.002 | 0.003 | 1.2 $f'_c$ |
| | $D_R$ | 0.006 | 0.006 | 0.006 | 0.006 | 0.006 | 0.006 | 0.006 | 0.006 | 0.006 | 0.006 | 0.006 | 0.006 | See note 1 |
| | $F_R/F_U$ | 0.1 | 0.1 | 0.1 | 0.1 | 0.1 | 0.1 | 0.01 | 0.01 | 0.01 | 0.01 | 0.01 | 0.2 | |
| Inelastic Shear Material | $K_0$ (ksi) | 50 | 50 | 50 | 50 | 50 | 50 | 50 | 50 | 145 | 145 | 145 | 560 | 145 = $\rho E_s$ |
| | $F_U$ (ksi) | 0.64 | 0.64 | 0.64 | 0.64 | 0.64 | 0.64 | 0.64 | 0.64 | 0.204 | 0.204 | 0.7 | 0.71 | 0.204 = 3.5$\sqrt{f'}$ |
| | $D_L$ | 0.0256 | 0.0256 | 0.0154 | 0.0154 | 0.0154 | 0.0154 | 0.0154 | 0.0154 | 0.003 | 0.003 | 0.005 | 0.0075 | |
| | $D_R$ | 0.064 | 0.064 | 0.0384 | 0.032 | 0.0256 | 0.0256 | 0.0256 | 0.0256 | 0.007 | 0.007 | 0.007 | 0.0085 | 0.17 = 0.6/3.5 |
| | $F_R/F_U$ | 0.2 | 0.4 | 0.4 | 0.5 | 0.5 | 0.5 | 0.5 | 0.5 | 0.5 | 0.17 | 0.17 | 0.4 | (FEMA 306) |
| Diagonal Compression Material | $K_0$ (ksi) | 3300 | 3300 | 3300 | 3300 | 3300 | 3300 | (Same as Inelastic Concrete Material) | (Same as Inelastic Concrete Material) | (Same as Inelastic Concrete Material) | (Same as Inelastic Concrete Material) | (Same as Inelastic Concrete Material) | (Same as Inelastic Concrete Material) | |
| | $F_U$ (ksi) | 4.08 | 4.08 | 4.08 | 4.08 | 4.08 | 4.08 | | | | | | | |
| | $D_L$ | - | - | - | - | - | - | | | | | | | |
| | $D_R$ | - | - | - | - | - | - | | | | | | | |
| | $F_R/F_U$ | - | - | - | - | - | - | | | | | | | |
| Match of Initial Stiffness | | OK | OK | OK | OK | OK | OK | Fair | Fair | Good | Good | Good | Poor | |
| Match of Peak Strength | | OK | Good | OK | OK | OK | OK | Fair | Fair | Poor | Poor | Poor | Fair | |
| Match of Strength Degradation | | OK | Poor | Fair | OK | Fair | Poor | Poor | Poor | Poor | Poor | Fair | Poor | |
| Match of Failure Pattern | | - | - | - | - | - | Fair | OK | OK | Fair | Fair | Poor | Poor | |

Note 1: Value of DL=0.002 and DR=0.006 corresponded to Park and Pauley [1975]

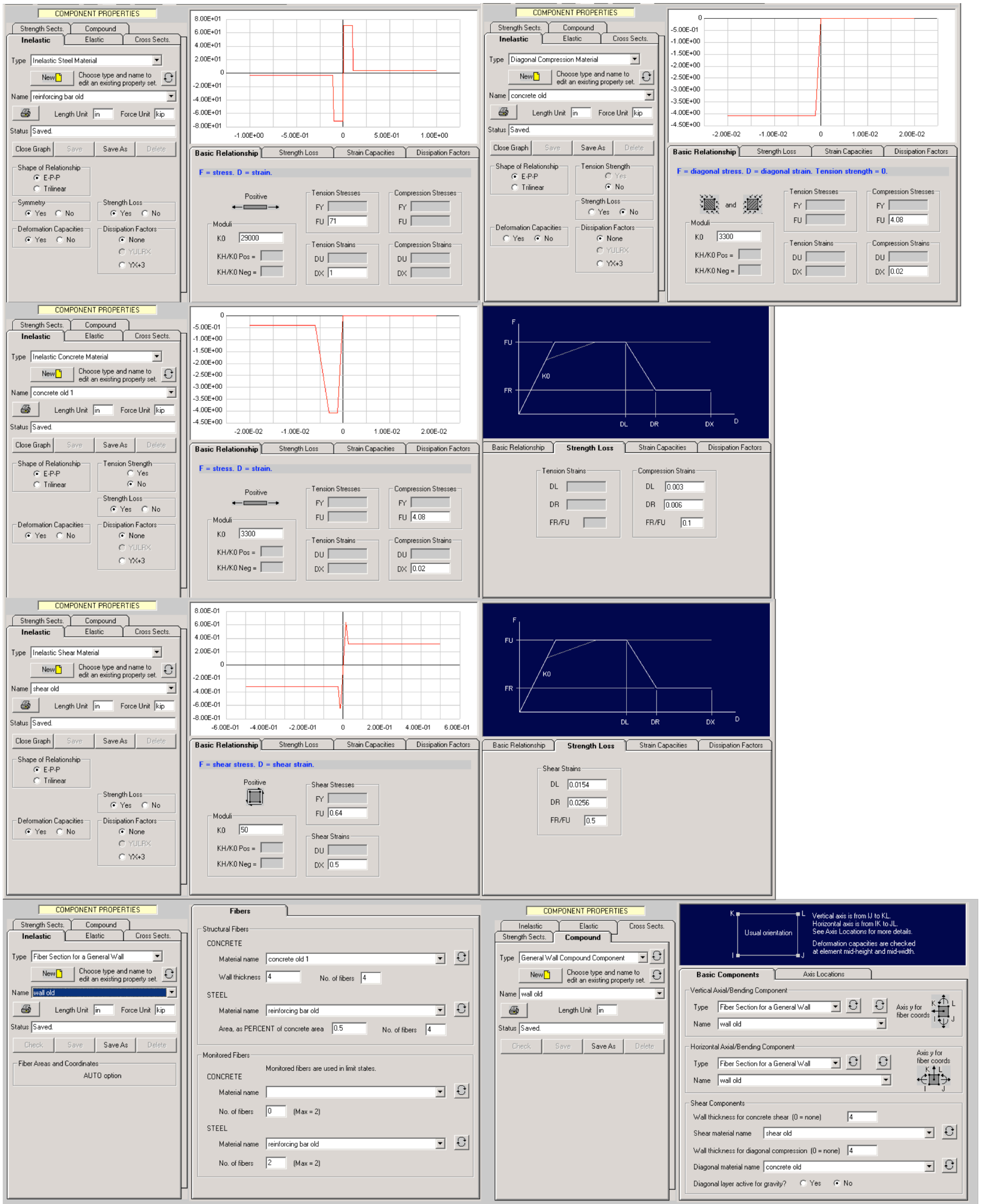

**Figure 5-4:** ***RAM Perform* input properties for calibration to test specimen (Run 4)**

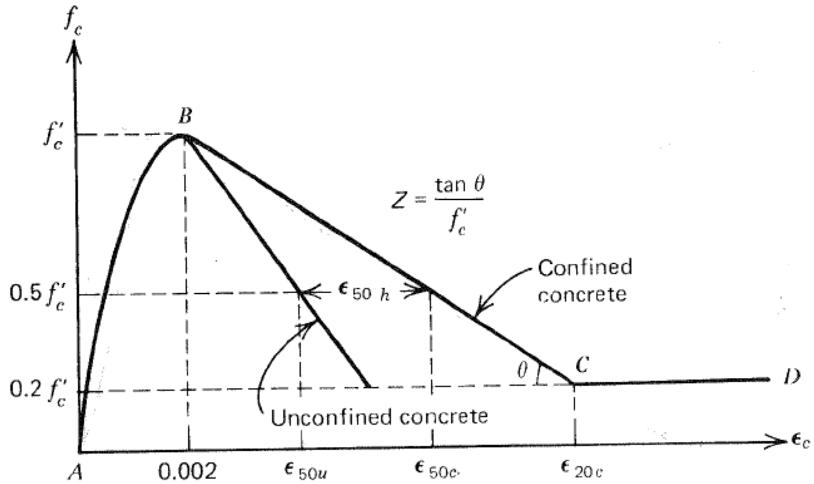


**Figure 5-5: Stress-strain curve for concrete confined by rectangular hoops, Park + Pauley**

# 6. Application on an 8-story steel moment frame building

# 7. Key Technical Issues

## *7.1. Analysis approach*

## *7.2. Residual drift*

**Estimated effect of residual displacement**

Specific research (outside the scope of the Task 508 project) is recommended to establish the effect of residual displacement.

Pending more specific results, the following procedure is used to estimate residual drift. See the notation section for the precise definitions of the variables used.

The static residual drift, $\Delta_{rs}$, is determined from the SPO and assumed unloading stiffness, according to the seismic assessment procedure.

**The expected dynamic residual drift, $\Delta_{rd}$ is assumed to be a factor $\gamma_1$ times $\Delta_{rs}$. The factor is assumed to depend on the type of seismic-force-resisting system, as it relates to the global hysteresis loop shape of the earthquake response. Specifically, the structural components of the seismic force-resisting system that respond nonlinearly influence the hysteresis loop shape. Hysteresis loop shapes with better displacement restoring**

**characteristics – for example those with a positive slope to the "hysteresis center curve" [MacRae 1995] are given a smaller value of $\gamma_1$. Recommended values of $\gamma_1$ are shown in**

**Table 7-2: Values of $\gamma 1$, ratio of dynamic to static residual drift.**

.

The reduction in global drift capacity, $\square_{re}$ is assumed to be a factor $\gamma_2$ times $\square_{rd}$. The factor is assumed to depend on the strength degradation of the SPO curve. The factor $\gamma_2$ is taken to depend on the average slope, $\alpha_i$, of the SPO between the damage state and the approximate collapse drift. Figure 7-1 shows how $\alpha_i$ is determined. It is taken as the ratio to the initial stiffness slope. A negative value of $\alpha_i$ indicates strength degradation. A positive value of $\alpha_i$ indicates hardening. **Error! Reference source not found.** shows the assumed relationship between $\gamma_2$ and $\alpha_i$.

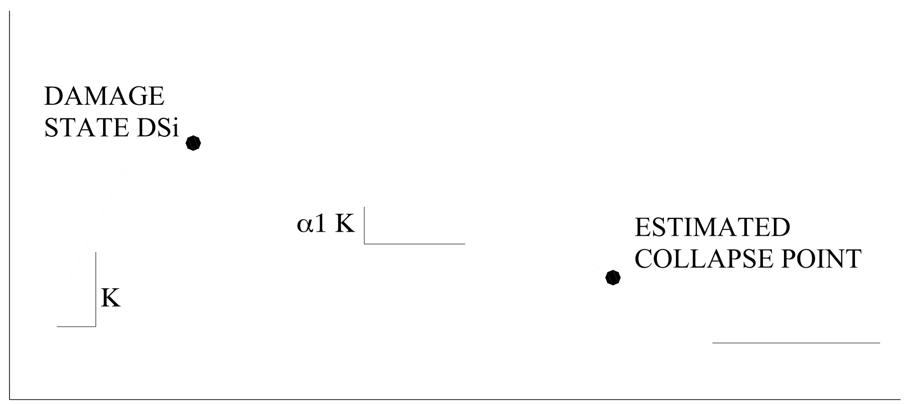


**Figure 7-1: Determining $\alpha_i$, slope factor effecting residual drift for $DS_i$.**

**Table 7-1: Determining $\gamma_2$**

| **Strength Degradation beyond Damage State i** | $\gamma_2$ |
|---|---|
| High Degradation | 0.9 |
| Moderate Degradation | 0.7 |
| Zero Degradation | 0.5 |
| Strength Increasing | 0.3 |

**Table 7-2: Values of $\gamma_1$, ratio of dynamic to static residual drift.**

| Example Structure Types | Hysteresis Loop Shapes | $\gamma_1$ |
|---|---|---|
| • eam<br>• 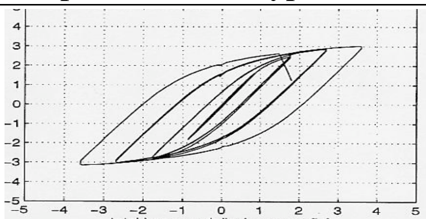<br>• Steel Unbonded Braced Frame | | 0.3 |
| • Flexural plastic hinging in concrete walls or concrete moment frames<br>• Plywood or OSB sheathed walls<br>• Diaphragm-yielding structures (e.g., tilt-ups) with plywood or OSB sheathed diaphragms.<br>• Steel concentric braced frames<br>• Structures not otherwise classified | 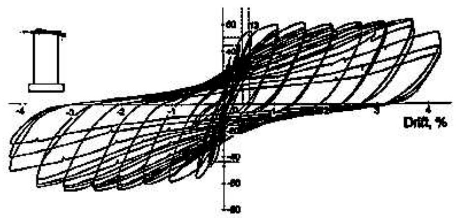 | 0.2 |
| • Foundation rocking structures<br>• Other structures with high restoring force from gravity load and rocking-type hysteresis loop shapes. | 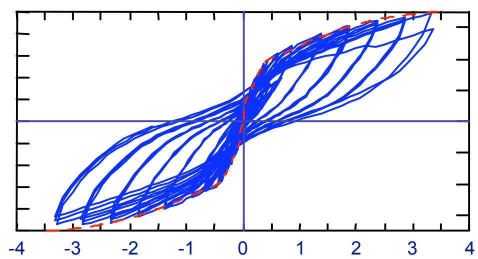 | 0.1 |
| • Structures specifically designed for minimal residual drift, such as precast hybrid moment frames [PRESSS]. | 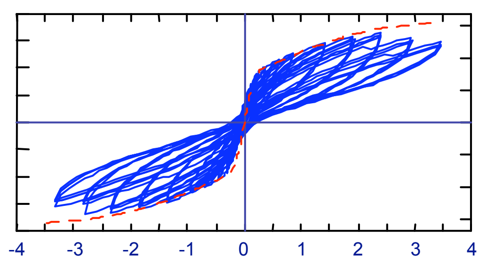 | 0 |





### *7.3. Building period shift and effect*

### *7.4. Tagging criteria*

**Tagging criteria A – based on the probability of collapse for the aftershock seismic hazard.**

This option for tagging criteria would be the most technically sophisticated and correct approach, but it requires knowledge of the aftershock seismic hazard and a selection of acceptable collapse probabilities. To date, there has not been much research focused on aftershock seismic hazard. There is the potential that in the near future, more specific data on aftershock seismic hazard could be used in tagging criteria. Research (outside the scope of this project) is recommended in this area.

**Tagging criteria B – based on the probability of collapse of the damaged structure, using the pre-earthquake seismic hazard**

Under this option, the tagging criteria is shown graphically in Figure 21, and is explained as *follows*:

*If the increase in the probability of collapse is less than 10% ($P/P_0 < 1.10$), then the tagging condition is Green.* In other words, if $P/P_0 < 1.10$, the ability of the building to survive an earthquake has not been significantly changed by whatever damage has occurred. As is customary in post-earthquake inspection, if a building has not suffered any consequential damage, then it is given a Green tag. Even if it is a highly vulnerable building, it is given a green tag because the earthquake did not change its vulnerability.

*If the increase in the probability of collapse is greater than 10%* ($P/P_0 > 1.10$)*, then the tagging condition depends on the probability of collapse in an aftershock.* In the absence of aftershock hazard information, this is assumed to correlate to the magnitude of ground shaking, expressed by Return Period, that would cause collapse. The return period corresponds to the pre-earthquake seismic hazard at the site, i.e., assuming that that hazard has not changed by the occurrence of the damaging earthquake.

> *If the return period to cause collapse is greater than 1000 years, then the tagging condition is Green.* For $RP > 1000$ years, the building has an ability to survive earthquake collapse that is equivalent to or better than that assumed for new structures in conformance to the latest building codes. Therefore, despite the damage sustained, the building is given a Green tag.

If the return period to cause collapse is between 250 an 1000 years, then the tagging condition is Yellow.

> *If the return period to cause collapse is less than 250 years, then the tagging condition is Red.* A building that has been damaged ($P/P_0 > 1.10$) and will collapse under the relatively small RP < 250 ground motions is considered under enough risk that it warrants a Red tag rather than a Yellow tag.

For this criteria the trigger values of $P/P_0 = 1.10$, $RP = 250$, and $RP = 1000$ are selected by the judgment of the authors, and could be adjusted as appropriate.

**Tagging Criteria C – based on the ability to sustain an aftershock proportional to the main shock.**

Under this option, the tagging criteria is as follows:

*If the damaged structure can withstand, without collapse, an aftershock with $S_a$ equal to that of the damaging earthquake, then the tagging condition is Green.*

*If the damaged structure collapses under the above test, but can withstand an aftershock with $S_a$ equal to 0.75 times that of damaging earthquake, then the tagging conditions is Yellow. If the damaged structure collapses under an aftershock with $S_a$ equal to 0.75 times that of damaging earthquake, then the tagging condition is Red.*

# 8. Conclusions

This project described in this report investigates the practical application and potential of performance-based seismic assessment methods. The project explores issues that may affect the wider application in practice of seismic and structural engineering procedures that use state of the art techniques.

## *8.1 Overall findings*

In general, the project finds that:

- The Advanced Seismic Assessment Guidelines are a logical and rational method that appears to be technically sound.
- The Guidelines can be implemented using a variety of structural analysis approaches, ranging from hand-calculated building response to fully computerized analysis of intact and damaged structures.
- The results of the procedure depend on the technical definition of what collapse potential should correspond to a red-tag, yellow-tag, or green-tag occupancy. This report investigate several options for tagging criteria and generally recommends what is defined as Tagging Criteria D, with correlation to engineering judgment.
- The results of the procedure depend on key assumptions and practices related to evaluating the intact and damaged structure. These practices include:
    - Whether the analysis truly identifies and incorporates the structural behavior modes that will govern the seismic response. (This is a key aspect of any seismic evaluation procedure).
    - How degraded components are assumed to respond, which must be based on available research results and technical approaches.
    - Estimating the residual drift in a structure, and the effect of that residual drift on displacement demand. This report gives recommendations based on a structure's peak plastic drift, hysteresis loop shape, and strength degradation characteristics.
- For the most effective application of the Guidelines, research is needed on the structural response of degraded components, specifically in the following areas:
    - For steel moment frame structures, tests of beam-column connections are needed, where the tests are taken to displacements beyond flange fracture. (While there have been many tests of such connections, very few have continued testing beyond flange fracture.)
    - For concrete wall structures, a review and assessment of past laboratory testing would be useful, considering behavior modes including flexure, shear, and foundation rocking. There are a reasonable number of tests available, but appropriate recommendations for seismic evaluation assumptions have not been developed or verified.

- Advanced computer models of structural elements – in particular, multi-layer nonlinear finite element models of concrete walls, and nonlinear fiber models of fracturing steel beam connections – should be calibrated to experimental testing.

### 8.2 Specific recommendations on implementation

In addition to the overall conclusions of the report, the items below summarize some key recommendations to engineers who are using the Guidelines, indicating sections of this report that may be especially helpful:

- Engineers using the assessment procedure may find the step-by-step description of applying the guidelines, Section 2.7, to be a useful example.
- A key step for an engineer applying the procedure is how to calculate the SPO of a damaged structure. This report contains examples of different ways that the SPO can be calculated. The procedure for calculating the SPO should be based on:
  - The intact SPO and the damage state $DS_i$
  - Effective residual deformation, $\square_{re}$
  - Reloading initial stiffness, $K_i$
  - Reloading hardening stiffness, $K_{hi}$

  Given this data, the SPO can be graphically constructed. Alternatively, changing material properties using appropriate nonlinear analysis software can be an effective approach
- For various types of structures, the engineer needs to know how to estimate unloading and reloading global stiffness, and global hardening stiffness as a function of damage state. This report gives recommendations for steel moment frames. Alternatively the engineer can use nonlinear software with appropriate modifications to material properties to account for damage. This report gives an example of this approach, applicable to concrete wall buildings.
- The engineer must account for the effect of residual deformation on the deformation capacity under subsequent shaking. The report section 7.2 gives an approximate approach that attempts to account for the key variables of hysteresis loop shape and strength degradation. Further research is recommended to assess the effects of residual deformation.
- Engineers may find a plot of $S_a/S_{a10/50}$ , such as shown in Figures 18, helpful in explaining the IDAs for different damage states are compared on the same graph.
- Converting the IDA plot to one of return period versus roof drift, such as shown in Figure 19 and 22, can help illustrate to engineers how the IDAs interact with the green, yellow, and red conditions of tagging criteria B.

## 9. References

ATC 20, 1989, *Procedures for Postearthquake Safety Evaluation of Buildings*, Applied Technology Council (ATC), ATC: Redwood City, California.

ATC 20-2, 1995, *Addendum to the ATC-20 Postearthquake Building Safety Evaluation Procedures*, Applied Technology Council (ATC), ATC: Redwood City, California.

ATC, 1999, *Evaluation of Earthquake Damaged Concrete and Masonry Wall Buildings*, *Basic Procedures Manual* prepared by the Applied Technology Council (ATC-43 project) for the Partnership for Response and Recovery, published by the Federal Emergency Management Agency, Report No. *FEMA 306*, Washington D.C.

ATC, 1999, *Evaluation of Earthquake Damaged Concrete and Masonry Wall Buildings*, *Technical Resources*, prepared by the Applied Technology Council (ATC-43 project) for the Partnership for Response and Recovery, published by the Federal Emergency Management Agency, Report No. *FEMA 307*, Washington D.C.

Barda, Felix, John W Hanson, and W. Gene Corley, "Shear Strength of Low-Rise Walls with Boundary Elements", Research and Development Bulletin RD043.01D, preprinted with permission from ACI Symposium *Reinforced Concrete Structures in Seismic Zones*, American Concrete Institute, by Portland Cement Association, 1976.

Bazzurro P., Cornell C.A., Menun C. and M. Motahari, 2002, "Advanced Seismic Assessment Guidelines", prepared for Pacific Gas and Electric/PEER, February 28 draft.

Park, R. and T. Paulay, Reinforced Concrete Structures, A Wiley-Interscience Publication, New York, 1975.

Paulay, T. and M. J. N. Priestley, 1992, *Seismic Design of Reinforced Concrete and Masonry Buildings*, John Wiley and Sons, New York

Vamvatsikos D., Cornell C.A**, "**Direct Estimation of the Seismic Demand and Capacity of Oscillators with Multi-Linear Static Pushovers through Incremental Dynamic Analysis" *Proceedings of the 7th National Conference on Earthquake Engineering*, Boston, July 2002